ANALYSIS OF HEAT TRANSFER IN SEVERAL MEDIA

Thesis by

Satwindar Singh Sadhal

In Partial Fulfillment of the Requirements

for the Degree of

Doctor of Philosophy

California Institute of Technology

Pasadena, California

1979

(Submitted September 26, 1978)

ACKNOWLEDGMENTS

I take this opportunity to express my sincere gratitude to Professor Milton S. Plesset who, since the inception of this investigation, has shared some of his wisdom with me in the form of constructive and scholarly advice. I am deeply indebted to Miss Helen Burrus for her excellent work in the laborious task of typing this thesis which involved generous amounts of her personal time and energy. My thanks also go to Miss Cecilia Lin for her artistic inkwork in preparing the figures and to Miss Patricia Sahagian who briefly undertook the typing during the short absence of Miss Burrus. I gratefully acknowledge financial support from the Natural Sciences and Engineering Research Council Canada, the California Institute of Technology and the National Science Foundation (Grant No. ENG75-22676).

ABSTRACT

Analytical solutions to three heat transfer problems, each involving more than one medium, are obtained by using some exact and approximate methods.

I. In particular, for the analysis of nucleate boiling at a solid surface, a single bubble is simulated by a point source (or a sink) of liquid. A solution of the boundary layer type is obtained for a constant point sink, and it is used to estimate the microlayer thickness, a quantity useful in determining some features of latent heat transfer due to vapor flow within the bubble.

II. The thermal effects of droplets condensing on, or evaporating from, a solid surface are analyzed by solving the steady heat-conduction equation for a spherical segment droplet on a semi-infinite solid with suitable boundary and interface conditions. Expressions for the temperatures, the overall heat flow and the lifetime of an evaporating droplet are obtained. From these expressions, the effects of the solid properties and the contact angle are predicted.

III. Estimates of long-time thermal contact resistances are obtained by considering the transient thermal response of two semi-infinite bodies in contact over (1) a circular disk; and (2) a series of identical, equally spaced strips. The unsteady heat equation is solved by using suitable interface conditions with each solid being at an initially uniform but different temperature. The solution is valid for large values of the Fourier number.

TABLE OF CONTENTS

LIST OF FIGURES

INTRODUCTION

Many of the interesting problems in heat transfer involve more than one medium, and quite often the analyses of these problems cannot be treated by considering each medium separately. That is, the analyses require the simultaneous treatment of all the media involved, rather than an independent treatment of each medium. In some cases, however, one medium may be effectively approximated by, let us say, a surface, or a line, or even a point. In this thesis, we investigate three important problems in heat transfer, each problem involving more than one medium.

In the first problem we deal with the vapor bubbles of nucleate boiling which grow and collapse at a solid surface. The analysis of the heat transfer requires an estimate of heat transfer due to conduction through the "microlayer" of liquid between the vapor bubble and the solid wall, and the latent heat transport due to the evaporation from the microlayer. Such an estimate requires the knowledge of the microlayer thickness. The calculation of the thickness is a well-defined theoretical problem in fluid dynamics but an exact analysis seems impracticable and approximations are, therefore, necessary. In the present study we describe the liquid flow outside the bubble by a source (growing bubble) or by a sink (collapsing bubble) on a rigid plane (see Fig. 1.1). In this way we essentially reduce this two-medium problem to a one-medium problem so far as the fluid dynamics is concerned. The vapor medium properties are described by the source or sink strength. Results, however, are obtained only for a collapsing bubble. For a growing bubble we encounter analytical

difficulties, presumably because of the possible reverse flows which are suspected to exist for the case of a point source on a rigid plane. The flow from a line source on a plane is known to have this reverse flow (see Fig. 1.3).

In the second problem we study droplets, condensing on or evaporating from a solid surface (see Fig. 2.1), and obtain expressions for the quasisteady thermal resistances. This problem involves three media — solid, liquid and vapor; but the effect of the vapor, for an evaporating droplet, may be decoupled from the solid and liquid effects which remain coupled with each other. For a condensing droplet, the interactions of the properties of all three media are coupled. It will be made evident that the contribution of each medium to the overall thermal resistance cannot be separated from the contributions of the other media. This interaction takes place because the interfaces of the media are not uniform temperature surfaces except at the liquid-vapor interface for an evaporating droplet.

The third problem deals with the transient thermal resistance between two different solids having imperfect thermal contact. In this case we analyze the transient thermal response of two semi-infinite solid bodies, the plane surfaces of which are brought into contact. Initially, each body is at a different uniform temperature. We consider the possibilities when the contact is established over (1) a finite circular disk; and (2) a series of equally spaced identical strips. Over these regions of perfect contact we require the temperatures and the heat fluxes to be continuous. Along the interface where there is no contact, we may have heat transfer due to the presence of air.

At atmospheric pressures, however, the effect of the air medium can be ignored, and we may assume that the regions of no contact are insulated. The problem then reduces to the heat equation for two media, and approximate solutions are obtained by a long-time perturbation scheme.

For all these problems the solutions, although approximate, are analytical. As a result, we obtain a clear view of the effect of the properties of the different media.

PART 1

AN ANALYTICAL ESTIMATE OF THE MICROLAYER THICKNESS IN NUCLEATE BOILING

Nomenclature

m_s	=	$R^2\dot{R}$ = source strength
m	=	$-R^2\dot{R}$ = sink strength
p	=	pressure
$R(t)$	=	bubble radius
R_o	=	maximum bubble radius
r	=	spherical distance from origin
t	=	time
t_o	=	bubble lifetime
U	=	free-field radial velocity
u	=	radial velocity within the boundary layer
w	=	velocity normal to wall
z	=	distance normal to wall
δ	=	boundary layer thickness
δ_o	=	microlayer thickness
$\langle\delta_o\rangle$	=	average value of δ_o
η	=	$z(\lvert m_s\rvert/2\nu r^3)^{\frac{1}{2}}$ = similarity variable
ν	=	kinematic viscosity
ρ	=	density of liquid
ϕ	=	velocity potential

1.1 Introduction

Among the phenomena of interest in nucleate boiling at a solid surface is the enhanced heat transfer that takes place with the onset of such boiling. In the physical situation of present concern one has a large temperature gradient in the liquid in the neighborhood of the solid. Vapor bubbles grow and collapse at the solid with a lifetime of the order of a millisecond or less. These nucleate boiling bubbles have characteristically a maximum size of about 0.5 mm. The analysis of the dynamics of such vapor bubbles is important for the understanding of the physical mechanism of the increased heat transfer from a hot solid to a liquid in nucleate boiling conditions.

To explain the increased heat transfer with nucleate boiling two mechanisms have been suggested. The first supposes that the growing and collapsing of a bubble produces a stirring of the liquid in the region of the large temperature gradient near the solid. This "microconvection" is then supposed to produce the increase in heat transfer. Because of viscosity the bubble growth and collapse have associated with them a viscous layer between the bubble base and the solid (see Fig. 1.1). This viscous layer is known as the "microlayer". The second mechanism supposes that the important contribution comes from the transport of latent heat. In this latter mechanism the heat from the hot wall is conducted through the microlayer and is transported from the bubble base to the cooler bubble cap in the form of latent heat of vaporization from the microlayer. The contribution of this latent heat transport in subcooled nucleate boiling has been studied by Plesset and Prosperetti [1].

In the determination of heat transfer rates due to these mechanisms the thickness of the microlayer plays an important role and has been the subject of several investigations. From a theoretical point of view the calculation of the thickness of the microlayer is a well-defined problem in fluid dynamics. However, previous attempts [2, 3] to solve this problem have led to solutions which have been developed and applied to slowly growing bubbles. These growing bubbles are observed in situations in which the temperature gradient in the liquid in the neighborhood of the solid is much smaller than the gradients which apply to nucleate boiling. The vapor bubbles which grow in such moderate temperature gradients not only grow much more slowly but also attain sizes of the order of several millimeters. These do not usually collapse on the solid but detach from it to collapse at a distance from it. Measurements of the microlayer thickness for such bubbles have been made by Jawurek [4] and by Voutsinos and Judd [5] with use of optical interferometry. For the small, short-lived nucleate boiling bubbles such measurements are not yet available.

For a spherical vapor bubble of radius R(t) growing or collapsing in an unbounded liquid such as water the velocity potential in the liquid viewed as a perfect fluid is

$$\phi(r, t) = \frac{R^2 \dot{R}}{r} \quad , \tag{1.1}$$

where $\dot{R} \equiv dR/dt$ is the velocity at the bubble boundary. This motion is the same as the motion produced by a point source (or a sink) of liquid of strength

$$m_s = R^2\dot{R} \quad . \tag{1.2}$$

Viscous effects for such unbounded spherical motion in water are unimportant. A bubble growing (collapsing) at a solid wall usually has a nearly hemispherical shape and the liquid motion away from the wall can be described by (1.1-1.2). At the wall, however, the no-slip condition applies and we have a viscous boundary layer. The motion of the liquid is similar to the case of a point source (sink) in an unbounded liquid where we introduce a rigid plane containing the point.

In the present analysis, we obtain an estimate of the microlayer thickness during the collapse of a bubble from the known solution [8] to the boundary layer equations for a constant point sink on a plane. That is to say, we simulate a bubble of time-varying radius R(t) by a point sink of liquid on a rigid plane in a semi-infinite liquid (see Fig. 1.1). The strength of the sink is taken to be $m = -R^2\dot{R}$ (i.e., $m_s = -m$). An estimate of the microlayer thickness during the growth of the bubble could not be obtained in a corresponding way because of analytical difficulties in obtaining the boundary layer solution for a point source on a plane. In fact, such a solution does not even exist. An attempt to obtain a solution by the usual similarity variable method leads to physically meaningless results [6, 7]. A steady state boundary layer solution for a constant point sink is, however, available [8] and a calculation of the boundary layer thickness is used to give an estimate of the microlayer thickness for a collapsing bubble.

1.2 Boundary Layer Solution for a Point Sink on a Plane

The boundary layer solution for a constant point sink given by Rosenhead [8] is presented in the present study with a more detailed derivation. The analysis is based on the general class of axisymmetric solutions by Mangler [9] and Geis [10]. With the boundary layer approximation, the momentum equation for incompressible, axisymmetric flow near a plane is given by

$$u \frac{\partial u}{\partial r} + w \frac{\partial u}{\partial z} = - \frac{1}{\rho} \frac{\partial p}{\partial r} + \nu \frac{\partial^2 u}{\partial z^2} \quad , \tag{1.3}$$

where u is the radial velocity along the plane, w is the velocity normal to the plane, r is the spherical distance from the origin, z is the distance normal to the plane, ν is the kinematic viscosity, p is the pressure and ρ is the density. The continuity equation in these coordinates is

$$\frac{\partial}{\partial r} (ru) + \frac{\partial}{\partial z} (rw) = 0 \quad . \tag{1.4}$$

This set of equations is valid within the boundary layer provided the usual assumption of the boundary layer being thin is valid.

The potential flow outside the boundary layer is given in terms of the free-field velocity U as

$$U(r) = - \frac{m}{r^2} \quad , \tag{1.5}$$

where the source strength is taken to be $m_s = - m = R^2 \dot{R}$ (i.e., the

strength of the sink is $m = -R^2\dot{R} > 0$). From the exact momentum equation for inviscid flow, we obtain the pressure term

$$-\frac{1}{\rho}\frac{\partial p}{\partial r} = U\frac{dU}{dr} = -\frac{2m^2}{r^5} \quad . \tag{1.6}$$

In the boundary layer approximation it is assumed that (1.6) describes the pressure distribution within the viscous layer as well as outside it. As a result, equation (1.3) becomes

$$u\frac{\partial u}{\partial r} + w\frac{\partial u}{\partial z} = -\frac{2m^2}{r^5} + \nu\frac{\partial^2 u}{\partial z^2} \quad . \tag{1.7}$$

For the set of equations (1.7) and (1.4) it is found that

$$\eta = z\left(\frac{m}{2\nu r^3}\right)^{\frac{1}{2}} , \qquad m = -R^2\dot{R} > 0 \quad , \tag{1.8}$$

is a suitable similarity variable. We now assume that the radial velocity u within the viscous layer can be expressed as

$$u = U(r)f'(\eta) = -\frac{m}{r^2}f'(\eta) \quad , \tag{1.9}$$

where f is an undetermined function of η. In order to satisfy the continuity equation (1.4), we require

$$w = \left(\frac{m\nu}{2r^3}\right)^{\frac{1}{2}}[f - 3\eta f'] \quad . \tag{1.10}$$

Upon the substitution of (1.9) and (1.10) into (1.7), we obtain

$$f''' - ff'' + 4(1 - f'^2) = 0 \quad , \tag{1.11}$$

which is a special case of the Falkner-Skan equation. The no-slip and the zero normal velocity conditions require that

$$f(0) = f'(0) = 0 \quad , \tag{1.12}$$

and in order that $u \to U$ away from the plane, f has to satisfy the requirement

$$f'(\eta) \to 1 \qquad \text{as} \qquad \eta \to \infty \quad . \tag{1.13}$$

A numerical solution to this set of equations (1.11-1.13) is available [8], and it can be used to obtain the flow velocity at any point. A similar analysis for a point source is carried out in Section 1.4, but it does not lead to a physically meaningful solution.

1.3 Microlayer Thickness

If the boundary layer thickness is defined as the distance in which the flow velocity has attained 99% of the potential flow velocity, then from (1.9) it follows that

$$f'(\eta) < 0.99 \quad . \tag{1.14}$$

From the numerical solution of (1.11-1.13) we find that (1.14) requires that

$$z\left(\frac{m}{2\nu r^3}\right)^{\frac{1}{2}} = \eta \lesssim 2 \quad . \tag{1.15}$$

Therefore, the boundary layer is the region

$$0 < z \lesssim 2\left(\frac{2\nu r^3}{m}\right)^{\frac{1}{2}} \quad , \tag{1.16}$$

and hence the boundary layer thickness is given by

$$\delta \simeq 2\left(\frac{2\nu r^3}{m}\right)^{\frac{1}{2}} \quad . \tag{1.17}$$

There is, of course, some arbitrariness in the determination of the boundary layer thickness. If the thickness is defined as $f'(\eta) = 0.999$, then one finds $\delta \simeq 3(2\nu r^3/m)^{\frac{1}{2}}$; and if one takes $f'(\eta) = 0.95$ one finds $\delta \simeq 0.9(2\nu r^3/m)^{\frac{1}{2}}$.

An estimate of the microlayer thickness δ_o can be obtained if we find a suitable expression for m and then interpret δ as δ_o. The expression for m must be consistent with the assumption that it be a constant and it should fit the experimental data for $R(t)$.

The above results are valid only for the collapse of the bubble, and we take $t = 0$ as the time when the bubble radius $R(t)$ is a maximum R_o, i.e.,

$$R(0) = R_o \quad . \tag{1.18}$$

If t_o is taken as the total bubble lifetime, then we require

$$R(\tfrac{1}{2} t_o) = 0 \quad . \tag{1.19}$$

In addition, $R(t)$ must satisfy

$$R^2 \dot{R} = -m \quad , \tag{1.20}$$

where m is taken to be a constant. Simple integration of (1.20), subject to the conditions (1.18) and (1.19), yields

$$R(t) = R_o (1 - \frac{2t}{t_o})^{\frac{1}{3}} \quad , \tag{1.21}$$

and

$$m = \frac{2}{3} \frac{R_o^3}{t_o} \quad , \tag{1.22}$$

which upon substitution into (1.17) gives the microlayer thickness as

$$\delta_o \simeq 2(3\nu t_o)^{\frac{1}{2}} (\frac{r}{R_o})^{3/2} \quad . \tag{1.23}$$

This expression may be averaged over the region beneath the bubble to give

$$< \delta_o > \simeq \frac{8}{7} (3\nu t_o)^{\frac{1}{2}} \quad , \tag{1.24}$$

where $< \delta_o >$ is the average value of δ_o.

In the next section we discuss the problem of the point source and show the difficulties we encounter in an attempt to obtain a boundary layer solution.

1.4 Point Source on a Plane

For a point source we take the free-field velocity as

$$U(r) = \frac{m_s}{r^2} , \qquad m_s = R^2\dot{R} > 0 , \tag{1.25}$$

and the pressure term for inviscid flow is

$$-\frac{1}{\rho}\frac{\partial p}{\partial r} = U\frac{dU}{dr} = -\frac{2m_s^2}{r^5} . \tag{1.26}$$

If we use this term as an approximation in the momentum equation (1.3), we obtain

$$u\frac{\partial u}{\partial r} + w\frac{\partial u}{\partial z} = -\frac{2m_s^2}{r^5} + \nu\frac{\partial^2 u}{\partial z^2} . \tag{1.27}$$

For the set of equations (1.4) and (1.27) we find

$$\eta = z\left(\frac{m_s}{2\nu r^3}\right)^{\frac{1}{2}} , \qquad m_s = R^2\dot{R} > 0, \tag{1.28}$$

to be a suitable similarity variable. By letting

$$u = U(r)f'(\eta) = \frac{m_s}{r^2} f'(\eta) , \tag{1.29}$$

and

$$w = \left(\frac{m_s\nu}{2r^3}\right)^{\frac{1}{2}}[-f + 3\eta f'] , \tag{1.30}$$

we satisfy the continuity equation (1.4). Upon the substitution of (1.29) and (1.30) into (1.27) we obtain

$$f''' + ff'' - 4(1 - f'^2) = 0 , \tag{1.31}$$

which is a special case of

$$f''' + ff'' + \beta(1 - f'^2) = 0 \ . \tag{1.32}$$

The no-slip and the zero normal velocity conditions require that

$$f(0) = f'(0) = 0 \ , \tag{1.33}$$

and in order that $u \to U$ away from the plane, f must satisfy the requirement

$$f'(\eta) \to 1 \quad \text{as} \quad \eta \to \infty \ . \tag{1.34}$$

For this set of equations (1.32-1.34), it was shown by Hartree [6] that the solution is not unique for $\beta_o < \beta < 0$, where $\beta_o = -0.1988$. We encounter the nonuniqueness because the condition (1.34) at ∞ is satisfied, regardless of the choice of the integration constants. Two of the integration constants are fixed by (1.33) but one remains free and therefore, the solution is not unique. It was later shown by Stewartson [7] that for $\beta < \beta_o$ ($\beta = -4$, in the present case), any solution satisfying (1.32-1.34) has $f' > 1$ for some values of $\eta > 1$. In view of (1.29), this would mean that the radial velocity would increase from a value zero at the plane to a value greater than m_s/r^2 within the viscous layer and then approach the potential flow from above. Such behavior is unrealistic and is rejected as being physically unacceptable.

1.5 Discussion

The information about the boundary layer thickness just described can be used to estimate the heat transfer rate due to evaporation from the microlayer. A question arises concerning the accuracy of the description of the collapse motion which is determined by taking m to be a constant. In Fig. 1.2, $R(t)/R_o$ from (1.21), which is a direct result of this assumption, is shown as a function of t/t_o together with the data from measurements by Gunther and Kreith [11] and by Gunther [12]; also plotted on the same graph are the best fits of these data. The assumption that m is a constant is seen to be fairly good for $0 < t \lesssim \frac{1}{4}t_o$, but is less accurate as $t \to \frac{1}{2}t_o$. We should also remark that the bubble velocity at the maximum radius for fixed m is not zero while for the growing and collapsing bubble $\dot{R} = 0$, at the maximum radius. The results given by (1.23) and (1.24) cannot be compared with any available experimental data because none of these deal with collapsing bubbles of nucleate boiling.

A valid solution for a time varying m would be of considerable value but it appears to be exceedingly difficult to obtain analytically. For a constant point source a solution of the boundary layer type does not exist and it appears that the exact solution is quite complicated. Presumably, the difficulty in the potential solution for a point source arises from the regions of reverse flows so that one does not have a monopole potential flow. The existence of such reverse flows can be inferred from the exact solutions of the Navier-Stokes equations for the viscous flows from a line source in a two-dimensional channel [13-15] (see Fig. 1.3).

The analytical model presented here for the microlayer thickness has a significant advantage of simplicity. It also gives some useful information regarding the variation of the microlayer thickness along the solid boundary.

REFERENCES

[1] Plesset, M. S., and Prosperetti, A., "The Contribution of Latent Heat Transport in Subcooled Nucleate Boiling", International Journal of Heat and Mass Transfer 21, 725-734 (1978).

[2] Cooper, M. G., and Lloyd, A. J., "The Microlayer Thickness in Nucleate Boiling", International Journal of Heat and Mass Transfer 12, 895-913 (1969).

[3] Olander, R. R., and Watts, R. G., "An Analytical Expression for the Microlayer Thickness in Nucleate Boiling", Journal of Heat Transfer 91, 178-180 (1969).

[4] Jawurek, H. H., "Simultaneous Determination of Microlayer Geometry and Bubble Growth in Nucleate Boiling", International Journal of Heat and Mass Transfer 12, 843-848 (1969).

[5] Voutsinos, C. M., and Judd, R. L., "Laser Interferometric Investigation of the Microlayer Evaporation Phenomenon", Journal of Heat Transfer 97, 88-92 (1975).

[6] Hartree, D. R., "On an Equation Occurring in Falkner and Skan's Approximate Equations of the Boundary Layer", Proceedings of the Cambridge Philosophical Society 33, 223-239 (1937).

[7] Stewartson, K., "Further Solutions of the Falkner-Skan Equation", Proceedings of the Cambridge Philosophical Society 50, 454-465 (1954).

[8] Rosenhead, L., (Ed.), Laminar Boundary Layers , Oxford (1963).

[9] Mangler, W., "Boundary Layers on Bodies of Revolution in Symmetrical Flow", Ber. aerodyn. VersAnst. Göttingen 45/A/17 (1945).

[10] Geis, T., "Ähnliche Grenzschichten an Rotationskörpern", 50 Jahre Grenzschichtforschung (Editors: Görtler, H., and Tollmien, W.), Vieweg, Braunschweig, 294-303 (1955).

[11] Gunther, F. C., and Kreith, F., "Photographic Study of Bubble Formation in Heat Transfer to Subcooled Water", Progress Report No. 4-120, Jet Propulsion Laboratory, Pasadena (1950).

[12] Gunther, F. C., "Photographic Study of Surface-Boiling Heat Transfer to Water with Forced Convection", Journal of Applied Mechanics 18, 115-123 (1951).

[13] Jeffery, G., "The Two-Dimensional Steady Motion of a Viscous Fluid", Philosophy Magazine (6) 29, 455-465 (1915).

[14] Hamel, G., "Spiralförminge Bewegungen zäher Flussigkeiten", Jber. dtsch. MatVer 25, 34-60 (1917).

[15] Rosenhead, L., "The Steady Two-Dimensional Radial Flow of Viscous Fluid Between Two Inclined Plane Walls", Proceedings of the Royal Society A 175, 436-467 (1940).

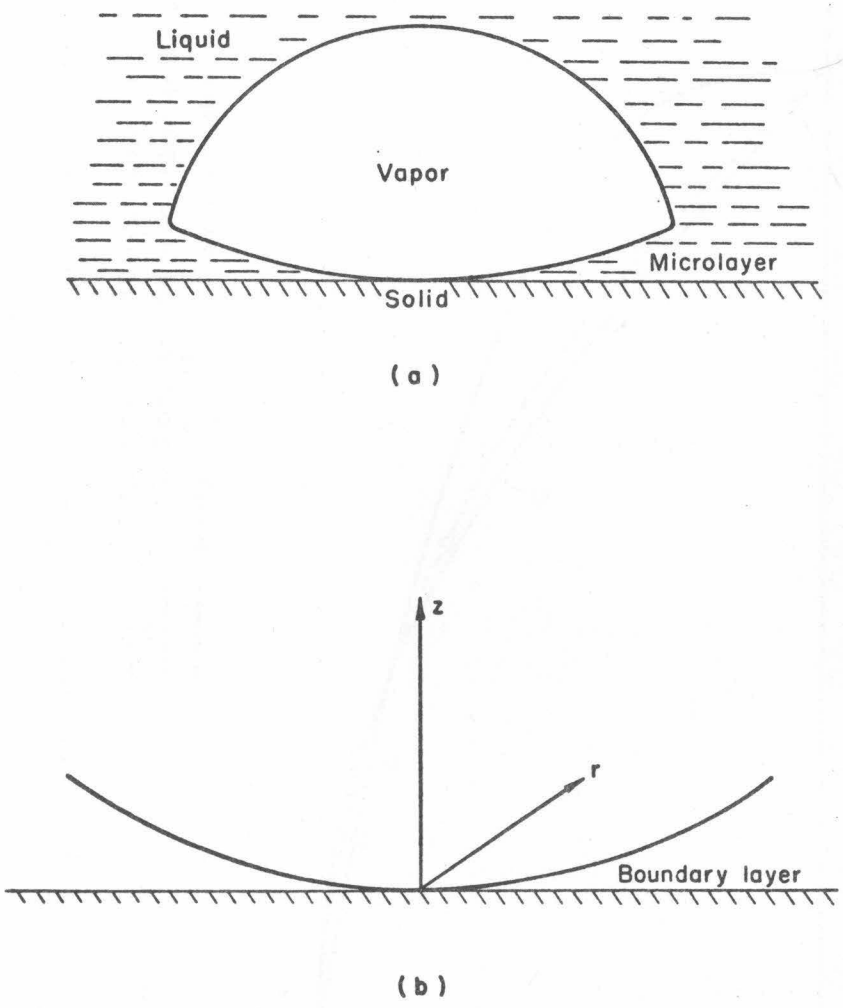

Fig. 1.1. (a) A diagrammatic representation of a typical nucleate boiling vapor bubble with a viscous microlayer.

(b) Mathematical model (point source or sink).

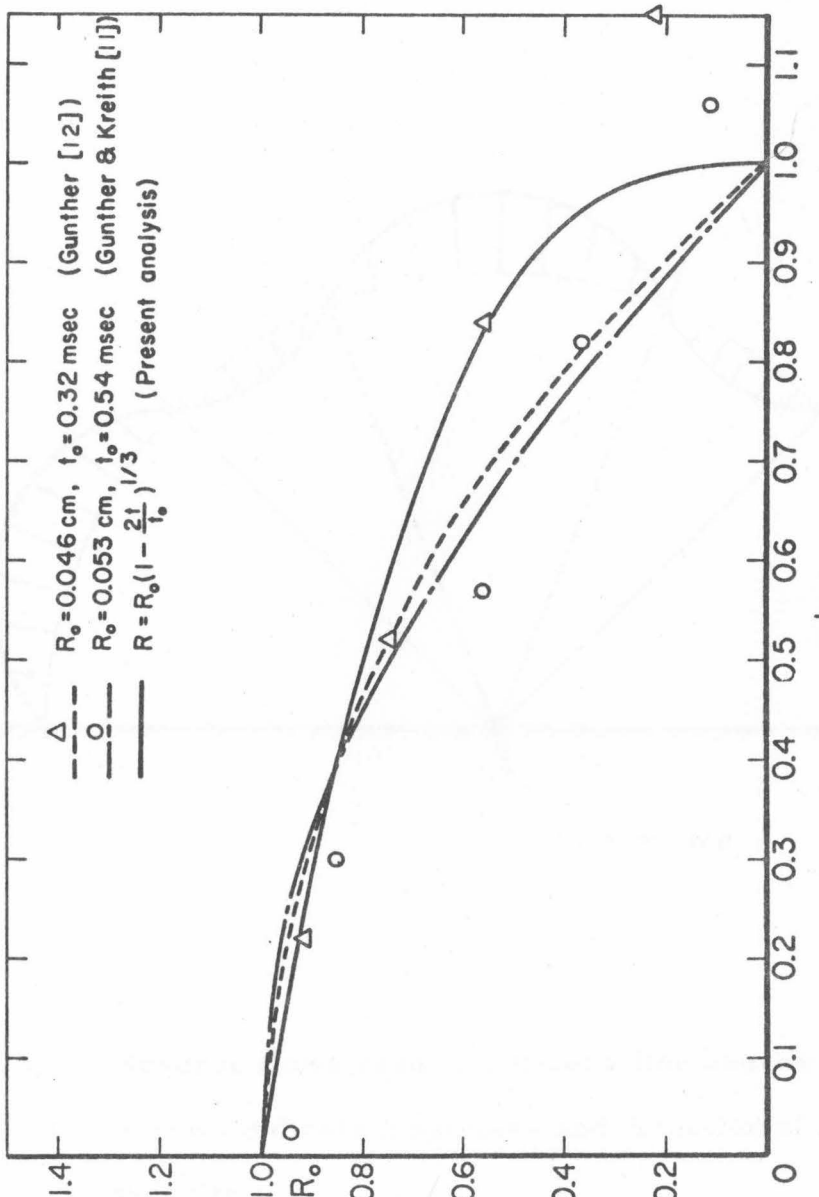

Fig. 1.2. A comparison of R(t) obtained by assuming constant m with experiment data and their best fits.

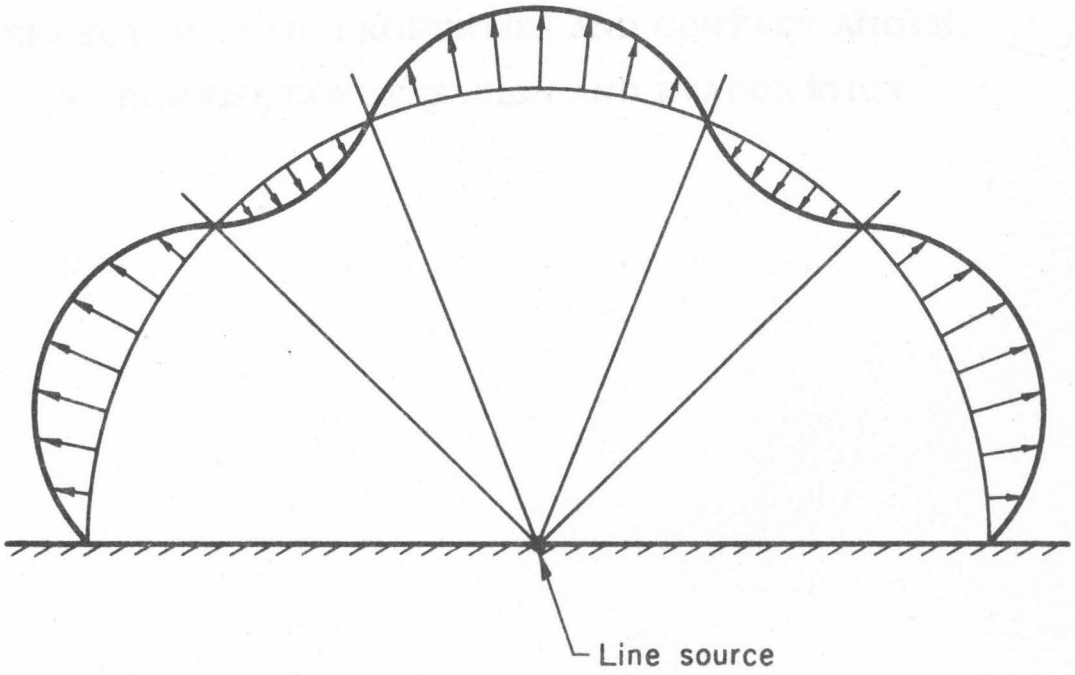

Fig. 1.3. Reverse flows resulting from a line source on a plane; arrows indicate magnitude and direction of the fluid velocity.

PART 2

EFFECT OF SOLID PROPERTIES AND CONTACT ANGLE IN DROPWISE CONDENSATION AND EVAPORATION

Nomenclature

$Bi = h\rho/k_1$	=	Biot number
D_1	=	spatial region of droplet
D_2	=	spatial region of semi-infinite solid
∂D_{12}	=	solid-liquid interface
∂D_{1v}	=	liquid-vapor interface
∂D_{2v}	=	solid-vapor interface
$f(\tau)$	=	correction factor
$g(\theta, Bi)$	=	correction function
h	=	heat-transfer coefficient
k_1	=	thermal conductivity of liquid
k_2	=	thermal conductivity of solid
Nu	=	$Q/[k_1\rho \lvert T_o - T_v \rvert]$ = Nusselt number
$p^e(T)$	=	equilibrium vapor pressure at temperature T
$P_{-\frac{1}{2}+i\tau}(x)$	=	Legendre function of complex degree, $-\frac{1}{2}+i\tau$
q	=	heat flux
Q	=	overall heat flow
R	=	universal gas constant/molecular weight of vapor
T_1^*	=	temperature distribution in liquid
T_2^*	=	temperature distribution in solid
T_{if}^*	=	temperature distribution of solid-liquid interface

T_c^* = temperature at center of solid-liquid interface

T_v = vapor temperature

T_o = temperature at large distance into solid

T_1 = $(T_1^* - T_o)/(T_v - T_o)$ = dimensionless temperature distribution in liquid

T_2 = $(T_2^* - T_o)/(T_v - T_o)$ = dimensionless temperature distribution in solid

T_{if} = $(T_{if}^* - T_o)/(T_v - T_o)$ = dimensionless temperature distribution of solid-liquid interface

T_c = $(T_c^* - T_o)/T_v - T_o)$ = dimensionless temperature of center of solid-liquid interface

t = time

t_o = lifetime of an evaporating droplet

V = volume of droplet

α = spatial coordinate

β = spatial coordinate

β_o = $\theta + \pi$

γ = accommodation coefficient

ϵ = k_1/k_2

θ = contact angle

λ	=	latent heat of vaporization
ρ	=	base radius of droplet
ρ_o	=	initial radius of evaporating droplet
ρ_ℓ	=	density of liquid
$\rho^e(T)$	=	equilibrium vapor density at temperature T

2.1 Introduction

In view of the large heat fluxes observed in dropwise condensation, this subject has received a considerable amount of attention. Although the analysis and the physical fundamentals of the reverse process, dropwise evaporation, are similar in many respects, most of the effort has been concentrated on the condensation problem. Due to the complexity of these heat-and-mass transfer processes, an exact analysis is virtually impracticable. However, several models have been proposed to approximate the condensation process but oversimplifications invalidate some of these. For example, Fatica and Katz [1], Sugawara and Michiyoshi [2], and Nijaguna [3] have considered steady heat conduction in a single droplet with a discontinuity in the temperature along the edge. The discrepancy due to this discontinuity was recognized by Ahrendts [4], Hurst and Olson [5] and Umur and Griffith [6] and it was later shown [7] that such a model is inadmissible because it predicts an infinite amount of heat flow across the droplet. Other models [4, 6, 7] are incomplete in the sense that the condenser material properties could not be considered and their validity is, therefore, restricted to cases in which the thermal resistance between the droplet and the vapor is dominant. However, there has been some interest in understanding the effect of the condenser material properties, and in one of the first analyses Mikic [8] suggested that the effect was due to large droplets behaving as inactive areas constricting the heat flow. Recently, this idea was further pursued by Hannemann and Mikic [9] with some modifications of the original model. Earlier, Hurst and

Olson [5] considered the condenser material properties by numerically solving the heat equation for a hemispherical droplet on a flat-disk shaped condenser.

In the present study both evaporation and condensation of droplets are analyzed and the effect of the condenser (evaporator) material is dealt with by solving the steady heat-conduction equation for a geometry consisting of a droplet in the form of a spherical segment on a semi-infinite solid (see Fig. 2.1). This model assumes that the influence on a droplet due to surrounding droplets is negligible. The results of this analysis show that for a liquid like water condensing on (evaporating from) a metallic solid the temperature within the solid approaches the far-field value rapidly with distance from the edge of the droplet. Therefore, it is quite reasonable to assume that the range of influence of a droplet is restricted to a distance which is of the order of the droplet size and droplets so distributed may be regarded as isolated. However, a large droplet near several very small ones has a strong influence on them, and the present analysis is not valid for such cases. The model also restricts the validity of the results to systems having condensers (evaporators) more than a few droplet radii thick. Thin solid sheets such as foils are excluded. For the droplets of interest (less than 1 mm diameter) the assumed droplet shape is quite reasonable because the effect of gravity is much weaker than that of surface tension. Also for such droplets the viscous forces dominate over gravity, and free convection can be neglected (the Grashof number is less than 10 for water). One need not consider the transient effects in the heat conduction because the condensation or evaporation appears to be much slower than diffusion.

That is, the time it takes for the droplet size to change by an amount comparable with the original size is much longer than the time it takes for the latent heat to diffuse into or out of the droplet. In solving the steady condensation problem, the transfer of latent heat into the liquid droplet due to the vapor flow is approximated by a mixed boundary condition involving a heat-transfer coefficient, h, which is calculated by using Plesset's formula [10, 11] for vapor flow onto a liquid sphere. By using such a boundary condition we match the heat fluxes on each side of the liquid-vapor interface. The vapor with a far-field temperature T_v deposits a heat flux $h(T_v - T_s)$ onto the cooler liquid surface having a temperature distribution T_s. This flux is equated with the heat flux conducted into the droplet. For an evaporating droplet, it follows from Plesset's results [10] that the temperature of the liquid-vapor interface can be taken equal to the far-field vapor temperature T_v. The solid-vapor interface for both cases is taken to be insulated because the thermal conductivity of the vapor is much smaller than that of the solid. This condition is not only realistic but also necessary to obtain a nontrivial bounded solution for the temperature. Along the solid-liquid interface perfect thermal contact is assumed and therefore the temperature and the heat flux are required to be continuous. At large distances into the solid the temperature is taken to be a constant, T_o. For this model, exact solutions are found for an evaporating droplet ($T_o > T_v$). For the case of a condensing droplet ($T_o < T_v$) exact solutions are found for some special values of h and approximate solutions for other values of h. These solutions are then used to obtain expressions for the overall heat flow Q across the droplet, the rate of change of the droplet size, and the lifetime for an evaporating droplet.

2.2 Mathematical Formulation

For the model described in Section 2.1, the temperature distribution is given by

$$\nabla^2 T_j^* = 0, \qquad \text{in } D_j, \quad j = 1, 2, \tag{2.1}$$

where T_1^* and T_2^* are the temperature distributions in the droplet and the solid respectively, and D_1 and D_2 are the corresponding spatial regions. The boundary conditions discussed may be stated as

$$-k_1 \frac{\partial T_1^*}{\partial n} = h[T_1^* - T_v], \qquad \text{for } T_o < T_v; \quad \text{on } \partial D_{1v}, \tag{2.2}$$

or

$$T_1^* = T_v, \qquad \text{for } T_v < T_o; \quad \text{on } \partial D_{1v}, \tag{2.2'}$$

$$T_1^* = T_2^*, \qquad \text{on } \partial D_{21}, \tag{2.3}$$

$$k_1 \frac{\partial T_1^*}{\partial n} = k_2 \frac{\partial T_2^*}{\partial n}, \qquad \text{on } \partial D_{21}, \tag{2.4}$$

$$\frac{\partial T_2^*}{\partial n} = 0, \qquad \text{on } \partial D_{2v}, \tag{2.5}$$

and, at a large distance into the solid,

$$T_2^* = T_o, \tag{2.6}$$

where $\partial/\partial n$ is the outward normal derivative, ∂D_{1v} is the liquid-vapor interface, ∂D_{21} is the solid-liquid interface, ∂D_{2v} is the

solid-vapor interface, k_1 and k_2 are the thermal conductivities of the liquid and the solid, respectively; h is the liquid-vapor heat-transfer coefficient, T_v is the vapor temperature and T_o is the temperature of the solid at large distances from the droplet. To satisfy this set of equations (2.1-2.6) one resorts to a toroidal coordinate system involving the transformation [12]

$$z + ir = i\rho \coth\left[\tfrac{1}{2}(\alpha + i\beta)\right] , \tag{2.7}$$

where z and r are the coordinates for cylindrical geometry, ρ is the droplet radius, and α and β are the transformed coordinates (see Fig. 2.2). With this coordinate system, for axial symmetry, one finds that equation (2.1) becomes

$$\frac{\partial}{\partial\alpha}\left[\frac{\sinh\alpha}{\cosh\alpha - \cos\beta}\,\frac{\partial T_j}{\partial\alpha}\right] + \frac{\partial}{\partial\beta}\left[\frac{\sinh\alpha}{\cosh\alpha - \cos\beta}\,\frac{\partial T_j}{\partial\beta}\right] = 0 ,$$

$$0 \le \alpha < \infty,\ j = 1,2; \quad \pi \le \beta < \beta_o,\ j = 1; \quad 0 < \beta \le \pi,\ j = 2, \tag{2.8}$$

where $T_j = (T_j^* - T_o)/(T_v - T_o)$. The variables cannot be separated directly for this equation. However, by making the transformation [12],

$$T_j = (2\cosh\alpha - 2\cos\beta)^{\frac{1}{2}} v_j , \qquad j = 1,2, \tag{2.9}$$

and by substitution into (2.8), one finds that the equation for v_j,

$$\frac{\partial^2 v_j}{\partial \alpha^2} + \frac{\partial^2 v_j}{\partial \beta^2} + \coth \alpha \frac{\partial v_j}{\partial \alpha} + \frac{1}{4} v_j = 0 ,$$

$$0 \leq \alpha < \infty, \; j = 1, 2; \quad \pi \leq \beta < \beta_o, \; j = 1; \quad 0 < \beta \leq \pi, \; j = 2 ,$$

(2.10)

can be separated. The boundary conditions (2.2-2.6) transform into

$$(1 + \frac{\sin\beta_o}{2Bi}) v_1 + \frac{1}{2Bi} (2 \cosh \alpha - 2 \cos \beta_o) \frac{\partial v_1}{\partial \beta}$$

$$= \frac{1}{(2 \cosh \alpha - 2 \cos \beta_o)^{\frac{1}{2}}}, \qquad \text{for } T_o < T_v; \; \beta = \beta_o; \; 0 \leq \alpha < \infty,$$

(2.11)

or

$$v_1 = \frac{1}{(2 \cosh \alpha - 2 \cos \beta_o)^{\frac{1}{2}}}, \qquad \text{for } T_v < T_o; \; \beta = \beta_o; \; 0 \leq \alpha < \infty,$$

(2.11')

$$v_1 = v_2 , \qquad \beta = \pi; \; 0 \leq \alpha < \infty , \tag{2.12}$$

$$\epsilon \frac{\partial v_1}{\partial \beta} = \frac{\partial v_2}{\partial \beta} , \qquad \beta = \pi; \; 0 \leq \alpha < \infty , \tag{2.13}$$

$$\frac{\partial v_2}{\partial \beta} = 0 , \qquad \beta = 0; \; 0 \leq \alpha < \infty , \tag{2.14}$$

and

$$v_2 < \infty , \qquad \alpha, \beta \to 0 , \tag{2.15}$$

where $\epsilon = k_1/k_2$, and $Bi = h\rho/k_1$ is the Biot number. In the coordinate system used, $\beta = \beta_o$ corresponds to the liquid-vapor interface, $\beta = \pi$ to the solid-liquid interface, and $\beta = 0$ to the solid-vapor

interface (see Fig. 2.2). At large distances from the droplet $\alpha, \beta \to 0$ and therefore, equation (2.6) is satisfied because the factor $(2\cosh\alpha - 2\cos 2\beta)^{\frac{1}{2}}$ in (2.9) goes to zero.

Since all the boundary conditions are specified at constant values of β, we require a solution involving oscillatory functions in α. A general solution of this type for equation (2.10) is [12]

$$v_j = \int_0^\infty [A_j(\tau)\cosh\beta\tau + B_j(\tau)\sinh\beta\tau] P_{-\frac{1}{2}+i\tau}(\cosh\alpha)d\tau\,, \qquad j = 1, 2, \tag{2.16}$$

where $A_j(\tau)$ and $B_j(\tau)$ are function of τ depending on the boundary conditions, and $P_{-\frac{1}{2}+i\tau}(\cosh\alpha)$ is the Legendre function of complex degree, $-\frac{1}{2} + i\tau$. By choosing v_1 and v_2 to be the following special forms:

$$v_1 = \int_0^\infty \frac{\Phi(\tau)\sinh(\beta_o-\beta)\tau + \Psi(\tau)\sinh(\beta-\pi)\tau}{\sinh(\beta_o-\pi)\tau} P_{-\frac{1}{2}+i\tau}(\cosh\alpha)d\tau\,, \tag{2.17}$$

and

$$v_2 = \int_0^\infty \frac{\Phi(\tau)\cosh\beta\tau}{\cosh\pi\tau} P_{-\frac{1}{2}+i\tau}(\cosh\alpha)d\tau\,, \tag{2.18}$$

the boundary conditions (2.12), (2.14) and (2.15) are satisfied. Upon satisfying (2.13) we find that

$$\Psi(\tau) = \Phi(\tau)\left[\frac{1}{\epsilon}\tanh\pi\tau\,\sinh(\beta_o-\pi)\tau + \cosh(\beta_o-\pi)\tau\right]. \tag{2.19}$$

In order to obtain $\Psi(\tau)$ [and hence, $\Phi(\tau)$] we need to satisfy (2.11) or (2.11') as the case may be. In the next section we deal with an evaporating droplet in which case we satisfy (2.11') exactly.

2.3 An Exact Solution for an Evaporating Droplet

Equation (2.11') can be easily satisfied by expanding its right side, $(2\cosh\alpha - 2\cos\beta_o)^{-\frac{1}{2}}$, in the integral form [12],

$$\frac{1}{(2\cosh\alpha - 2\cos\beta_o)^{\frac{1}{2}}} = \int_o^\infty \frac{\cosh(\beta_o - \pi)\tau}{\cosh\pi\tau} P_{-\frac{1}{2}+i\tau}(\cosh\alpha)d\tau \,. \tag{2.20}$$

Upon the substitution of (2.17) and (2.20) into (2.11'), we obtain

$$\int_o^\infty \Psi(\tau)P_{-\frac{1}{2}+i\tau}(\cosh\alpha)d\tau = \int_o^\infty \frac{\cosh(\beta_o - \pi)\tau}{\cosh\pi\tau} P_{-\frac{1}{2}+i\tau}(\cosh\alpha)d\tau \,. \tag{2.21}$$

This equation may be inverted by making use of the fact that an arbitrary function $g(\alpha)$, subject to the condition that $\int_o^\infty \alpha\,|g(\alpha)|\,d\alpha < \infty$, may be expanded as

$$g(\alpha) = \int_o^\infty G(\tau)P_{-\frac{1}{2}+i\tau}(\cosh\alpha)d\tau \,, \tag{2.22}$$

where G is given by the Mehler-Fock transform [12],

$$G(\eta) = \eta\tanh\pi\eta\int_o^\infty g(\alpha)P_{-\frac{1}{2}+i\eta}(\cosh\alpha)\sinh\alpha\,d\alpha \,, \tag{2.23}$$

of $g(\alpha)$. These relations clearly imply the orthogonality of the transform in the Dirac delta sense, i.e.,

$$\delta(\eta-\tau) = \eta\tanh\pi\eta\int_o^\infty P_{-\frac{1}{2}+i\tau}(\cosh\alpha)P_{-\frac{1}{2}+i\eta}(\cosh\alpha)\sinh\alpha d\alpha \,. \tag{2.24}$$

Therefore, based on this orthogonality property, we obtain from (2.21)

$$\Psi(\tau) = \frac{\cosh(\beta_o - \pi)\tau}{\cosh \pi\tau} \quad . \tag{2.25}$$

From (2.19) it follows that

$$\Phi(\tau) = \frac{\epsilon}{[\tanh \pi\tau \tanh(\beta_o - \pi)\tau + \epsilon]\cosh \pi\tau} \quad . \tag{2.26}$$

The heat flux, $q(\alpha)$, across the solid-liquid interface may be written as

$$q(\alpha) = -k_2 \left(\frac{\cosh \alpha - \cos \pi}{\rho}\right) \left.\frac{\partial T_2^*}{\partial \beta}\right|_{\beta=\pi}$$

$$= \frac{k_2}{2\rho} (T_o - T_v)(2 \cosh \alpha - 2 \cos \pi) \int_o^\infty \tau \tanh \pi\tau \, \Phi(\tau) P_{-\frac{1}{2}+i\tau}(\cosh \alpha) d\tau. \tag{2.27}$$

The overall heat flow, Q, is obtained by integrating $q(\alpha)$ over the solid-liquid interface as follows:

$$Q = \int_o^\infty 2\pi \left(\frac{\rho}{2 \cosh \alpha - 2 \cos \pi}\right)^2 q(\alpha) \sinh \alpha d\alpha$$

$$= \frac{4\pi k_1 \rho (T_o - T_v)}{\epsilon} \int_o^\infty \frac{\sinh \alpha d\alpha}{(2\cosh\alpha - 2\cos\pi)^{\frac{1}{2}}} \left[\int_o^\infty \tau \tanh \pi\tau \, \Phi(\tau) P_{-\frac{1}{2}+i\tau}(\cosh\alpha) d\tau\right]. \tag{2.28}$$

By letting $\beta_o = \pi$ in (2.20) we may represent $(2 \cosh \alpha - 2 \cos \pi)^{-\frac{1}{2}}$ as an integral. Upon doing so in (2.28) we find that

$$Q = \frac{4\pi k_1 \rho (T_o - T_v)}{\epsilon} \int_o^\infty \sinh\alpha d\alpha \left[\int_o^\infty \frac{1}{\cosh \pi\eta} P_{-\frac{1}{2} + i\eta}(\cosh\alpha) d\eta \right]$$

$$\times \left[\int_o^\infty \tau \tanh \pi\tau \, \Phi(\tau) P_{-\frac{1}{2} + i\tau}(\cosh \alpha) d\tau \right] , \qquad (2.29)$$

which, upon making use of the orthogonality relation (2.24), becomes

$$Q = \frac{4\pi k_1 \rho (T_o - T_v)}{\epsilon} \int_o^\infty \frac{\Phi(\tau)}{\cosh \pi\tau} \, d\tau = 4\pi k_1 \rho (T_o - T_v) \int_o^\infty \frac{\operatorname{sech}^2 \pi\tau}{[\tanh \pi\tau \tanh \theta\tau + \epsilon]} , \qquad (2.30)$$

where $\theta = (\beta_o - \pi)$ is the contact angle. This result may be written in the dimensionless form

$$Nu = 4\pi \int_o^\infty \frac{\operatorname{sech}^2 \pi\tau \, d\tau}{[\tanh \pi\tau \tanh \theta\tau + \epsilon]} , \qquad (2.31)$$

where $Nu = Q/[k_1 \rho (T_o - T_v)]$ is defined as the Nusselt number. It appears that an exact expression for the integral is not known and therefore, it is evaluated numerically and the results are presented in Fig. 2.3.

For most liquids evaporating from metallic solids $\epsilon \sim 0.01$ and for such cases most of the contribution to the integral takes place near $\tau = 0$. It would therefore be a good approximation to replace $\tanh \theta\tau$ in the demoniator by $(\theta/\pi)\tanh \pi\tau$. By the further substitution $x = \tanh \pi\tau$, the integral takes the form

$$Nu \simeq \frac{4\pi}{\theta} \int_o^1 \frac{dx}{[x^2 + \frac{\pi\epsilon}{\theta}]} = 4\left(\frac{\pi}{\theta\epsilon}\right)^{\frac{1}{2}} \tan^{-1}\left[\left(\frac{\theta}{\pi\epsilon}\right)^{\frac{1}{2}}\right] , \qquad 2.32)$$

which for $\theta \gg 0$ can be further approximated as

$$Nu \simeq \frac{2\pi^{3/2}}{(\theta\epsilon)^{\frac{1}{2}}} , \tag{2.33}$$

or

$$Q \simeq \frac{2\pi^{3/2}}{\theta^{\frac{1}{2}}} (k_1 k_2)^{\frac{1}{2}} \rho(T_o - T_v) . \tag{2.34}$$

Equation (2.32) is exact for $\theta = 0$ and $\theta = \pi$, and agrees with (2.31) to within 20% for other contact angles when $\epsilon \leq 0.01$.

The solid-liquid interface temperature distribution T_{if}^* can be obtained from (2.17) or (2.18) as

$$T_{if} = \frac{T_o - T_{if}^*}{T_o - T_v} = (2\cosh\alpha + 2)^{\frac{1}{2}} \int_o^\infty \frac{\epsilon \operatorname{sech} \pi\tau}{[\tanh \pi\tau \tanh \theta\tau + \epsilon]} P_{-\frac{1}{2}+i\tau}(\cosh\alpha) d\tau . \tag{2.35}$$

For the special case of a hemispherical droplet, this expression becomes

$$T_{if} = 2\left(\frac{\epsilon}{1+\epsilon}\right)\cosh^{\frac{1}{2}}\alpha \int_o^\infty \frac{P_{-\frac{1}{2}+i\tau}(\cosh\alpha) d\tau}{[\cosh \pi\tau - \frac{1}{1+\epsilon}]} . \tag{2.36}$$

By using the integral representation for $\alpha > 0$ in (2.36)

$$P_{-\frac{1}{2}+i\tau}(\cosh\alpha) = \frac{2}{\pi} \int_o^\alpha \frac{\cos \tau\phi}{(2\cosh\alpha - 2\cosh\phi)^{\frac{1}{2}}} d\phi \tag{2.37}$$

and integrating with respect to τ, we find that the expression for T_{if} reduces to

$$T_{if} = \frac{4}{\pi} \frac{\epsilon}{(2\epsilon + \epsilon^2)^{\frac{1}{2}}} \cosh \tfrac{1}{2}\alpha \int_0^{\alpha} \frac{\sinh\left\{\left[1 - \frac{1}{\pi}\cos^{-1}\left(\frac{1}{1+\epsilon}\right)\right]\phi\right\}}{\sinh\phi\,[2\cosh\alpha - 2\cosh\phi]^{\frac{1}{2}}}\, d\phi. \quad (2.38)$$

The temperature at the edge of the droplet is obtained [by letting $\alpha \to \infty$ in (2.38)] to be T_v. By letting $\alpha \to 0$ in (2.36), the temperature T_c^* at the center of the base is found to be given by

$$T_c = \frac{T_o - T_c^*}{T_o - T_v} = 2\epsilon\left(\frac{1+\epsilon}{2\epsilon + \epsilon^2}\right)^{\frac{1}{2}}\left[1 - \frac{1}{\pi}\cos^{-1}\left(\frac{1}{1+\epsilon}\right)\right], \quad (2.39)$$

which may be approximated as $T_c \simeq (2\epsilon)^{\frac{1}{2}}$. These calculations clearly show that the base temperature varies from a value close to T_o at the center to T_v at the edge and is clearly not uniform.

From the heat flow results, the diminishing rate of the droplet size can be calculated and used to find the time it takes to vanish. The rate of change of volume V is given by [7]

$$\frac{dV}{dt} = \pi\rho^2 \frac{(1 - \cos\theta)^2(2 + \cos\theta)}{\sin^3\theta} \frac{d\rho}{dt} \quad (2.40)$$

and the volume evaporation rate of the liquid in $Q/(\lambda\,\rho_\ell)$, where λ is the latent heat of vaporization and ρ_ℓ is the density of the liquid. Therefore, the rate of change of the droplet base radius is obtained as

$$\frac{d\rho}{dt} = -\frac{k_1(T_o - T_v)Nu}{\rho\lambda\rho_\ell\pi} \frac{\sin^3\theta}{(1 - \cos\theta)^2(2 + \cos\theta)}, \quad (2.41)$$

which upon integration leads to

$$\rho = \rho_o \left[1 - \frac{2k_1(T_o - T_v)Nu}{\pi\lambda\rho_\ell \rho_o^2} \frac{\sin^3\theta}{(1-\cos\theta)^2(2+\cos\theta)} t \right]^{\frac{1}{2}} , \qquad (2.42)$$

where ρ_o is the initial radius. It is not difficult to see that the droplet takes a time

$$t_o = \frac{\pi\lambda\rho_\ell \rho_o^2 (1-\cos\theta)^2(2+\cos\theta)}{2k_1(T_o - T_v)\sin^3\theta \, Nu} , \qquad (2.43)$$

to vanish.

Similar calculations can be carried out for a condensing droplet but it turns out that the expression for Nu is much more complicated and involves the droplet radius ρ. The details are discussed in the next section.

2.4 Approximate Solution for a Condensing Droplet

For a condensing droplet instead of satisfying (2.11') one needs to satisfy (2.11) in order to determine $\Phi(\tau)$ used in equations (2.17 - 2.19). However, an attempt to do so yields a double integral equation for $\Phi(\tau)$ with very complicated kernels. An explicit expression for $\Phi(\tau)$ can only be found for $Bi = \frac{1}{2}\sin\theta$ and $Bi \to \infty$. Therefore, approximate solutions are sought and one such solution can be obtained by finding a suitable function $f(\tau)$ satisfying

$$V_1\Big|_{\beta=\beta_o} = \int_o^\infty \Psi(\tau) P_{-\frac{1}{2}+i\tau}(\cosh\alpha)d\tau$$

$$= (2\cosh\alpha - 2\cos\beta_o)\int_o^\infty \Psi(\tau)f(\tau)P_{-\frac{1}{2}+i\tau}(\cosh\alpha)d\tau \ . \tag{2.44}$$

Substitution of (2.19) and (2.44) into (2.11) leads to

$$\int_o^\infty \Big\{(1+\frac{\sin\beta_o}{2Bi})f(\tau)[\frac{1}{\epsilon}\tanh\pi\tau\sinh(\beta_o-\pi)\tau + \cosh(\beta_o-\pi)\tau] + \frac{1}{2Bi}\tau$$

$$\times [\frac{1}{\epsilon}\tanh\pi\tau + \tanh(\beta_o-\pi)\tau]\cosh(\beta_o-\pi)\tau\Big\}\Phi(\tau)P_{-\frac{1}{2}+i\tau}(\cosh\alpha)d\tau$$

$$= \frac{1}{[2\cosh\alpha - 2\cos\beta_o]^{3/2}} \ , \tag{2.45}$$

where the right side may be written in the integral form

$$\frac{1}{(2\cosh\alpha - 2\cos\beta_o)^{3/2}} = -\frac{1}{\sin\beta_o}\int_o^\infty \frac{\tau \sinh(\beta_o - \pi)\tau}{\cosh \pi\tau} P_{-\frac{1}{2}+i\tau}(\cosh\alpha)d\tau \ . \tag{2.46}$$

By the substitution of this integral representation into (2.45) and by the inversion of the integrals we obtain

$$\Phi(\tau) = \frac{\operatorname{sech} \pi\tau}{(1 - \frac{\sin\theta}{2Bi})\frac{\sin\theta}{\tau\tanh\theta\tau} f(\tau)[\frac{1}{\epsilon}\tanh\pi\tau\tanh\theta\tau + 1] + \frac{\sin\theta}{2Bi}[\frac{1}{\epsilon}\frac{\tanh\pi\tau}{\tanh\theta\tau} + 1]}, \tag{2.47}$$

where $\theta = (\beta_o - \pi)$ as in Section 2.3. Here $f(\tau)$ is still an unknown function and may be determined as an approximation by equating the total heat flow across the liquid-vapor interface to that across the solid-liquid interface.

The total heat flow Q across the liquid-vapor interface is given by the Nusselt number Nu as

$$Nu = \frac{Q}{k_l \rho (T_v - T_o)} = \int_S Bi\left[1 - T_l\Big|_{\beta=\beta_o}\right] dS \ , \tag{2.48}$$

where S denotes the surface over which we integrate. In order to integrate $T_l\big|_{\beta=\beta_o}$ over S we write (2.48) in terms of α and θ as follows:

$$Nu = \int_o^\infty \frac{8\pi Bi}{(2\cosh\alpha + 2\cos\theta)^2}\left[1 - T_l\Big|_{\beta=\beta_o}\right]\sinh\alpha \, d\alpha \ , \tag{2.49}$$

which, in view of (2.9), may be written as

$$Nu = \int_0^\infty \frac{8\pi Bi}{(2\cosh\alpha + 2\cos\theta)^{3/2}} \left\{ \frac{1}{(2\cosh\alpha + 2\cos\theta)^{\frac{1}{2}}} - v_1 \Big|_{\beta=\beta_o} \right\} \sinh\alpha \, d\alpha. \tag{2.50}$$

By making use of the integral representations (2.17), (2.20) and (2.46) we obtain

$$Nu = 8\pi Bi \int_0^\infty \left\{ \frac{1}{\sin\theta} \int_0^\infty \frac{\eta \sinh\theta\eta}{\cosh\pi\eta} P_{-\frac{1}{2}+i\eta}(\cosh\alpha) d\eta \right\}$$

$$\times \left\{ \int_0^\infty \left[\frac{\cosh\theta\tau}{\cosh\pi\tau} - \Psi(\tau) \right] P_{-\frac{1}{2}+i\tau}(\cosh\alpha) d\tau \right\} \sinh\alpha \, d\alpha \, . \tag{2.51}$$

The substitution of (2.19) and (2.47) into (2.51) and the use of the orthogonality relation (2.24) yield

$$Nu = 4\pi \int_0^\infty \frac{\left(\frac{f(\tau)\sin\theta}{\tau\tanh\theta\tau} - 1\right)\frac{2Bi}{\sin\theta} + \frac{\left[\frac{\tanh\pi\tau}{\tanh\theta\tau} - \frac{f(\tau)\sin\theta}{\tau\coth\pi\tau} + \epsilon\left(1 - \frac{f(\tau)\sin\theta}{\tau\tanh\theta\tau}\right)\right]}{\tanh\pi\tau\tanh\theta\tau + \epsilon}}{\frac{\cosh\pi\tau\sinh\pi\tau}{\cosh\theta\tau\sinh\theta\tau}\left\{\left(1 - \frac{\sin\theta}{2Bi}\right)\frac{f(\tau)\sin\theta}{\tau\tanh\theta\tau} + \frac{\frac{\sin\theta}{2Bi}\left[\frac{\tanh\pi\tau}{\tanh\theta\tau} + \epsilon\right]}{\left[\tanh\pi\tau\tanh\theta\tau + \epsilon\right]}\right\}} d\tau \, . \tag{2.52}$$

If the heat flow calculation is carried out at the solid-liquid interface, the expression for the Nusselt number is

$$Nu = \frac{1}{\epsilon}\int_S (2\cosh\alpha - 2\cos\pi)\left.\frac{\partial T_2}{\partial\beta}\right|_{\beta=\pi} dS$$

$$= \frac{4\pi}{\epsilon}\int_0^\infty (2\cosh\alpha + 2)\left.\frac{\partial T_2}{\partial\beta}\right|_{\beta=\pi} \frac{\sinh\alpha\, d\alpha}{(2\cosh\alpha + 2)^2}$$

$$= \frac{4\pi}{\epsilon}\int_0^\infty \frac{\sinh\alpha\, d\alpha}{(2\cosh\alpha + 2)^{\frac{1}{2}}} \int_0^\infty \tau\tanh\pi\tau\ \Phi(\tau)P_{-\frac{1}{2}+i\tau}(\cosh\alpha)d\tau\ ,$$

(2.53)

which, in view of (2.28 -2.30), becomes

$$Nu = \frac{4\pi}{\epsilon}\int_0^\infty \frac{\Phi(\tau)}{\cosh\pi\tau}\ d\tau\ . \qquad (2.54)$$

The substitution of (2.47) in the above expression leads to

$$Nu = 4\pi\int_0^\infty \frac{\operatorname{sech}^2\pi\tau\, d\tau}{(1 - \frac{\sin\theta}{2Bi})\frac{f(\tau)\sin\theta}{\tau\tanh\theta\tau}[\tanh\pi\tau\tanh\theta\tau + \epsilon] + \frac{\sin\theta}{2Bi}[\frac{\tanh\pi\tau}{\tanh\theta\tau} + \epsilon]}.$$

(2.55)

If one requires that the integrands in (2.52) and (2.55) be identical, one obtains

$$f(\tau) = \frac{\tau\tanh\theta\tau}{\sin\theta}. \qquad (2.56)$$

It must be pointed out here that this expression for $f(\tau)$ is not necessarily exact. The above procedure for obtaining $f(\tau)$ is effectively equivalent to integrating the boundary condition (2.11) and hence, all the information cannot be obtained. Also, it is quite clear that to require the integrals in (2.52) and (2.55) to be equal, it is not necessary for the integrands to be identical. Therefore, it is appropriate to write, instead of (2.56),

$$f(\tau) \simeq \frac{\tau \tanh \theta\tau}{\sin \theta} . \tag{2.57}$$

By the substitution of (2.57) into (2.52) or (2.55), the expression for Nu becomes

$$\mathrm{Nu} \simeq 4\pi \int_0^\infty \frac{\operatorname{sech}^2 \pi\tau \, d\tau}{\tanh \pi\tau \, \tanh \theta\tau + \epsilon + \frac{\sin \theta}{2\mathrm{Bi}} \frac{\tanh \pi\tau \, \tanh \theta\tau}{\sinh^2 \theta\tau}} . \tag{2.58}$$

In the next section this expression is compared with some exact ones for special limiting cases.

2.5 Comparison with Exact Solutions

For the case $Bi \to \infty$, the boundary condition (2.11) simplifies to

$$v_1\Big|_{\beta=\beta_o} = \frac{1}{(2\cosh\alpha - 2\cos\beta_o)^{\frac{1}{2}}} , \tag{2.59}$$

which is the same as (2.11'). Therefore, the expression for Nu should be the same as (2.31) and that indeed is the case when $Bi \to \infty$ in (2.58).

When $Bi = \frac{1}{2}\sin\theta$, the first term on the left-hand side of (2.11) is zero and $\Phi(\tau)$ turns out to be independent of $f(\tau)$. Since the only approximation in (2.52) and (2.55) is the knowledge of $f(\tau)$, the result (2.58) is exact for the case in which it is unaffected by $f(\tau)$, namely $Bi = \frac{1}{2}\sin\theta$.

Further comparisons of (2.58) can be made with a set of results from the analysis by Sadhal and Martin [7] in which a solution was obtained by assuming the droplet base temperature to be uniform at T_o. For $0 \le \theta \le \pi/2$, the expression for the Nusselt number was given by

$$Nu \simeq \frac{2\pi Bi}{(1+\mu_o)} \frac{\left[(1-a_o)-(1+\mu_o)\sum_{n=1}^{\infty}\frac{a_n P'_n(\mu_o)}{n(n+1)}\right]}{\left[(1-a_o)-\sum_{n=1}^{\infty} a_n P_n(\mu_o)\right]} , \tag{2.60}$$

where

$$a_o = \frac{1}{2}(1-\mu_o) + \frac{1}{4}\phi\mu_o^2 , \tag{2.61}$$

$$a_1 = \frac{\frac{3}{4}(1 - \mu_o^2) + \frac{1}{2}\phi\mu_o^2}{1 + (1 - \mu_o^2)^{\frac{1}{2}}/\mathrm{Bi}} , \qquad (2.62)$$

$$a_n = \frac{(2n+1)}{2} \frac{\left[(1 - \mu_o^2)\frac{P_n'(\mu_o)}{n(n+1)} + \frac{\phi}{\mu_o}\frac{(1 - \mu_o^2)[P_n(\mu_o) - \mu_o P_n'(\mu_o)] - P_n(0)}{n(n-1) - 2}\right]}{\left[1 + \frac{n(1 - \mu_o^2)^{\frac{1}{2}}}{\mathrm{Bi}}\right]} ,$$

$$n \geq 2 , \qquad (2.63)$$

μ_o denotes $\cos\theta$, P_n denotes the Legendre polynomial of degree n, and $\phi = [1 - 2\theta/\pi]^{2\theta/\pi}$. This solution corresponds to the case $\epsilon = 0$ in the present analysis, and (2.58) has exact agreement with (2.60) for the trivial case $\theta = 0$, i.e.,

$$\mathrm{Nu}\Big|_{\theta=0,\ \epsilon=0} = \pi\,\mathrm{Bi} . \qquad (2.64)$$

However, for θ near $\pi/2$, in (2.58) Nu behaves like $\sim \mathrm{Bi}^{\frac{1}{2}}$ for large Bi while numerical calculation of (2.60) indicates that $\mathrm{Nu} \sim \ell n\ \mathrm{Bi}$. The latter analysis is known to be exact for $\theta = \pi/2$ and therefore (2.58) does not hold for large Bi when $\epsilon = 0$.

To make use of the information available from all the exact solutions, a correction $g(\theta, \mathrm{Bi})$ is made to the factor $\sin\theta/(2\,\mathrm{Bi})$ in (2.58) so that Nu may be written as

$$Nu \simeq 4\pi \int_0^{\infty} \frac{\operatorname{sech}^2 \pi\tau \; d\tau}{\tanh \pi\tau \tanh \theta\tau + \epsilon + [\frac{\sin\theta}{2Bi} + g(\theta, Bi)] \frac{\tanh \pi\tau \tanh \theta\tau}{\sinh^2 \theta\tau}} \, . \tag{2.65}$$

The correction function $g(\theta, Bi)$ is chosen so that when $\epsilon = 0$, (2.65) yields approximately the same results as those obtained in [7] and so that the exact solutions remain unaffected. Since logarithmic behavior in Bi is required and without $g(\theta, Bi)$, (2.65) would behave like $\sim Bi^{\frac{1}{2}}$, it is appropriate to choose $g(\theta, Bi) \sim (\ell n\ Bi)^{-2}$. Furthermore, $g(\theta, Bi)$ is required to be zero when $Bi = \frac{1}{2} \sin\theta$ and ϵ are both zero because, at these values, (2.58) is exact. After a few trials, a suitable expression for the correction function is found to be

$$g(\theta, Bi) = 1.8 \sin^3\theta (1 - \frac{\sin\theta}{2\ Bi})^{14} (1 - \frac{1}{2Bi}) [\ell n (\frac{\sin\theta}{2\ Bi})]^{-2} \, . \tag{2.66}$$

It is important to mention that since the results (2.60 - 2.63) were restricted to contact angles $0 \leq \theta \leq \pi/2$, the same condition must apply to (2.65).

Results from the numerical integration of (2.65) are presented in Fig. 2.4. It can be seen that for large values ϵ the dependence of Nu on ϵ is quite strong but, depending on the value of Bi, it gets weaker as ϵ becomes smaller.

The droplet growth rate for this case also is given by (2.41) but since Nu is a complicated function of ρ, straightforward integration is not possible.

2.6 Calculation of the Liquid-Vapor Heat-Transfer Coefficient

There has been considerable interest in the problem of vapor flow to a liquid surface. The difficulty, generally, has been in including the effect of the bulk velocity of the vapor, and some authors [13, 14] have dealt with this problem by introducing correction factors. However, in Plesset's work [10] on the flow of vapor between parallel liquid surfaces, the bulk velocity for low Mach number was considered implicitly. This result was later extended by Plesset and Prosperetti [11] for vapor flow between spherical and cylindrical surfaces.

In particular, for flow from an inner sphere of radius R_v and temperature T_v to an outer spherical cavity boundary of radius R_s and temperature T_s, the bulk velocity u_s at the cavity is given [11] by

$$u_s = \gamma\left(\frac{RT_s}{2\pi}\right)^{\frac{1}{2}} \frac{p^e(T_v) - p^e(T_s)}{p^e(T_v) + \left(\frac{R_s}{R_v}\right)^2 \left(\frac{T_v}{T_s}\right)^{\frac{1}{2}} p^e(T_s)}, \qquad (2.67)$$

where γ is the accommodation coefficient, $p^e(T_v)$ and $p^e(T_s)$ are the equilibrium vapor pressures at temperatures T_v and T_s respectively, and R is the ratio of the universal gas constant to the molecular weight of the liquid and the vapor. This result can also be applied to vapor flowing from an outer cavity boundary of radius R_v and temperature T_v to an inner sphere of radius R_s and temperature T_s. For this case, in the limit $R_v \to \infty$, (2.67) takes the form

$$u_s = \gamma\left(\frac{RT_s}{2\pi}\right)^{\frac{1}{2}} \frac{p^e(T_v) - p^e(T_s)}{p^e(T_v)} , \tag{2.68}$$

from which the vapor flux J is evaluated to be

$$J = u_s \rho^e(T_s) = \gamma \frac{p^e(T_v) - p^e(T_s)}{(2\pi R T_s)^{\frac{1}{2}}} \tag{2.69}$$

where $\rho^e(T_s) = p^e(T_s)/(RT_s)$ is the equilibrium vapor density at temperature T_s.

From the Clausius-Clapeyron equation $p^e(T_v)$ and $p^e(T_s)$ can be related

$$\frac{p^e(T_s)}{p^e(T_v)} = \exp\left[-\frac{\lambda}{RT_s}\left(1 - \frac{T_s}{T_v}\right)\right] , \tag{2.70}$$

where λ is the latent heat of vaporization. For T_s very close to T_v, this may be further approximated by

$$p^e(T_s) \simeq p^e(T_v)\left[1 - \frac{\lambda}{RT_s T_v}(T_v - T_s)\right] . \tag{2.71}$$

Upon substitution of this approximation into (2.69), the heat flux $q = J\lambda$ is found to be

$$q = \gamma \frac{p^e(T_v)\lambda^2}{(2\pi)^{\frac{1}{2}} T_s^{3/2} T_v R^{3/2}} (T_v - T_s) , \tag{2.72}$$

and by noting that $T_s^{3/2}\, T_v \simeq T_v^{5/2}$, the heat-transfer coefficient $h = q/(T_v - T_s)$ may be expressed as

$$h = \gamma \frac{p^e(T_v)\lambda^2}{(2\pi)^{\frac{1}{2}} R^{3/2} T_v^{5/2}} \quad . \tag{2.73}$$

This is the result for vapor flowing onto a liquid sphere and due to symmetry it is also valid for a hemisphere. For the general case of vapor flowing onto an arbitrary spherical segment an expression for h is not available but may, nevertheless, be approximated by (2.73).

By taking the accommodation coefficient γ to be unity as recommended by Nabavian and Bromley [14], numerical calculations for water at $T_v = 373K$ show that $h \simeq 7.7 \times 10^6$ Watts/(m^2 - K). The Biot number $Bi = h\rho/k_l$ for droplets ranging in size from 10 μm to 1 mm varies from about 100 to 10,000.

2.7 Discussion

The results of the present study clearly illustrate the importance of the material properties of the solid and of the droplet contact angle for both evaporating and condensing droplets. For an evaporating droplet the liquid-vapor interface temperature is set at T_v. If the solid properties are ignored by setting the droplet base temperature to be $T_o \neq T_v$, calculations show that the total heat flow Q would become unbounded, which is of course unrealistic. This behavior is made quite clear by equations (2.30-2.31) from which we see that if $k_2 \to \infty$ (i.e., $\epsilon \to 0$), then $Nu \to \infty$. The overall behavior for $\theta \sim 1$ may be summed up by equation (2.34) which predicts Q as being proportional to $(k_1 k_2)^{\frac{1}{2}}$. The dependence of Q on the contact angle is well described by (2.32).

For a condensing droplet, the analysis shows a strong dependence of Q on ϵ for $\ell n\ Bi \sim 1/\epsilon^{\frac{1}{2}}$ or $\ell n\ Bi > 1/\epsilon^{\frac{1}{2}}$. When $\ell n\ Bi \gg 1/\epsilon^{\frac{1}{2}}$, the dependence of Q is dominated by ϵ and it approaches the value $Q \propto (k_1 k_2)^{\frac{1}{2}}$ given by equations (2.32-2.34). Calculations for water condensing on metals show that Bi varies from about 100 to 10,000 while ϵ varies from about 0.001 to 0.01. Therefore, the importance of considering the condenser properties is evident, especially for large droplets and/or for small contact angles. Interestingly, the behavior $Q \propto (k_1 k_2)^{\frac{1}{2}}$ agrees very well with the three experimental data points reported in the work of Griffith and Lee [15]. This result differs from that of Nijaguna and Abdelmessih [16] who obtained $Q \propto k_2^{\frac{1}{2}}$ by considering the transient response of a thin film of liquid on a semi-infinite solid. Such behavior is to be

expected because it is an intrinsic property of transient heat flows in all simple geometries. However, in the present analysis the proportionality of Q with $(k_1 k_2)^{\frac{1}{2}}$ is the result of the edge effects of the droplet with the solid surface around it being insulated. Another important implication of the very large Biot numbers is that the solid-liquid interface temperature approaches high nonuniformity as in the case of an evaporating droplet. Therefore, it would be incorrect, under the circumstances described, to add the separate resistances of the droplet and the solid. In general, the criterion for the separability of resistances is the existence of an isotherm along the desired surface of separation. For small droplets, however, the Biot number may be small enough so that the overall resistance may be that of the droplet alone.

To obtain a more precise theoretical prediction, one can calculate the average heat flow across a given area by adding the individual flow rates across droplets for a known size distribution. Since the properties of the solid, the liquid, and the vapor are all considered simultaneously, such calculations would be a step closer to a more complete theory in the study of droplets.

REFERENCES

[1] Fatica, N. and Katz, D. L., "Dropwise Condensation", Chemical Engineering Progress 45, 661-674 (1949).

[2] Sugawara, S. and Michiyoshi, I., "Dropwise Condensation", Memoirs of Faculty of Engineering, Kyoto University 18(2), 84-111 (1956).

[3] Nijaguna, B. T., "Drop Nusselt Number in Dropwise Condensation", Applied Scientific Research 29, 226-236 (1974).

[4] Ahrendts, J., "Der Warmleitwiderstand eines Kondensattropfens", Warme-und Stroffübertagung 5, 239-244 (1972).

[5] Hurst, C. J. and Olson, D. R., "Conduction through Droplets during Dropwise Condensation", Journal of Heat Transfer 95, 12-20 (1973).

[6] Umur, A. and Griffith, P., "Mechanism of Dropwise Condensation", Journal of Heat Transfer 87, 275-282 (1965).

[7] Sadhal, S. S. and Martin, W. W., "Heat Transfer through Drop Condensate using Differential Inequalities", International Journal of Heat and Mass Transfer 20, 1401-1407 (1977).

[8] Mikic, B., "On Mechanism of Dropwise Condensation", International Journal of Heat and Mass Transfer 12, 1311-1323 (1969).

[9] Hannemann, R. J. and Mikic, B. B., "An Analysis of the Effect of Surface Thermal Conductivity on the Rate of Heat Transfer in Dropwise Condensation", International Journal of Heat and Mass Transfer 19, 1299-1307 (1976).

[10] Plesset, M. S., "Note on the Flow of Vapor Between Liquid Surfaces", Journal of Chemical Physics 20, 790-793 (1952).

[11] Plesset, M. S. and Prosperetti, A., "Flow of Vapor in a Liquid Enclosure", Journal of Fluid Mechanics 78, 433-444 (1976).

[12] Lebedev, N. N., Special Functions and Their Application, Dover Publications, Inc., New York, N. Y. (1972).

[13] Schrage, R. W., A Theoretical Study of Interphase Mass Transfer , Columbia University Press, New York, N. Y. (1953).

[14] Nabavian, K. and Bromley, L. A., "Condensation Coefficient of Water", Chemical Engineering Science 18, 651-660 (1963).

[15] Griffith, P. and Lee, M. S., "The Effect of Surface Thermal Properties and Finish on Dropwise Condensation", International Journal of Heat and Mass Transfer 10, 697-707 (1967).

[16] Nijaguna, B. T. and Abdelmessih, A. H., "Precoalescence Drop Growth Model for Dropwise Condensation ", ASME 71-WA/HT-47 (1971).

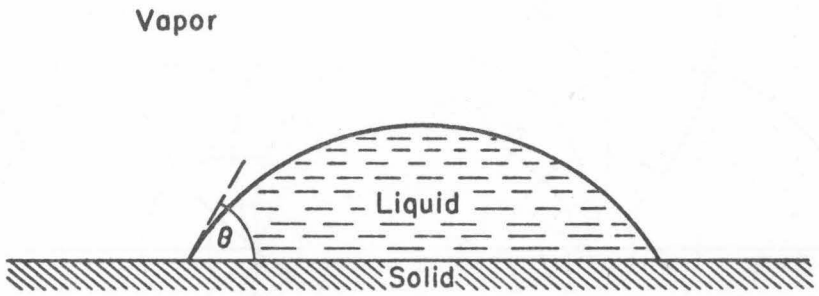

Fig. 2.1. Physical model for the analysis.

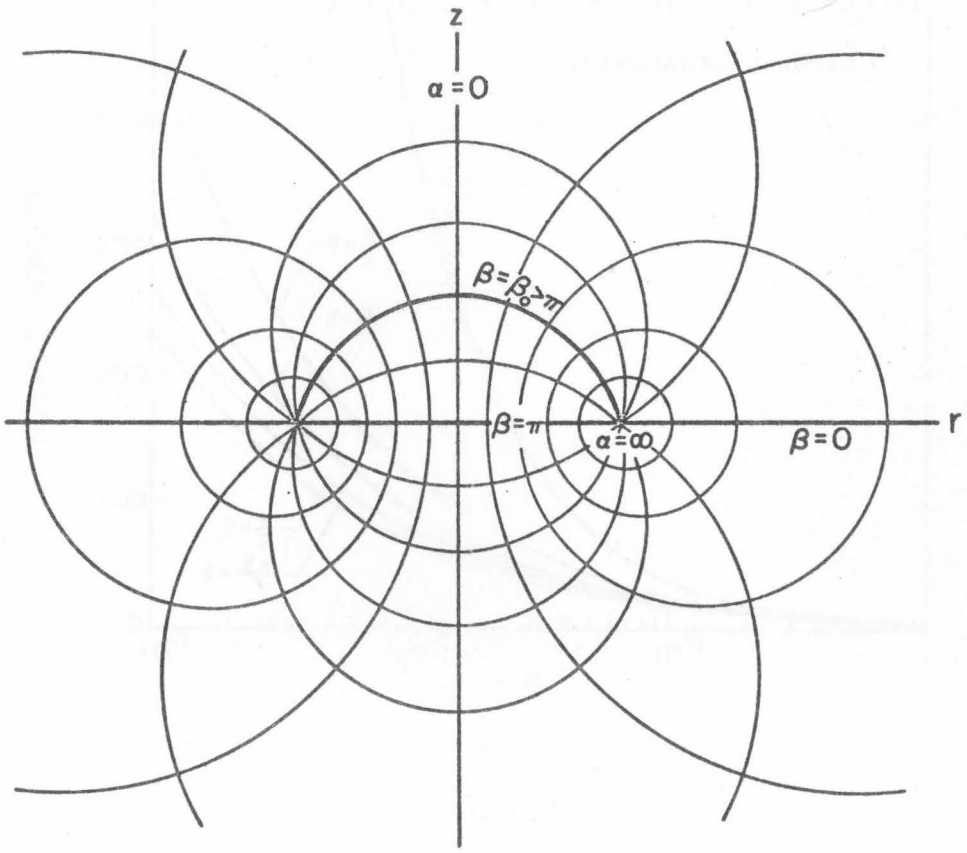

Fig. 2.2. Toroidal coordinate system.

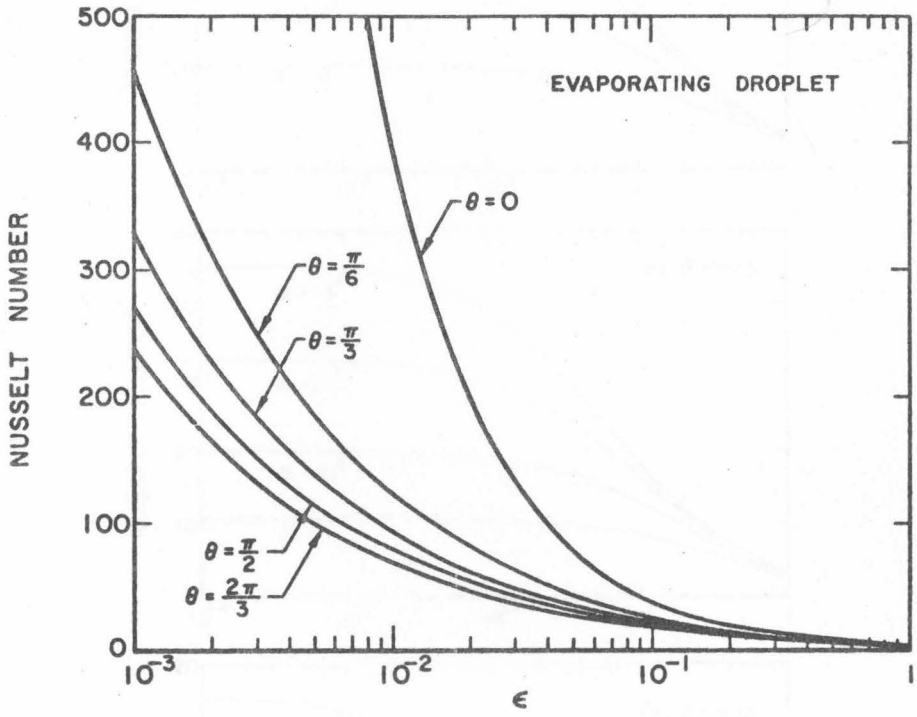

Fig. 2.3. Variation of evaporating droplet Nusselt number with conductivity ratio $\epsilon = k_1/k_2$ for different contact angles.

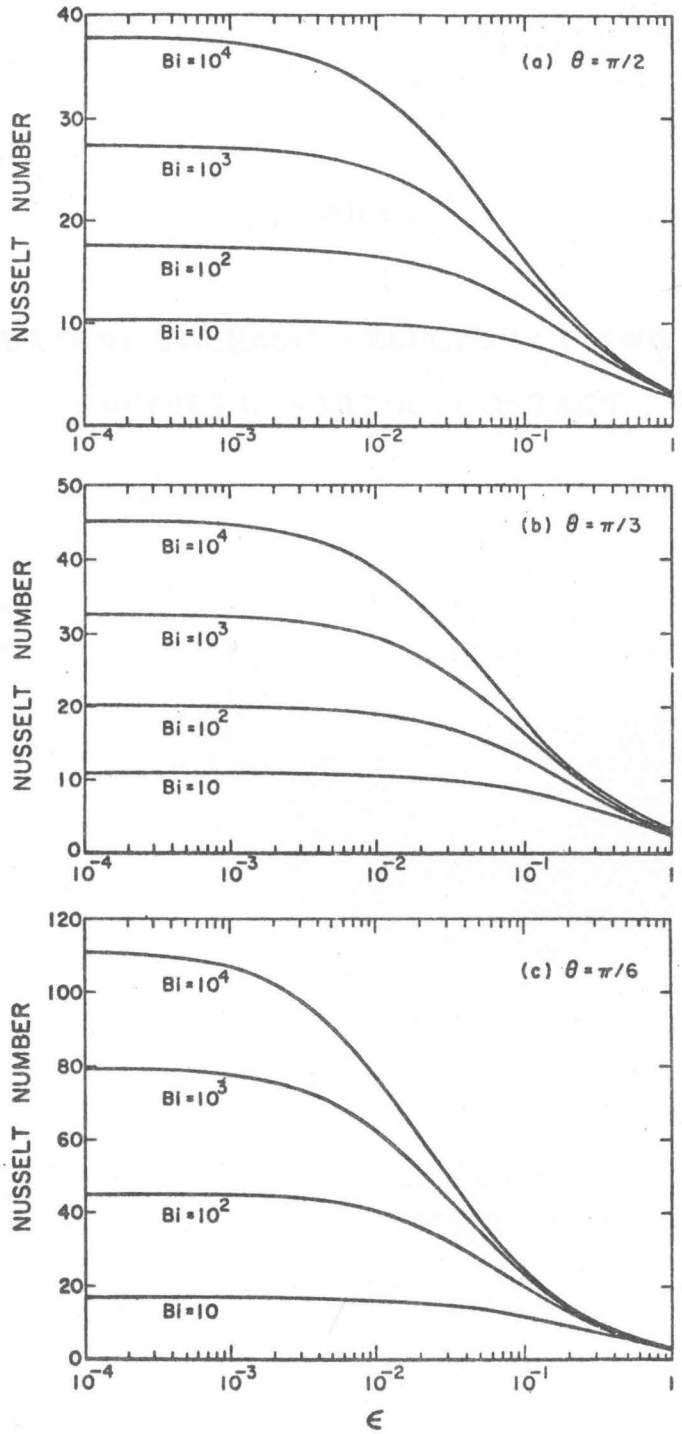

Fig. 2.4. Condensing droplet Nusselt number as a function of conductivity ratio $\epsilon = k_1/k_2$ for different Biot numbers: contact angles (a) $\pi/2$, (b) $\pi/3$, and (c) $\pi/6$.

PART 3

TRANSIENT THERMAL RESPONSE OF TWO SOLID BODIES IN PARTIAL CONTACT

Nomenclature

a	=	radius of disk of contact
c^*	=	half-width of regions of no contact
c	=	$c^*\pi/\ell$ = dimensionless half-width of regions of no contact
Fo_i	=	$\begin{cases} \kappa_i t/a^2 \\ \kappa_i t/\ell^2 \end{cases}$ = Fourier number
k_1	=	thermal conductivity of solid 1
k_2	=	thermal conductivity of solid 2
ℓ	=	width of lines of symmetry
$\mathcal{L}$	=	Laplace transform operator
$\mathcal{L}^{-1}$	=	inverse Laplace transform operator
p	=	Laplace transform parameter
$P_n(x)$	=	Legendre polynomial of degree n
q	=	heat flux
q_{av}	=	average heat flux
r	=	cylindrical radial coordinate
R	=	thermal resistance
R_{ss}	=	steady-state thermal resistance
R_{fc}	=	full-contact thermal resistance
t	=	time
T_1	=	temperature distribution in solid 1
T_2	=	temperature distribution in solid 2

T_{10} = initial temperature of solid 1

T_{20} = initial temperature of solid 2

x^* = cartesian coordinate

x = $x^*\pi/\ell$ = dimensionless cartesian coordinate

y^* = cartesian coordinate

y = $y^*\pi/\ell$ = dimensionless cartesian coordinate

z = cylindrical coordinate

$\delta_{j,k}$ = Kronecker delta

ϵ = oblate spheroidal coordinate

η = oblate spheroidal coordinate

θ_1 = dimensionless temperature distribution in solid 1

θ_2 = dimensionless temperature distribution in solid 2

$\textcircled{H}_1$ = Laplace transform of θ_1

$\textcircled{H}_2$ = Laplace transform of θ_2

κ_1 = thermal diffusivity of solid 1

κ_2 = thermal diffusivity of solid 2

Ψ_1 = Legendre transform of $\textcircled{H}_1$

Ψ_2 = Legendre transform of $\textcircled{H}_2$

3.0 Introduction

It is well known that when the plane surfaces of two bodies are brought together the actual contact does not take place over the entire interfacial area but over a fraction of that area. As a result for any heat flow taking place across the interface, the flow lines are constricted and lead to what is termed "contact resistance". Over the region where there is no contact, heat may be transported by the air present between the surfaces. At atmospheric pressures, however, this heat transfer may be neglected, and it is quite reasonable to assume that the areas of no contact are insulated. Under such an assumption we have a well-defined, heat-conduction problem but the general irregularity of the contacting areas makes an exact analysis virtually impracticable. For cases in which the actual contact takes place over a small fraction of the total interfacial area, one can model a single area of contact by assuming it to be a circular disk between two semi-infinite solids. The areas around the disk can be taken to be insulated (see Fig. 3.0.1). The steady-state solution for heat flow in this geometry is well known [1] and the transient case has been dealt with numerically by Schneider et al. [2]. In an approximate analysis, Heasley [3] obtained a solution to the transient case by assuming the region of contact to be a perfectly conducting sphere between two semi-infinite solids (see Fig. 3.0.2). This model makes the unrealistic assumption that there is a spherical isotherm passing symmetrically through the two solids. Other models by Heasley [3] involve one-dimensional approximations of the heat equation and their validity is

very restricted. In the present study the problem as posed by Schneider et al. [2] is solved analytically by using a long-time perturbation scheme based on the work done by Norminton and Blackwell [4] for heat flow from an isothermal disk. That is, a solution to the time-dependent heat equation is found for the problem in which two different solids at different uniform initial temperatures are brought into contact over a finite circular disk. The solution is valid for long time, large thermal diffusivities or for small areas of contact; that is, large Fourier numbers.

This model is only meaningful if the areas of contact are sufficiently small (or sufficiently isolated). If, however, the fraction of the area in contact is large, the interface may be modelled in two dimensions by equally spaced identical strips of perfect contact with the rest of the area of each surface being insulated (see Fig. 3.0.3). The steady heat conduction problem for this case has been dealt with by Dundurs and Panek [5]. Since this is a two-dimensional case, steady temperatures at large distances from the interface cannot be kept finite. An exact analytical solution for the transient case has not yet been found but in the present analysis a solution valid for large time or for large fraction of contact is obtained. This latter model is particularly useful for machined surfaces.

In the first part of the analysis that follows, we obtain a solution for the case in which the contact is over a disk. The solution for the other model is given in the second part.

3.1 Unsteady Heat Flow in Two Semi-Infinite Solids with a Circular Region of Contact

3.1.1 Statement of Problem

Two semi-infinite solids at different initial temperatures are brought together and perfect thermal contact is established over a finite circular region (see Fig. 3.0.1). The rest of the areas of the contacting planes are assumed to be insulated. Far away from the contact areas the temperature in each solid is taken to be fixed at the initial value.

To adapt to the geometry one resorts to the oblate spheroidal coordinate system. The prolate and the oblate coordinate systems were used by Norminton and Blackwell [4] to obtain the large-time temperature distribution for one-medium heat flow from isothermal spheroids and the isothermal circular disk. In the present analysis the case of the disk is generalized to that of two media, with the disk temperature being nonuniform and time-varying.

The oblate spheroidal coordinate system involves the transformation

$$r = a[(1 + \epsilon^2)(1 - \eta^2)]^{\frac{1}{2}} , \qquad 0 \leq \epsilon , \tag{3.1.1}$$

$$z = a\epsilon\eta , \qquad 0 \leq \eta \leq 1 , \tag{3.1.2}$$

$$\phi = \phi , \qquad 0 \leq \phi < 2\pi , \tag{3.1.3}$$

where (r, z, ϕ) are the usual cylindrical coordinates, (ϵ, η, ϕ) are the transformed spheroidal coordinates (see Fig. 3.1.1) and a is

the radius of the disk. In these coordinates the heat equation

$$\nabla^2 T_i = \frac{1}{\kappa_i} \frac{\partial T_i}{\partial t} , \qquad i = 1, 2, \tag{3.1.4}$$

for axial symmetry takes the form

$$\frac{1}{a^2(\epsilon^2 + \eta^2)} \left\{ \frac{\partial}{\partial \epsilon}\left[(1 + \epsilon^2) \frac{\partial T_i}{\partial \epsilon}\right] + \frac{\partial}{\partial \eta}\left[(1 - \eta^2) \frac{\partial T_i}{\partial \eta}\right] \right\} = \frac{1}{\kappa_i} \frac{\partial T_i}{\partial t} ,$$

$$i = 1, 2,$$

$$t > 0; \; 0 < \epsilon < \infty; \; 0 < \eta \leq 1 , \tag{3.1.5}$$

where t is the time, T_1 is the temperature distribution in the hotter solid (say, solid 1), T_2 is the temperature distribution in the other solid (solid 2), and k_1 and k_2 are the corresponding thermal diffusivities. The initial boundary conditions are given by

$$\left.\begin{aligned} T_1 &= T_{10} \\ T_2 &= T_{20} \end{aligned}\right\} , \qquad t = 0; \quad 0 \leq \epsilon < \infty; \; 0 \leq \eta \leq 1, \tag{3.1.6}$$

$$\left.\begin{aligned} T_1 &= T_2 \\ k_1 \frac{\partial T_1}{\partial \epsilon} &= -k_2 \frac{\partial T_2}{\partial \epsilon} \end{aligned}\right\} , \qquad \epsilon = 0; \quad t > 0; \; 0 \leq \eta \leq 1, \tag{3.1.7}$$

$$\left.\begin{aligned} T_1 &= T_{10} \\ T_2 &= T_{20} \end{aligned}\right\} , \qquad \epsilon \to \infty; \quad t > 0; \; 0 \leq \eta \leq 1, \tag{3.1.8}$$

and

$$\frac{\partial T_1}{\partial \eta} = \frac{\partial T_2}{\partial \eta} = 0, \qquad \eta = 0; \qquad t > 0;\ 0 \leq \epsilon < \infty . \qquad (3.1.9)$$

Here k_1 and k_2 are the thermal conductivities of the solids 1 and 2, respectively.

3.1.2 Analysis

It is convenient to redefine the dependent variables T_1 and T_2 in dimensionless forms as

$$\theta_1 = \frac{T_1 - T_{10}}{T_{10} - T_{20}} = \frac{T_1 - T_{20}}{T_{10} - T_{20}} - 1 \ , \qquad (3.1.10)$$

and

$$\theta_2 = \frac{T_2 - T_{20}}{T_{10} - T_{20}} \ . \qquad (3.1.11)$$

As a result the equations (3.1.5-3.1.9) become

$$\frac{\partial}{\partial \epsilon}\left[(1 + \epsilon^2) \frac{\partial \theta_i}{\partial \epsilon}\right] + \frac{\partial}{\partial \eta}\left[(1 - \eta^2) \frac{\partial \theta_i}{\partial \eta}\right] = \frac{a^2(\epsilon^2 + \eta^2)}{\kappa_i} \frac{\partial \theta_i}{\partial t} \ ,$$

$$t > 0; \ 0 < \epsilon < \infty, \ 0 < \eta \leq 1, \qquad (3.1.12)$$

subject to

$$\theta_1 = \theta_2 = 0, \qquad t = 0; \ 0 \leq \epsilon < \infty, \ 0 \leq \eta \leq 1, \qquad (3.1.13)$$

$$\left.\begin{aligned} \theta_1 + 1 &= \theta_2 \\ k_1 \frac{\partial \theta_1}{\partial \epsilon} &= -k_2 \frac{\partial \theta_2}{\partial \epsilon} \end{aligned}\right\} \ , \qquad \epsilon = 0; \ t > 0; \ 0 \leq \eta \leq 1 \ , \qquad (3.1.14)$$

$$\theta_1 = \theta_2 = 0 \ , \qquad \epsilon \to \infty, \quad t > 0; \ 0 \leq \eta \leq 1, \qquad (3.1.15)$$

and

$$\frac{\partial \theta_1}{\partial \eta} = \frac{\partial \theta_2}{\partial \eta} = 0 \qquad \eta = 0; \quad t > 0; \quad 0 \leq \epsilon < \infty, \qquad (3.1.16)$$

where the symbol i, henceforth will denote i = 1, 2.

By taking the Laplace transform of θ_i with respect to time we obtain

$$\frac{\partial}{\partial \epsilon}\left[(1+\epsilon^2)\frac{\partial \Theta_i}{\partial \epsilon}\right] + \frac{\partial}{\partial \eta}\left[(1-\eta^2)\frac{\partial \Theta_i}{\partial \eta}\right] = \frac{pa^2(\epsilon^2+\eta^2)}{\kappa_i}\Theta_i ,$$

$$0 < \epsilon < \infty; \; 0 < \eta \leq 1, \qquad (3.1.17)$$

subject to

$$\left.\begin{aligned} \Theta_1 + \frac{1}{p} &= \Theta_2 \\ k_1 \frac{\partial \Theta_1}{\partial \epsilon} &= -k_2 \frac{\partial \Theta_2}{\partial \epsilon} \end{aligned}\right\}, \qquad \epsilon = 0; \quad 0 \leq \eta \leq 1, \qquad (3.1.18)$$

$$\Theta_1 = \Theta_2 , \qquad \epsilon \to \infty; \quad 0 \leq \eta \leq 1, \qquad (3.1.19)$$

$$\frac{\partial \Theta_1}{\partial \eta} = \frac{\partial \Theta_2}{\partial \eta} = 0, \qquad \eta = 0; \quad 0 \leq \epsilon < \infty, \qquad (3.1.20)$$

where

$$\Theta_i(\epsilon, \eta, p) = \int_0^\infty e^{-pt}\, \theta_i(\epsilon, \eta, t)dt , \qquad (3.1.21)$$

We now take the Legendre transform of Θ_i with respect to η. In view of the boundary condition (3.1.20), only the even powers of η

are needed and therefore we make the transform involving only the even order Legendre polynomials. Thus

$$\Phi_{2m,i}(\epsilon, p) = \int_0^1 \Theta_i(\epsilon, \eta, p) P_{2m}(\eta) d\eta \ , \qquad (3.1.22)$$

where m is used to denote $m = 0, 1, 2, \ldots$ unless otherwise specified, and $P_{2m}(\eta)$ denotes the Legendre polynomial of degree $2m$. As a result of (3.1.22), equations (3.1.17-3.1.22), transform into

$$\frac{d}{d\epsilon}\left[(1+\epsilon^2)\frac{d\Phi_{2m,i}}{d\epsilon}\right] - 2m(2m+1)\Phi_{2m,i}$$

$$= \frac{a^2 p}{\kappa_i}\left[a_{2m}\Phi_{2m-2,i} + (\epsilon^2 + b_{2m})\Phi_{2m,i} + c_{2m}\Phi_{2m+2,i}\right] \ ,$$

$$0 < \epsilon < \infty \ , \qquad (3.1.23)$$

subject to

$$\left.\begin{aligned} \Phi_{0,1} + \frac{1}{p} &= \Phi_{0,2} \quad , \quad m = 0 \\ \Phi_{2m,1} &= \Phi_{2m,2} \quad , \quad m = 1, 2, 3, \ldots \\ k_1 \frac{d\Phi_{2m,1}}{d\epsilon} &= -k_2 \frac{d\Phi_{2m,2}}{d\epsilon} \quad , \quad m = 1, 2, 3, \ldots \end{aligned}\right\} \quad \epsilon = 0, \qquad (3.1.24)$$

and

$$\Phi_{2m,1} = \Phi_{2m,2} \quad , \quad \epsilon \to \infty \ , \qquad (3.1.25)$$

where

$$a_{2m} = \frac{2m(2m-1)}{(4m+1)(4m-1)} \quad ,$$

$$b_{2m} = \frac{8m^2+4m-1}{(4m-1)(4m+3)} \quad ,$$

and

$$c_{2m} = \frac{(2m+1)(2m+2)}{(4m+1)(4m+3)} \quad .$$

For $\epsilon \to \infty$, $\Phi_{2m,i}$ is found to behave as $\exp[-(p/\kappa_i)^{\frac{1}{2}} a\epsilon]$ and therefore, a dependent variable substitution [4]

$$\Phi_{2m,i}(\epsilon, p) = f_{2m,i}(\epsilon, p) \exp[-(p/\kappa_i)^{\frac{1}{2}} a\epsilon] \quad , \qquad (3.1.26)$$

is used. This substitution transforms equations (3.1.23-3.1.25) into

$$\frac{d}{d\epsilon}[(1+\epsilon^2)\frac{df_{2m,i}}{d\epsilon}] - 2m(2m+1)f_{2m,i}$$

$$= 2(\frac{p}{\kappa_i})^{\frac{1}{2}} a[(1+\epsilon^2)\frac{df_{2m,i}}{d\epsilon} + \epsilon f_{2m,i}]$$

$$+ (\frac{p}{\kappa_i})a^2[a_{2m}f_{2m-2,i} + (b_{2m}-1)f_{2m,i} + c_{2m}f_{2m+2,i}] \quad ,$$

$$0 < \epsilon < \infty, \qquad (3.1.27)$$

subject to

$$\left.\begin{aligned} f_{2m,1} + \frac{1}{p}\,\delta_{2m,0} &= f_{2m,2} \\ k_1\left[\frac{df_{2m,1}}{d\epsilon} - \left(\frac{p}{\kappa_1}\right)^{\frac{1}{2}} a f_{2m,1}\right] &= -\,k_2\left[\frac{df_{2m,2}}{d\epsilon} - \left(\frac{p}{\kappa_2}\right)^{\frac{1}{2}} a f_{2m,2}\right] \end{aligned}\right\} , \qquad \epsilon = 0 , \tag{3.1.28}$$

and

$$f_{2m,i} \to 0 \qquad \text{as} \qquad \epsilon \to \infty . \tag{3.1.29}$$

The symbol $\delta_{j,k}$ denotes the Kronecker delta.

As we can see, an exact solution to equation (3.1.27) is not straightforward, and approximate solutions have to be sought. Norminton and Blackwell [4] obtained an approximate solution by first finding the Green's function to the left side of (3.1.27), i.e., by finding a solution to

$$\frac{d}{d\epsilon}\left[(1+\epsilon^2)\frac{dG_{2m}}{d\epsilon}\right] - 2m(2m+1)G_{2m} = \delta(\epsilon - \beta) , \tag{3.1.30}$$

This Green's function was relatively simple to obtain because the problem involved only one medium and the boundary conditions were easy to satisfy. In the present case, however, similar calculations get too cumbersome. As an alternative we assume a perturbation expansion for $f_{2m,i}(\epsilon, p)$ in powers of $p^{\frac{1}{2}}$.

3.1.3 Solution by Perturbation

By letting

$$f_{2m,i}(\epsilon, p) = \frac{1}{p}\left[f^{(0)}_{2m,i}(\epsilon) + p^{\frac{1}{2}} f^{(1)}_{2m,i}(\epsilon) + p f^{(2)}_{2m,i}(\epsilon) + \cdots\cdots\right] \tag{3.1.31}$$

and substituting it into (3.1.27-3.1.29) we obtain the following.

Order p^0

$$\frac{d}{d\epsilon}\left[(1+\epsilon^2)\frac{df^{(0)}_{2m,i}}{d\epsilon}\right] - 2m(2m+1) f^{(0)}_{2m,i} = 0,$$

$$0 < \epsilon < \infty, \tag{3.1.32}$$

subject to

$$\left.\begin{aligned} f^{(0)}_{2m,1} + \delta_{2m,0} &= f^{(0)}_{2m,2} \\ k_1 \frac{df^{(0)}_{2m,1}}{d\epsilon} &= -k_2 \frac{df^{(0)}_{2m,2}}{d\epsilon} \end{aligned}\right\}, \qquad \epsilon = 0, \tag{3.1.33}$$

and

$$f^{(0)}_{2m,i} = 0, \qquad \epsilon \to 0. \tag{3.1.34}$$

For $m = 0$, straightforward integration of the above set (3.1.32-3.1.34) gives the leading term

$$f^{(0)}_{0,i}(\epsilon) = A_i \cot^{-1}\epsilon, \tag{3.1.35}$$

where

$$\left.\begin{aligned} A_1 &= -\frac{2}{\pi}\frac{k_2}{(k_1+k_2)} \quad , \\ \text{and} \qquad & \\ A_2 &= \frac{2}{\pi}\frac{k_1}{(k_1+k_2)} \quad , \end{aligned}\right\} \tag{3.1.36}$$

For $m \geq 1$, $f^{(0)}_{2m,i} = 0$ satisfies (3.1.32-3.1.34) and is, therefore, the solution.

Order $p^{\frac{1}{2}}$

$$\frac{d}{d\epsilon}\left[(1+\epsilon^2)\frac{df^{(1)}_{2m,i}}{d\epsilon}\right] - 2m(2m+1)f^{(1)}_{2m,i}$$

$$= \frac{2a}{\kappa_i^{\frac{1}{2}}}\left[(1+\epsilon^2)\frac{df^{(0)}_{2m,i}}{d\epsilon} + \epsilon\, f^{(0)}_{2m,i}\right] , \qquad 0 < \epsilon < \infty , \tag{3.1.37}$$

subject to

$$\left.\begin{aligned} & f^{(1)}_{2m,i} = f^{(1)}_{2m,2} \\ & k_1\frac{df^{(1)}_{2m,1}}{d\epsilon} + k_2\frac{df^{(1)}_{2m,2}}{d\epsilon} = a\left[\frac{k_1}{\kappa_1^{\frac{1}{2}}} f^{(0)}_{2m,1} + \frac{k_2}{\kappa_2^{\frac{1}{2}}} f^{(0)}_{2m,2}\right] \end{aligned}\right\} , \qquad \epsilon = 0 , \tag{3.1.38}$$

and

$$f^{(1)}_{2m,i} = 0 , \qquad \epsilon \to \infty . \tag{3.1.39}$$

Upon the substitution of (3.1.35) and (3.1.36) into (3.1.37-3.1.39) we obtain

$$\frac{d}{d\epsilon}\left[(1+\epsilon^2)\frac{df^{(1)}_{0,i}}{d\epsilon}\right] = \frac{2aA_i}{\kappa_i^{\frac{1}{2}}}\left[-1+\epsilon\cot^{-1}\epsilon\right], \qquad m=0, \qquad (3.1.40)$$

$$\frac{d}{d\epsilon}\left[(1+\epsilon^2)\frac{df^{(1)}_{2m,i}}{d\epsilon}\right] - 2m(2m+1)f^{(1)}_{2m,i} = 0, \quad m=1,2,3,\ldots$$

$$0 < \epsilon < \infty, \qquad (3.1.41)$$

subject to

$$\left.\begin{aligned} &f^{(1)}_{2m,1} = f^{(1)}_{2m,2}, \\ &k_1\frac{df^{(1)}_{0,1}}{d\epsilon} + k_2\frac{df^{(1)}_{0,2}}{d\epsilon} = \frac{\pi a}{2}\left[\frac{k_1A_1}{\kappa_1^{\frac{1}{2}}} + \frac{k_2A_2}{\kappa_2^{\frac{1}{2}}}\right], \qquad m=0, \\ &k_1\frac{df^{(1)}_{2m,1}}{d\epsilon} + k_2\frac{df^{(1)}_{2m,2}}{d\epsilon} = 0, \qquad m=1,2,3,\ldots. \end{aligned}\right\}$$

$$\epsilon = 0, \qquad (3.1.42)$$

and

$$f^{(1)}_{2m,i} = 0, \qquad \epsilon \to \infty. \qquad (3.1.43)$$

By integrating (3.1.40) with respect to ϵ once, and dividing the result by $(1+\epsilon^2)$ we find that

$$\frac{df_{0,i}^{(1)}}{d\epsilon} = \frac{aA_i}{\kappa_i^{\frac{1}{2}}}\left[\cot^{-1}\epsilon - \frac{\epsilon}{1+\epsilon^2}\right] - \frac{B_i}{1+\epsilon^2}\ , \tag{3.1.44}$$

where $-B_i$ denotes integration constants. By the substitution of (3.1.44) into (3.1.42) we see that

$$\frac{k_1A_1}{\kappa_1^{\frac{1}{2}}}\frac{\pi}{2} - k_1B_1 + \frac{k_2A_2}{\kappa_2^{\frac{1}{2}}}\frac{\pi}{2} - k_2B_2 = \frac{\pi}{2}\left[\frac{k_1A_1}{\kappa_1^{\frac{1}{2}}} + \frac{k_2A_2}{\kappa_2^{\frac{1}{2}}}\right]\ ,$$

which clearly results in

$$k_1B_1 + k_2B_2 = 0\ . \tag{3.1.45}$$

Further integration of (3.1.44) with respect to ϵ yields

$$f_{0,i}^{(1)} = \frac{aA_i}{\kappa_i^{\frac{1}{2}}}\left[\epsilon\cot^{-1}\epsilon + C_i\right] + B_i\cot^{-1}\epsilon\ , \tag{3.1.46}$$

where C_i denotes the second set of integration constants. In order to satisfy (3.1.38) we require $C_1 = C_2 = -1$ and the substitution of (3.1.46) into (3.1.42) leads to

$$-\frac{aA_1}{\kappa_1^{\frac{1}{2}}} + (\tfrac{\pi}{2})B_1 = -\frac{aA_2}{\kappa_2^{\frac{1}{2}}} + (\tfrac{\pi}{2})B_2\ . \tag{3.1.47}$$

Upon solution of the set of algebraic equations (3.1.45) and (3.1.47), explicit expressions for B_1 and B_2 are found to be

$$B_1 = \frac{2a}{\pi} \frac{k_2}{(k_1 + k_2)} \left[\frac{A_1}{\kappa_1^{\frac{1}{2}}} - \frac{A_2}{\kappa_2^{\frac{1}{2}}} \right] ,$$

and

$$B_2 = - \frac{2a}{\pi} \frac{k_1}{(k_1 + k_2)} \left[\frac{A_1}{\kappa_1^{\frac{1}{2}}} - \frac{A_2}{\kappa_2^{\frac{1}{2}}} \right] . \qquad (3.1.48)$$

For $m \geq 1$, we again have a trivial solution

$$f^{(1)}_{2m,\,i}(\epsilon) = 0 , \qquad (3.1.49)$$

which satisfies (3.1.41-3.1.43).

Order p

$$\frac{d}{d\epsilon}\left[(1+\epsilon^2)\frac{df^{(2)}_{2m,\,i}}{d\epsilon}\right] - 2m(2m+1)f^{(2)}_{2m,\,i} = \frac{2a}{\kappa_i^{\frac{1}{2}}}\left[(1+\epsilon^2)\frac{df^{(1)}_{2m,i}}{d\epsilon} + \epsilon f^{(1)}_{2m,\,i}\right]$$

$$+ \frac{a^2}{\kappa_i}\left[a_{2m} f^{(0)}_{2m-2,\,i} + (b_{2m} - 1) f^{(0)}_{2m,\,i} + C_{2m} f^{(0)}_{2m+2,\,i}\right] ,$$

$$0 < \epsilon < \infty , \qquad (3.1.50)$$

subject to

$$\left.\begin{aligned} f^{(2)}_{2m,\,1} &= f^{(2)}_{2m,\,2} \\ k_1 \frac{df^{(2)}_{2m,\,1}}{d\epsilon} + k_2 \frac{df^{(2)}_{2m,\,2}}{d\epsilon} &= a\left[\frac{k_1}{\kappa_1^{\frac{1}{2}}} f^{(1)}_{2m,\,1} + \frac{k_2}{\kappa_2^{\frac{1}{2}}} f^{(1)}_{2m,\,2}\right] \end{aligned}\right\} ,$$

$$\epsilon = 0 , \qquad (3.1.51)$$

and

$$f^{(2)}_{2m,i} = 0, \qquad \epsilon \to \infty . \tag{3.1.52}$$

For $m = 0$, (3.1.50-3.1.53) take the form

$$\frac{d}{d\epsilon}[(1+\epsilon^2)\frac{df^{(2)}_{0,i}}{d\epsilon}] = \frac{2a^2A_i}{\kappa_i}[(\frac{2}{3}+2\epsilon^2)\cot^{-1}\epsilon - 2\epsilon] + \frac{2a}{\kappa_i^{\frac{1}{2}}}B_i[\epsilon\cot^{-1}\epsilon - 1],$$

$$0 < \epsilon < \infty, \tag{3.1.53}$$

subject to

$$f^{(2)}_{0,1} = f^{(2)}_{0,2}, \qquad \epsilon = 0, \tag{3.1.54a}$$

$$k_1\frac{df^{(2)}_{0,1}}{d\epsilon} + k_2\frac{df^{(2)}_{0,2}}{d\epsilon} = -a^2[\frac{A_1k_1}{\kappa_1} + \frac{A_2k_2}{\kappa_2}] + \frac{\pi}{2}a[\frac{k_1B_1}{\kappa_1^{\frac{1}{2}}} + \frac{k_2B_2}{\kappa_2^{\frac{1}{2}}}],$$

$$\epsilon = 0, \tag{3.1.54b}$$

and

$$f_{0,i} = 0, \qquad \epsilon \to \infty . \tag{3.1.55}$$

Upon integrating (3.1.53) with respect to ϵ once, and then dividing by $(1+\epsilon^2)$, we obtain

$$\frac{df^{(2)}_{0,i}}{d\epsilon} = \frac{4a^2A_i}{3\kappa_i}[\epsilon\cot^{-1}\epsilon - 1 + \frac{1}{1+\epsilon^2}] + \frac{aB_i}{\kappa_i^{\frac{1}{2}}}[\cot^{-1}\epsilon - \frac{\epsilon}{1+\epsilon^2}] - \frac{D_i}{1+\epsilon^2},$$

(3.1.56)

where $-D_i$ denotes a set of integration constants. In order to satisfy (3.1.54b) we require

$$k_1 D_1 + k_2 D_2 = a^2\left[\frac{A_1 k_1}{\kappa_1} + \frac{A_2 k_2}{\kappa_2}\right] . \tag{3.1.57}$$

The integration of (3.1.56) with respect to ϵ yields

$$f^{(2)}_{0,i} = \frac{2a^3 A_i}{3\kappa_i}\left[(\epsilon^2 - 1)\cot^{-1}\epsilon - \epsilon\right] + \frac{aB_i}{\kappa_i^{\frac{1}{2}}}\epsilon\cot^{-1}\epsilon + D_i\cot^{-1}\epsilon + E_i, \tag{3.1.58}$$

where the integration constants are denoted by E_i, which upon satisfying (3.1.55) is found to be

$$E_i = -\frac{aB_i}{\kappa_i^{\frac{1}{2}}} . \tag{3.1.59}$$

In addition to (3.1.57), another relation between D_1 and D_2 is obtained by satisfying (3.1.54a). This relation is given by

$$D_1 - D_2 = \frac{2}{\pi} a\left[\frac{B_1}{\kappa_1^{\frac{1}{2}}} + \frac{B_2}{\kappa_2^{\frac{1}{2}}}\right] + \frac{2}{3} a^2\left[\frac{A_1}{\kappa_1} - \frac{A_2}{\kappa_2}\right] . \tag{3.1.60}$$

Explicit expressions for D_1 and D_2 are found from these two relations as

$$D_1 = \frac{1}{(k_1+k_2)}\left[\frac{2}{\pi} ak_2\left(\frac{B_1}{\kappa_1^{\frac{1}{2}}} - \frac{B_2}{\kappa_2^{\frac{1}{2}}}\right) + a^2\left(\frac{3k_1+2k_2}{3\kappa_1} A_1 + \frac{k_2}{3\kappa_2} A_2\right)\right] ,$$

and

$$D_2 = \frac{1}{(k_1+k_2)}\left[-\frac{2}{\pi} ak_2\left(\frac{B_1}{\kappa_1^{\frac{1}{2}}} - \frac{B_2}{\kappa_2^{\frac{1}{2}}}\right) + a^2\left(\frac{k_1}{3\kappa_1} A_1 + \frac{2k_1+3k_2}{3\kappa_2} A_2\right)\right] .$$

(3.1.61)

For $m = 1$, (3.1.50-3.1.52) may be written as

$$\frac{d^2 f_{2,i}^{(2)}}{d\epsilon^2} + \frac{2\epsilon}{1+\epsilon^2} \frac{d^2 f_{2,i}^{(2)}}{d\epsilon} - \frac{6}{1+\epsilon^2} f_{2,i}^{(2)} = \frac{2a^2 A_i}{15\kappa_i} \frac{\cot^{-1}\epsilon}{1+\epsilon^2} ,$$

$$0 < \epsilon < \infty , \qquad (3.1.62)$$

subject to

$$f_{2,1}^{(2)} = f_{2,2}^{(2)} , \qquad \epsilon = 0 , \qquad (3.1.63a)$$

$$k_1 \frac{df_{2,1}^{(2)}}{d\epsilon} + k_2 \frac{df_{2,2}^{(2)}}{d\epsilon} = 0 , \qquad \epsilon = 0 , \qquad (3.1.63b)$$

and

$$f_{2,i}^{(2)} = 0 , \qquad \epsilon \to \infty . \qquad (3.1.64)$$

This set of equations may be solved by the variation of parameters. The homogeneous part of (3.1.62) has two solutions, y_1 and y_2 given by

$$y_1 = \frac{1}{2}[(1 + 3\epsilon^2)\cot^{-1}\epsilon - 3\epsilon] \quad , \tag{3.1.65}$$

and

$$y_2 = \frac{1}{2}(1 + 3\epsilon^2) \quad . \tag{3.1.66}$$

The particular solution to (3.1.62) may be written as

$$f^{(2)}_{2,i} = v_{1,i}(\epsilon)y_1(\epsilon) + v_{2,i}(\epsilon)y_2(\epsilon) \quad , \tag{3.1.67}$$

where

$$v_{1,i}(\epsilon) = -\int_{\epsilon_1}^{\epsilon} \frac{y_2(\xi)R_i(\xi)}{W(\xi)}\, d\xi \quad , \tag{3.1.68}$$

and

$$v_{2,i}(\epsilon) = \int_{\epsilon_2}^{\epsilon} \frac{y_1(\xi)R_i(\xi)}{W(\xi)}\, d\xi \quad . \tag{3.1.69}$$

Here $W(\xi)$ is the Wronskian,

$$W(\xi) = \begin{vmatrix} y_1(\xi) & y_2(\xi) \\ y_1'(\xi) & y_2(\xi) \end{vmatrix} = \frac{1}{1 + \xi^2} \tag{3.1.70}$$

and

$$R_i(\xi) = \frac{2}{15}\frac{a^2}{\kappa_i} A_i \frac{\cot^{-1}\xi}{1 + \xi^2} \tag{3.1.71}$$

is the function on the right side of (3.1.62). By simple integration in (3.1.68-3.1.69) we obtain

$$v_{1,i} = -\frac{a^2 A_i}{30\kappa_i}[\epsilon(1+\epsilon^2)\cot^{-1}\epsilon + \frac{1}{2}\epsilon^2] + F_i \quad , \tag{3.1.72}$$

and

$$v_{2,i} = \frac{a^2 A_i}{30\kappa_i}[\epsilon(1+\epsilon^2)(\cot^{-1}\epsilon)^2 - \frac{1}{2}(1+\epsilon^2)\cot^{-1}\epsilon - \frac{1}{2}\epsilon] + G_i \, , \tag{3.1.73}$$

where F_i and G_i denote integration constants. By the substitution of (3.1.72) and (3.1.73) into (3.1.67) we obtain

$$f^{(2)}_{2,i} = \frac{a^2 A_i}{60\kappa_i}[(\epsilon^2 - 1)\cot^{-1}\epsilon - \epsilon] + F_i \frac{1}{2}[(1+3\epsilon^2)\cot^{-1}\epsilon - 3\epsilon] + G_i \frac{1}{2}[1+3\epsilon^2] \, . \tag{3.1.74}$$

The condition (3.1.64) requires that $G_i = 0$. By satisfying (3.1.63a) we find

$$F_1 - F_2 = \frac{a^2}{30}[\frac{A_1}{\kappa_1} - \frac{A_2}{\kappa_2}] \, . \tag{3.1.75}$$

By further requiring (3.1.63b) on (3.1.74) another relation between F_1 and F_2 is found to be

$$k_1 F_1 + k_2 F_2 = 0. \tag{3.1.76}$$

From these two relations, explicit expressions for F_1 and F_2 are found to be given by

$$\left.\begin{aligned} F_1 &= \frac{k_2}{(k_1 + k_2)} \frac{a^2}{30} \left[\frac{A_1}{\kappa_1} - \frac{A_2}{\kappa_2}\right] , \\ \text{and} \\ F_2 &= -\frac{k_1}{(k_1 + k_2)} \frac{a^2}{30} \left[\frac{A_1}{\kappa_1} - \frac{A_2}{\kappa_2}\right] . \end{aligned}\right\} \qquad (3.1.77)$$

For $m \geq 2$, the solutions can readily be shown to be $f^{(2)}_{2m,\,i} = 0$.

Order $p^{3/2}$

$$\frac{d}{d\epsilon}\left[(1+\epsilon^2)\frac{df^{(3)}_{2m,\,i}}{d\epsilon}\right] - 2m(2m+1) f^{(3)}_{2m,\,i}$$

$$= \frac{2a}{\kappa_i^{\frac{1}{2}}}\left[(1+\epsilon^2)\frac{df^{(2)}_{2m,\,i}}{d\epsilon} + \epsilon f^{(2)}_{2m,\,i}\right] + \frac{a^2}{\kappa_i}(b_{2m} - 1) f^{(1)}_{2m,\,i} ,$$

$$0 < \epsilon < \infty , \qquad (3.1.78)$$

subject to

$$f^{(3)}_{2m,\,1} = f^{(3)}_{2m,\,2} , \qquad \epsilon = 0 , \qquad (3.1.79)$$

$$k_1 \frac{df^{(3)}_{2m,\,1}}{d\epsilon} + k_2 \frac{df^{(3)}_{2m,\,2}}{d\epsilon} = a\left[\frac{k_1}{\kappa_1^{\frac{1}{2}}} f^{(2)}_{2m,\,1} + \frac{k_2}{\kappa_2^{\frac{1}{2}}} f^{(2)}_{2m,\,2}\right] ,$$

$$\epsilon = 0 , \qquad (3.1.80)$$

and

$$f^{(3)}_{2m,i} = 0 , \qquad \epsilon \to \infty . \tag{3.1.81}$$

For $m = 0$, we have

$$\frac{d}{d\epsilon}[(1+\epsilon^2)\frac{df^{(3)}_{0,i}}{d\epsilon}] = \frac{2a}{\kappa_i^{\frac{1}{2}}}\left\{\frac{4}{3}\frac{a^2A_i}{\kappa_i}[\epsilon(1+\epsilon^2)\cot^{-1}\epsilon - \epsilon^2]\right.$$

$$+ \frac{aB_i}{\kappa_i^{\frac{1}{2}}}[(1+\epsilon^2)\cot^{-1}\epsilon - \epsilon] - D_i + \frac{2}{3}\frac{a^2A_i}{\kappa_i}[\epsilon(\epsilon^2-1)\cot^{-1}\epsilon - \epsilon^2]$$

$$+ \frac{aB_i}{\kappa_i^{\frac{1}{2}}}[\epsilon^2\cot^{-1}\epsilon - \epsilon] + D_i\epsilon\cot^{-1}\epsilon\Big\} - \frac{a^2}{\kappa_i}\frac{2}{3}\left\{\frac{aA_i}{\kappa_i^{\frac{1}{2}}}[\epsilon\cot^{-1}\epsilon - 1]\right.$$

$$+ \left.B_i\cot^{-1}\epsilon\right\} = \frac{2a^3A_i}{3\kappa_i^{3/2}}[(6\epsilon^3+\epsilon)\cot^{-1}\epsilon - 6\epsilon^2 + 1]$$

$$+ \frac{2a^2B_i}{3\kappa_i}[(6\epsilon^2+2)\cot^{-1}\epsilon - 6\epsilon] + \frac{2aD_i}{\kappa_i^{\frac{1}{2}}}[\epsilon\cot^{-1}\epsilon - 1] , \tag{3.1.82}$$

subject to

$$f^{(3)}_{0,1} = f^{(3)}_{0,2} , \qquad \epsilon = 0 , \tag{3.1.83a}$$

$$k_1\frac{df^{(3)}_{0,1}}{d\epsilon} + k_2\frac{df^{(3)}_{0,2}}{d\epsilon} = \frac{ak_1}{\kappa_1^{\frac{1}{2}}}[\frac{\pi}{2}(D_1 - \frac{2a^2A_1}{3\kappa_1}) - \frac{aB_1}{\kappa_1^{\frac{1}{2}}}]$$

$$+ \frac{ak_2}{\kappa_2^{\frac{1}{2}}}[\frac{\pi}{2}(D_2 - \frac{2a^2A_2}{3\kappa_2}) - \frac{aB_2}{\kappa_2^{\frac{1}{2}}}] ,$$

$$\epsilon = 0 , \tag{3.1.83b}$$

and

$$f^{(3)}_{0,i} = 0 \ , \qquad \epsilon \to \infty . \tag{3.1.84}$$

The integration of (3.1.82) once and the division of the result by $(1 + \epsilon^2)$ yields

$$\frac{df^{(3)}_{0,i}}{d\epsilon} = \frac{2a^3 A_i}{3\kappa_i^{3/2}}\left[\left(\frac{3}{2}\epsilon^2 - 1\right)\cot^{-1}\epsilon - \frac{3}{2}\epsilon + \frac{3}{2}\frac{\epsilon}{1+\epsilon^2}\right]$$

$$+ \frac{2a^2 B_i}{3\kappa_i}\left[2(\epsilon\cot^{-1}\epsilon - 1) + \frac{2}{1+\epsilon^2}\right] + \frac{aD_i}{\kappa_i^{\frac{1}{2}}}\left[\cot^{-1}\epsilon - \frac{\epsilon}{1+\epsilon^2}\right] - \frac{H_i}{1+\epsilon^2} \ , \tag{3.1.85}$$

where $-H_i$ denotes integration constants. By satisfying (3.1.80) we obtain a relation between H_1 and H_2 as

$$k_1 H_1 + k_2 H_2 = a^2\left[\frac{k_1 B_1}{\kappa_1} + \frac{k_2 B_2}{\kappa_2}\right] . \tag{3.1.86}$$

Further integration of (3.1.85) yields

$$f^{(3)}_{0,i} = \frac{a^3 A_i}{3\kappa_i^{3/2}}\left[(\epsilon^3 - 2\epsilon)\cot^{-1}\epsilon - \epsilon^2\right] + \frac{2a^2 B_i}{3\kappa_i}\left[(\epsilon^2 - 1)\cot^{-1}\epsilon - \epsilon\right]$$

$$+ \frac{aD_i}{\kappa_i^{\frac{1}{2}}}\epsilon\cot^{-1}\epsilon + H_i\cot^{-1}\epsilon + L_i \ , \tag{3.1.87}$$

where the integration constants are denoted by L_i, which upon requiring (3.1.81) to be satisfied turns out to be

$$L_i = \frac{7a^3 A_i}{9\kappa_i^{3/2}} - \frac{aD_i}{\kappa_i^{\frac{1}{2}}} \quad . \tag{3.1.88}$$

Equation (3.1.79) gives a second relation between H_1 and H_2 as

$$H_1 - H_2 = \frac{2a^2}{3}\left[\frac{B_1}{\kappa_1} - \frac{B_2}{\kappa_2}\right] - \frac{2}{\pi}(L_1 - L_2) \quad . \tag{3.1.89}$$

Simultaneous solution of (3.1.86) and (3.1.89) gives

$$\left.\begin{aligned} H_1 &= \frac{1}{(k_1+k_2)}\left\{\frac{2}{3}a^2 k_2\left[\frac{B_1}{\kappa_1} - \frac{B_2}{\kappa_2}\right] + a^2\left[\frac{k_1 B_1}{\kappa_1} + \frac{k_2 B_2}{\kappa_2}\right] - \frac{2}{\pi}k_2(L_1 - L_2)\right\}, \\ \text{and} \\ H_2 &= \frac{1}{(k_1+k_2)}\left\{-\frac{2}{3}a^2 k_1\left[\frac{B_1}{\kappa_1} - \frac{B_2}{\kappa_2}\right] + a^2\left[\frac{k_1 B_1}{\kappa_1} + \frac{k_2 B_2}{\kappa_2}\right] + \frac{2}{\pi}k_1(L_1 - L_2)\right\}. \end{aligned}\right\} \tag{3.1.90}$$

For $m \geq 1$, $f^{(3)}_{2m,i} = 0$ satisfies (3.1.78-3.1.81) and is therefore the solution.

Higher order terms may be obtained but the calculations become cumbersome. In the next section the solutions obtained are inverted to give temperature distributions valid for large values of the Fourier number, $Fo_i = a^2/(\kappa_i t)$.

3.1.4 Inversion of the Solutions

From (3.1.26) we see that

$$\Phi_{0,i}(\epsilon, p)= \frac{1}{p}[f^{(0)}_{0,i}(\epsilon)+ p^{\frac{1}{2}}f^{(1)}_{0,i}(\epsilon)+ pf^{(2)}_{0,i}(\epsilon)+ p^{3/2}f^{(3)}_{0,i}+\ldots]\exp[-(p/\kappa_i)^{\frac{1}{2}}a\epsilon] , \tag{3.1.91}$$

$$\Phi_{2,i}(\epsilon , p) = \frac{1}{p}[pf^{(2)}_{2,i}(\epsilon) + \ldots] \exp [-(p/\kappa_i)^{\frac{1}{2}}a\epsilon] , \tag{3.1.92}$$

and for $m \geq 2$, we may take $\Phi_{2m,i}(\epsilon, p) = 0$ up to an order $p^{\frac{1}{2}}\exp[-(p/\kappa_i)^{\frac{1}{2}} a\epsilon]$.

By carrying out the inverse Legendre transform on $\Phi_{2m,i}(\epsilon, p)$, we find that

$$\textcircled{H}_i(\epsilon, \eta, p) = \sum_{m=0}^{\infty} (4m+1)\Phi_{2m,i}(\epsilon, p)P_{2m}(\eta) \tag{3.1.93}$$

$$= \Bigg[\frac{1}{p}A_i\cot^{-1}\epsilon + \frac{1}{p^{\frac{1}{2}}}\{\frac{aA_i}{\kappa_i^{\frac{1}{2}}}(\epsilon\cot^{-1}\epsilon-1)+ B_i\cot^{-1}\epsilon\}$$

$$+ \{\frac{2a^2A_i}{3\kappa_i}[(\epsilon^2- 1)\cot^{-1}\epsilon -\epsilon] + \frac{aB_i}{\kappa_i^{\frac{1}{2}}}[\epsilon\cot^{-1}\epsilon -1] + D_i\cot^{-1}\epsilon\}$$

$$+ \{\frac{a^2A_i}{60\kappa_i}[(\epsilon^2- 1)\cot^{-1}\epsilon - \epsilon]+ \frac{1}{2}F_i[(1+3\epsilon^2)\cot^{-1}\epsilon -\epsilon]\}\frac{5}{2}(3\eta^2- 1)$$

$$+ p^{\frac{1}{2}}\{\frac{a^3A_i}{3\kappa_i^{3/2}}[\epsilon^3- 2\epsilon)\cot^{-1}\epsilon - \epsilon^2+\frac{7}{3}]+ \frac{2a^2B_i}{3\kappa_i}[(\epsilon^2- 1)\cot^{-1}\epsilon - \epsilon]$$

$$+ \frac{aD_i}{\kappa_i^{\frac{1}{2}}}[\epsilon\cot^{-1}\epsilon- 1]+ H_i\cot^{-1}\epsilon\}+ \ldots\Bigg] \exp[-(p/\kappa_i)^{\frac{1}{2}}a\epsilon] .$$

Upon the inversion of $\Theta_i(\epsilon, \eta, \rho)$ into the time domain by the Mellin integral, we obtain the dimensionless temperature distribution to be

$$\theta_i(\epsilon,\eta,t) = A_i(\cot^{-1}\epsilon)\,\mathrm{erfc}\left[\frac{a\epsilon}{2(\kappa_i t)^{\frac{1}{2}}}\right] + \left[\left\{\frac{aA_i}{\kappa_i^{\frac{1}{2}}}(\epsilon\cot^{-1}\epsilon - 1) + B_i\cot^{-1}\epsilon\right\}\frac{1}{(\pi t)^{\frac{1}{2}}}\right.$$

$$+ \left[\left\{\frac{2a^2A_i}{3\kappa_i}[(\epsilon^2-1)\cot^{-1}\epsilon - \epsilon] + \frac{aB_i}{\kappa_i^{\frac{1}{2}}}[\epsilon\cot^{-1}\epsilon - 1] + D_i\cot^{-1}\epsilon\right\}\right.$$

$$\left.\left. + \left\{\frac{a^2A_i}{60\kappa_i}[(\epsilon^2-1)\cot^{-1}\epsilon - \epsilon] + \frac{1}{2}F_i[(1+3\epsilon^2)\cot^{-1}\epsilon - 3\epsilon]\right\}\frac{5}{2}(3\eta^2-1)\right]\right.$$

$$\times \frac{a\epsilon}{2(\pi\kappa_i t)^{\frac{1}{2}}} + \left\{\frac{a^3A_i}{3\kappa_i^{3/2}}[(\epsilon^3-2\epsilon)\cot^{-1}\epsilon - \epsilon^2 + \frac{7}{3}] + \frac{2a^2B_i}{3\kappa_i}[(\epsilon^2-1)\cot^{-1}\epsilon - \epsilon]\right.$$

$$\left.\left. + \frac{aD_i}{\kappa_i^{\frac{1}{2}}}[\epsilon\cot^{-1}\epsilon - 1] + H_i\cot^{-1}\epsilon\right\}\left[\frac{a^2\epsilon^2}{4\kappa_i t} - \frac{1}{2}\right]\frac{1}{(\pi t^3)^{\frac{1}{2}}} + \ldots.\right]\right.$$

$$\times \exp\left[-\frac{a^2\epsilon^2}{4\kappa_i t}\right], \qquad (3.1.94)$$

which, after rearranging some terms, may be written as

$$\theta_i(\epsilon,\eta,t) = A_i(\cot^{-1}\epsilon)\,\mathrm{erfc}\left[\frac{a\epsilon}{2(\kappa_i t)^{\frac{1}{2}}}\right] + \left[\left\{A_i(\epsilon\cot^{-1}\epsilon - 1) + \frac{B_i\kappa_i^{\frac{1}{2}}}{a}\cot^{-1}\epsilon\right\}\right.$$

$$\times \frac{a}{(\pi\kappa_i t)^{\frac{1}{2}}} + \left[\frac{A_i}{6}[\epsilon^3\cot^{-1}\epsilon - \epsilon^2 - \frac{7}{3}] + \frac{B_i\kappa_i^{\frac{1}{2}}}{6a}[(\epsilon^2+2)\cot^{-1}\epsilon - \epsilon] + \frac{D_i\kappa_i}{2a^2}\right.$$

$$+ \left\{\frac{A_i}{48}[(\epsilon^3-\epsilon)\cot^{-1}\epsilon - \epsilon^2] + \frac{5F_i\kappa_i}{8a^2}[(3\epsilon^3+\epsilon)\cot^{-1}\epsilon - 3\epsilon^2]\right\}(3\eta^2-1)$$

$$\left.\left. - \frac{H_i\kappa_i^{3/2}}{2a^3}\cot^{-1}\epsilon\right]\frac{a^3}{(\pi\kappa_i^3 t^3)^{\frac{1}{2}}} + \ldots\right]\exp\left[-\frac{a^2\epsilon^2}{4\kappa_i t}\right]. \quad (3.1.95)$$

For small $a\epsilon/(4\kappa_i t)^{\frac{1}{2}}$ we may expand $\mathrm{erfc}[a\epsilon/(4\kappa_i t)^{\frac{1}{2}}]$ and $\exp[-a^2\epsilon^2/(4\kappa_i t)]$ to give

$$\theta_i(\epsilon,\eta,t) = A_i\cot^{-1}\epsilon + \left\{\frac{B_i\kappa_i^{\frac{1}{2}}}{a}\cot^{-1}\epsilon - A_i\right\}\frac{a}{(\pi\kappa_i t)^{\frac{1}{2}}}$$

$$+ \left[A_i[\frac{1}{6}\epsilon^3\cot^{-1}\epsilon + \frac{1}{12}\epsilon^2 - \frac{7}{18}] - \frac{B_i\kappa_i^{\frac{1}{2}}}{a}[(\frac{1}{12}\epsilon^2 - \frac{1}{3})\cot^{-1}\epsilon + \frac{1}{6}\epsilon]\right.$$

$$+ \frac{D_i\kappa_i}{2a^2} + \left\{\frac{A_i}{48}[(\epsilon^3-\epsilon)\cot^{-1}\epsilon - \epsilon^2] + \frac{5F_i\kappa_i}{8a^2}[3\epsilon^2+\epsilon)\cot^{-1}\epsilon - 3\epsilon^2]\right\}$$

$$\left.\times(3\eta^2-1) - \frac{H_i\kappa_i^{\frac{1}{2}}}{2a^3}\cot^{-1}\epsilon\right]\frac{a^3}{(\pi\kappa_i^3 t^3)^{\frac{1}{2}}} + \ldots\ldots \quad (3.1.96)$$

For the special case $k_1 \to \infty$ we have

$$A_1 = B_1\kappa_1^{\frac{1}{2}} = D_1\kappa_1 = F_1\kappa_1 = H_1\kappa_1^{3/2} = 0$$

and

$$A_2 = \frac{2}{\pi} ,$$

$$B_2\kappa_2^{\frac{1}{2}} = \frac{4a}{\pi^2} ,$$

$$D_2\kappa_2 = (\frac{8}{\pi^3} + \frac{4}{3\pi})a^2 ,$$

$$F_2\kappa_2 = \frac{a^2}{15\pi} ,$$

$$H_2\kappa_2^{3/2} = -[\frac{28}{9\pi^2} + \frac{16}{\pi^4}]a^3 .$$

The temperature distributions for this case may be written as

$$\frac{T_1 - T_{10}}{T_{10} - T_{20}} = \theta_1 = 0 , \qquad (3.1.97)$$

and

$$\frac{T_2 - T_{20}}{T_{10} - T_{20}} = \theta_2 = \frac{2}{\pi}(\cot^{-1}\epsilon)\,\mathrm{erfc}[\frac{a\epsilon}{2(\kappa_2 t)^{\frac{1}{2}}}] + \frac{1}{\pi^{\frac{1}{2}}}\Bigg[\{\frac{2}{\pi}(\epsilon\cot^{-1}\epsilon - 1) + \frac{4}{\pi^2}\cot^{-1}\epsilon\}$$

$$\times \frac{a}{(\kappa_2 t)^{\frac{1}{2}}} + \Bigg\{\frac{1}{3\pi}[\epsilon^3\cot^{-1}\epsilon - \epsilon^2 - \frac{1}{3}] + \frac{2}{3\pi^2}[\epsilon^2\cot^{-1}\epsilon - \epsilon] + \frac{4}{\pi^3}$$

$$+ \frac{1}{24\pi}[\epsilon^3\cot^{-1}\epsilon - \epsilon^2](3\eta^2 - 1) + (\frac{14}{9\pi^2} + \frac{8}{\pi^4})\cot^{-1}\epsilon\Bigg\}\frac{a^3}{(\kappa_2 t)^{\frac{1}{2}}} + \ldots.$$

$$\times \exp[-\frac{a^2\epsilon^2}{4\kappa_2 t}] . \qquad (3.1.98)$$

For $a\epsilon/(\kappa_2 t)^{\frac{1}{2}} \ll 1$, we have

$$\theta_2 = \frac{2}{\pi}\left[\cot^{-1}\epsilon + \frac{1}{\epsilon}\left[\frac{2}{\pi}\cot^{-1}\epsilon - 1\right]\frac{a\epsilon}{(\pi\kappa_2 t)^{\frac{1}{2}}}\right. \tag{3.1.99}$$

$$+ \left\{\frac{1}{12}\cot^{-1}\epsilon + \frac{1}{6\epsilon} - \frac{1}{6\pi\epsilon}\cot^{-1}\epsilon - \frac{1}{3\pi\epsilon^2} + \frac{5}{36\epsilon^3} + \frac{2}{\pi^2\epsilon^3}\right.$$

$$\left.\left. + \frac{1}{\epsilon^3}\left[\frac{7}{9\pi} + \frac{4}{\pi^3}\right]\cot^{-1}\epsilon + \frac{1}{4\epsilon}\left[\epsilon\cot^{-1}\epsilon - 1\right]\eta^2\right\}\frac{a^3\epsilon^3}{(\pi\kappa_2^3 t^3)^{\frac{1}{2}}}\right] + \ldots .$$

This result corresponds to the situation in which a semi-infinite solid, initially at a uniform temperature T_{20} , has a circular region at the surface exposed to a temperature T_{10} for $t > 0$; the remainder of the surface is insulated. The results of Norminton and Blackwell [4] agree with (3.1.98) and (3.1.99) only up to orders $a/(\pi\kappa_2 t)^{\frac{1}{2}} \times \exp[-a^2\epsilon^2/(4\kappa_2 t)]$ and $a\epsilon/(\pi\kappa_2 t)^{\frac{1}{2}}$, respectively. For the next higher order terms, the error in [4] is due to the omission of the term $f_{0,2}^{(3)}(\epsilon, p)$, which, as we can see in (3.1.94) makes a contribution of order $a^3/(\pi\kappa_2^3 t^3)^{\frac{1}{2}} \exp[-a^2\epsilon^2/(4\kappa_2 t)]$ along with $f_{0,2}^{(2)}(\epsilon, p)$ and $f_{2,2}^{(2)}(\epsilon, p)$.

3.1.5 Calculation of Heat Flow and Interface Temperature

The total heat flow, Q, across the interface is given by

$$Q = \int_0^1 \left[- k_2 \frac{1}{a\eta} \frac{\partial T_2}{\partial \epsilon} \bigg|_{\epsilon=0} \right] 2\pi a^2 \eta \, d\eta$$

$$= \int_0^1 \left[k_1 \frac{1}{a\eta} \frac{\partial T_1}{\partial \epsilon} \bigg|_{\epsilon=0} \right] 2\pi a^2 \eta \, d\eta$$

$$= 2\pi a k_1 (T_{10} - T_{20}) \int_0^1 \frac{\partial \theta_1}{\partial \epsilon} \bigg|_{\epsilon=0} d\eta$$

$$= 2\pi a k_1 (T_{10} - T_{20}) \int_0^1 \left\{ - A_1 - \frac{B_1 \kappa_1^{\frac{1}{2}}}{a} \frac{a}{(\pi \kappa_1 t)^{\frac{1}{2}}} \right.$$

$$+ \left[- \frac{B_1 \kappa_1^{\frac{1}{2}}}{2a} + \left(- \frac{A_1}{48} \frac{\pi}{2} + \frac{5 F_1 \kappa_1}{8a^2} \frac{\pi}{2} \right) (3\eta^2 - 1) \right.$$

$$\left. \left. + \frac{H_1 \kappa_1^{3/2}}{2a^3} \right] \frac{a^3}{(\pi \kappa_1^3 t^3)^{\frac{1}{2}}} + \ldots . \right\} d\eta$$

$$= 2\pi a k_1 (T_{10} - T_{20}) \left\{ - A_1 - \frac{B_1 \kappa_1^{\frac{1}{2}}}{a} \frac{a}{(\pi \kappa_1 t)^{\frac{1}{2}}} \right.$$

$$\left. + \left[- \frac{B_1 \kappa_1^{\frac{1}{2}}}{2a} + \frac{H_1 \kappa_1^{3/2}}{2a^3} \right] \frac{a^3}{(\pi \kappa_1^3 t^3)^{\frac{1}{2}}} + \ldots . \right\} . \qquad (3.1.100)$$

By the substitution of explicit expressions for A_1, B_1 and H_1 into (3.1.100) we obtain the following expression for the heat flow:

$$Q = 4a(T_{10}-T_{20})\frac{k_1k_2}{(k_1k_2)}\left\{1 + (\frac{2}{\pi})\frac{1}{(k_1+k_2)}\left[\frac{k_2}{\kappa_1^{\frac{1}{2}}} + \frac{k_1}{\kappa_2^{\frac{1}{2}}}\right]\frac{a}{(\pi t)^{\frac{1}{2}}}\right.$$

$$+ \frac{1}{2}(\frac{2}{\pi})\frac{1}{(k_1+k_2)^2}\left[\frac{4}{9}\left(\frac{k_1^2}{\kappa_1^{3/2}} + \frac{k_2^2}{\kappa_1^{3/2}}\right) - \frac{2}{9}k_1k_2\left(\frac{1}{\kappa_1^{3/2}} + \frac{1}{\kappa_2^{3/2}}\right)\right.$$

$$\left.\left. - (\frac{2}{\pi})^2\frac{1}{(k_1+k_2)^2}\left(\frac{k_2}{\kappa_1^{\frac{1}{2}}} + \frac{k_1}{\kappa_2^{\frac{1}{2}}}\right)^3\right]\frac{a^3}{(\pi t^3)^{\frac{1}{2}}} + \ldots\right\} . \qquad (3.1.101)$$

If we define the resistance as $R = (T_{10}-T_{20})/Q$, then we have, from (3.1.101),

$$R = R_{ss}\left\{1 + (\frac{2}{\pi})\frac{1}{(1+\frac{k_2}{k_1})}\left[\frac{k_2}{k_1}(\frac{\kappa_2}{\kappa_1})^{\frac{1}{2}} + 1\right](\pi Fo_2)^{-\frac{1}{2}}\right. \qquad (3.1.102)$$

$$+ \frac{1}{(1+\frac{k_2}{k_1})^2}\left[\frac{4}{9}\{(\frac{\kappa_2}{\kappa_1})^{3/2} + (\frac{k_2}{k_1})^2\} - \frac{2}{9}(\frac{k_2}{k_1})\{(\frac{\kappa_2}{\kappa_1})^{3/2} + 1\}\right.$$

$$\left.\left. - (\frac{2}{\pi})^2\frac{1}{(1+\frac{k_2}{k_1})}\{(\frac{k_2}{k_1})(\frac{\kappa_2}{\kappa_1})^{\frac{1}{2}} + 1\}^3\right](\pi Fo_2)^{-3/2} + \ldots\right\}^{-1} ,$$

where $R_{ss} = (k_1 + k_2)/[4a(T_{10} - T_{20})k_1k_2]$ is the steady-state

resistance and $Fo_2 = \kappa_2 t/a^2$ is the Fourier number based on the lower thermal diffusivity (i.e., $\kappa_2 < \kappa_1$). This result is presented in Fig. 3.1.2 for contacts between copper and steel, steel and glass, and copper and glass, with Fo_2 ranging between 1 and 10,000. The calculations show that the resistances for copper-glass and steel-glass contacts are almost the same. This behavior results because, for these cases, most of the resistance is that of the glass alone and the metals (steel or copper) make very little contribution.

The interface temperature, T_{if}, along the disk of contact is found by setting $\epsilon = 0$ in the expression for θ_2. By doing so we obtain

$$\theta_2\Big|_{\epsilon=0} = \frac{T_{if}-T_{20}}{T_{10}-T_{20}} = \frac{\pi}{2}A_2 + \left[\frac{B_2\kappa_2^{\frac{1}{2}}}{a}\left(\frac{\pi}{2}\right) - A_2\right]\frac{a}{(\pi\kappa_2 t)^{\frac{1}{2}}}$$

$$+ \left[-\frac{7}{18}A_2 + \frac{B_2\kappa_2^{\frac{1}{2}}}{3a}\left(\frac{\pi}{2}\right) + \frac{D_2\kappa_2}{2a^2} - \frac{H_2\kappa_2^{\frac{1}{2}}}{2a^3}\,\frac{\pi}{2}\right]$$

$$\times \frac{a^3}{(\pi\kappa_2^3 t^3)^{\frac{1}{2}}} + \cdots\cdots , \qquad (3.1.103)$$

which, upon the substitution of the explicit expressions for the various integration constants, becomes

$$\frac{T_{if}-T_{20}}{T_{10}-T_{20}} = \frac{k_1}{(k_1+k_2)} + \frac{2}{\pi}\frac{k_1k_2}{(k_1+k_2)^2}\left[\frac{1}{\kappa_1^{\frac{1}{2}}} - \frac{1}{\kappa_2^{\frac{1}{2}}}\right]\frac{a}{(\pi t)^{\frac{1}{2}}} + \frac{2}{\pi}\frac{k_1k_2}{(k_1+k_2)^3}$$

$$\times \left\{\frac{k_1-k_2}{6(\kappa_1\kappa_2)^{\frac{1}{2}}}\left[\frac{1}{\kappa_1^{\frac{1}{2}}} + \frac{1}{\kappa_2^{\frac{1}{2}}}\right] + \frac{2}{9}\left[\frac{k_2}{\kappa_1^{3/2}} - \frac{k_1}{\kappa_2^{3/2}}\right]\right.$$

$$- \frac{1}{9}\left[\frac{k_1}{\kappa_1^{3/2}} - \frac{k_2}{\kappa_2^{3/2}}\right] - \frac{1}{2}\left(\frac{2}{\pi}\right)^2\frac{1}{(k_1+k_2)}\left[\frac{k_2}{\kappa_1^{\frac{1}{2}}} + \frac{k_1}{\kappa_2^{\frac{1}{2}}}\right]^2$$

$$\left.\times \left[\frac{1}{\kappa_1^{\frac{1}{2}}} - \frac{1}{\kappa_2^{\frac{1}{2}}}\right]\right\} \frac{a^3}{(\pi t^3)^{\frac{1}{2}}} + \ldots . \qquad (3.1.104)$$

3.1.6 Discussion

The present work represents a generalization and a correction of the results obtained by Norminton and Blackwell [4]. In a numerical analysis by Schneider et al. [2], four combinations of solids were dealt with. In each case the ratio of the time-dependent resistance was plotted as a function of the Fourier number based on the lower thermal diffusivity. They showed that when the resistances ratio is plotted against the variable, $X = [1 + (\kappa_2/\kappa_1)^{\frac{1}{2}}] \times [\kappa_1\kappa_2/(\kappa_1 + \kappa_2)]t/a^2$, all the four cases lie close to a single curve. This curve, however, is not consistent with the individual plots they obtained, but it agrees approximately with equation (3.1.101) of the present study for Fourier numbers greater than unity.

The thermal resistance, in general, depends on the conductivity ratio, k_1/k_2, the diffusivity ratio, κ_1/κ_2, and the Fourier number $\kappa_2 t/a^2$, where we take $\kappa_2 < \kappa_1$. Schneider et al. [2] showed that for the cases they considered, the influence of the conductivity ratio appeared only in the steady-state part of the thermal resistance. They concluded that when the resistance is normalized with the steady-state value, the result depends only on the diffusivity ratio and the Fourier number. In the present study, however, equation (3.1.101) shows that the conclusion of Schneider et al. [2] is not necessarily valid. But it appears that for most materials of practical interest, the dependence on the conductivity is rather weak. This behavior results because large (small) conductivities generally represent large (small) diffusivities and any dependence on the conductivity ratio may be approximated by the diffusivity ratio.

3.2 Unsteady Heat Flow in Two Semi-Infinite Solids in Contact Over Equally Spaced Strips

3.2.1 Statement of Problem

Two semi-infinite solids initially at uniform but different temperatures are brought together and perfect thermal contact is established over a series of identical, equally spaced strips. The regions between these strips are assumed to be insulated. By recognizing the periodic nature of the problem, we can find planes of symmetry and we can require that the temperature distribution is an even function about these planes. These planes are taken to be a distance ℓ apart. As shown by broken lines in Fig. 3.0.3, the planes bisect the insulated regions and the regions of perfect contact. The insulated regions are shown by double lines and are taken to be a width $2c^*$.

The initially hotter solid is referred to as region 1 ($y^* > 0$) and the other solid as region 2 ($y^* < 0$), as shown in Fig. 3.0.3. The initial temperatures are denoted by T_{10} and T_{20} for regions 1 and 2, respectively. In the rest of the analysis the subscripts 1 and 2 are used in reference to the properties of the corresponding regions.

The conduction process is described by the heat equation which, under the conditions stated for the model, may be written as

$$\left.\begin{aligned} &\frac{\partial^2 T_1}{\partial x^{*2}} + \frac{\partial^2 T_1}{\partial y^{*2}} = \frac{1}{\kappa_1}\frac{\partial T_1}{\partial t}, \qquad t > 0;\ 0 \le x^* \le \ell;\ y^* > 0, \\ &\text{and} \\ &\frac{\partial^2 T_2}{\partial x^{*2}} + \frac{\partial^2 T_2}{\partial y^{*2}} = \frac{1}{\kappa_2}\frac{\partial T_2}{\partial t}, \qquad t > 0;\ 0 \le x^* \le \ell;\ y^* < 0, \end{aligned}\right\} \tag{3.2.1}$$

subject to

$$\left.\begin{aligned} &T_1 = T_{10}, \qquad t = 0;\ 0 \le x^* \le \ell;\ y^* \ge 0, \\ &T_2 = T_{20}, \qquad t = 0;\ 0 \le x^* \le \ell;\ y^* \le 0, \end{aligned}\right\} \tag{3.2.2}$$

$$\left.\begin{aligned} &\frac{\partial T_1}{\partial x^*} = 0, \qquad x^* = 0,\ x^* = \ell;\ t > 0;\ y^* \ge 0, \\ &\frac{\partial T_2}{\partial x^*} = 0, \qquad x^* = 0,\ x^* = \ell;\ t > 0;\ y^* \le 0, \end{aligned}\right\} \tag{3.2.3}$$

and

$$\left.\begin{aligned} &\left.\begin{aligned} &T_1 = T_2 \\ &k_1\frac{\partial T_1}{\partial y^*} = k_2\frac{\partial T_2}{\partial y^*} \end{aligned}\right], \qquad y^* = 0;\ t > 0;\ c^* < x^* \le \ell, \\ &\frac{\partial T_1}{\partial y^*} = \frac{\partial T_2}{\partial y^*} = 0, \qquad y^* = 0;\ t > 0;\ 0 \le x^* < c^*, \end{aligned}\right\} \tag{3.2.4}$$

where T_1 and T_2 denote the temperature distributions, k_1 and k_2 represent the thermal conductivities, κ_1 and κ_2 refer to the thermal diffusivities, x^* and y^* are the space coordinates, and t is the time.

3.2.2 Analysis

By introducing convenient dimensionless variables, $x = \pi x^*/\ell$, $y = \pi y^*/\ell$, $c = \pi c^*/\ell$, $\theta_1 = (T_1 - T_{20})/(T_{10} - T_{20})$ and $\theta_2 = (T_2 - T_{20})/(T_{10} - T_{20})$, we can write the equations (3.2.1-3.2.4) in the form

$$\left.\begin{aligned} \frac{\ell^2}{\pi^2 \kappa_1} \frac{\partial \theta_1}{\partial t} &= \frac{\partial^2 \theta_1}{\partial x^2} + \frac{\partial^2 \theta_1}{\partial y^2}, \quad t > 0; \quad 0 \le x \le \pi; \quad y > 0, \\ \frac{\ell^2}{\pi^2 \kappa_2} \frac{\partial \theta_2}{\partial t} &= \frac{\partial^2 \theta_2}{\partial x^2} + \frac{\partial^2 \theta_2}{\partial y^2}, \quad t > 0; \quad 0 \le x \le \pi; \quad y < 0, \end{aligned}\right\} \tag{3.2.5}$$

subject to

$$\left.\begin{aligned} \theta_1 &= 1, \quad t = 0; \quad 0 \le x \le \pi; \quad y \ge 0, \\ \theta_2 &= 0, \quad t = 0; \quad 0 \le x \le \pi; \quad y \le 0, \end{aligned}\right\} \tag{3.2.6}$$

$$\left.\begin{aligned} \frac{\partial \theta_1}{\partial x} &= 0, \quad x = 0, \quad x = \pi; \quad t > 0; \quad y \ge 0, \\ \frac{\partial \theta_2}{\partial x} &= 0, \quad x = 0, \quad x = \pi; \quad t > 0; \quad y \le 0, \end{aligned}\right\} \tag{3.2.7}$$

and

$$\left.\begin{aligned} &\theta_1 = \theta_2 \\ k_1 \frac{\partial \theta_1}{\partial y} &= k_2 \frac{\partial \theta_2}{\partial y} \end{aligned}\right], \qquad y = 0; \quad t > 0; \quad c < x \leq \pi ,$$

$$\frac{\partial \theta_1}{\partial y} = \frac{\partial \theta_2}{\partial y} = 0 , \qquad y = 0; \quad t > 0; \quad 0 \leq x < c . \tag{3.2.8}$$

Upon taking the Laplace transform of θ_i with respect to time, we obtain

$$\left.\begin{aligned} -\frac{\ell^2}{\pi^2 \kappa_1} + \frac{p\ell^2}{\pi^2 \kappa_1} \textcircled{H}_1 &= \frac{\partial^2 \textcircled{H}_1}{\partial x^2} + \frac{\partial^2 \textcircled{H}_1}{\partial y^2} , \qquad 0 \leq x \leq \pi; \quad y > 0 , \\ \frac{p\ell^2}{\pi^2 \kappa_2} \textcircled{H}_2 &= \frac{\partial^2 \textcircled{H}_2}{\partial x^2} + \frac{\partial^2 \textcircled{H}_2}{\partial y^2} , \qquad 0 \leq x \leq \pi; \quad y < 0 , \end{aligned}\right\} \tag{3.2.9}$$

subject to

$$\left.\begin{aligned} \frac{\partial \textcircled{H}_1}{\partial x} &= 0 , \quad x = 0 , \quad x = \pi; \quad y \geq 0 , \\ \frac{\partial \textcircled{H}_2}{\partial x} &= 0 , \quad x = 0 , \quad x = \pi; \quad y \leq 0 , \end{aligned}\right\} \tag{3.2.10}$$

and

$$\left.\begin{aligned} \Theta_1 &= \Theta_2 \\ k_1 \frac{\partial \Theta_1}{\partial y} &= k_2 \frac{\partial \Theta_2}{\partial y} \end{aligned}\right] \quad , \qquad y = 0;\ c < x \leq \pi \ , \qquad \left.\begin{aligned} \\ \\ \end{aligned}\right\}$$

$$\frac{\partial \Theta_1}{\partial y} = \frac{\partial \Theta_2}{\partial y} = 0 \ , \qquad y = 0;\ 0 \leq x < c \ , \qquad \left.\begin{aligned} \\ \\ \end{aligned}\right\} \qquad (3.2.11)$$

where

$$\Theta_i(x, y, p) = \int_0^\infty e^{-pt}\, \theta_i(x, y, t)\, dt \ , \qquad i = 1, 2, \qquad (3.2.12)$$

is the Laplace transform of $\theta_i(x, y, t)$.

In view of (3.2.10) the solution may be written as

$$\left.\begin{aligned} \Theta_1 &= \frac{1}{p} + \sum_{n=0}^{\infty} a_{n1} \exp[-(n^2 + p\ell^2/\pi^2\kappa_1)^{\frac{1}{2}} y] \cos nx, \\ &\qquad\qquad y \geq 0 \ , \\ \text{and} \\ \Theta_2 &= \sum_{n=0}^{\infty} a_{n2} \exp[(n^2 + p\ell^2/\pi^2\kappa_2)^{\frac{1}{2}} y] \cos nx, \\ &\qquad\qquad y \leq 0 \ . \end{aligned}\right\} \qquad (3.2.13)$$

By the substitution of (3.2.13) into (3.2.11) we see that we need to satisfy

$$\sum_{n=0}^{\infty} (a_{n2} - a_{n1}) \cos nx = \frac{1}{p} , \qquad c < x \leq \pi , \tag{3.2.14}$$

$$\sum_{n=0}^{\infty} \left[k_1 a_{n1} \left(n^2 + \frac{p\ell^2}{\pi^2 \kappa_1}\right)^{\frac{1}{2}} + k_2 a_{n2} \left(n^2 + \frac{p\ell^2}{\pi^2 \kappa_2}\right)^{\frac{1}{2}}\right] \cos nx = 0 ,$$

$$c < x \leq \pi , \tag{3.2.15}$$

and

$$\sum_{n=0}^{\infty} a_{n1} \left(n^2 + \frac{p\ell^2}{\pi^2 \kappa_1}\right)^{\frac{1}{2}} \cos nx = \sum_{n=0}^{\infty} a_{n2} \left(n^2 + \frac{p\ell^2}{\pi^2 \kappa_2}\right)^{\frac{1}{2}} \cos nx = 0 ,$$

$$0 \leq x < c . \tag{3.2.16}$$

Equation (3.2.15) can be satisfied by letting the coefficients of cos nx go to zero, i.e.,

$$a_{n1} = - \frac{k_2 \left[n^2 + \frac{p\ell^2}{\pi^2 \kappa_2}\right]^{\frac{1}{2}}}{k_1 \left[n^2 + \frac{p\ell^2}{\pi^2 \kappa_1}\right]^{\frac{1}{2}}} \; a_{n2} . \tag{3.2.17}$$

This relation reduces the set of equations (3.2.14-3.2.16) to

$$\sum_{n=0}^{\infty} a_{n2} \left[1 + \frac{k_2 \left(n^2 + \frac{p\ell^2}{\pi^2 \kappa_2}\right)^{\frac{1}{2}}}{k_1 \left(n^2 + \frac{p\ell^2}{\pi^2 \kappa_1}\right)^{\frac{1}{2}}}\right] \cos nx = \frac{1}{p} ,$$

$$c < x \leq \pi , \tag{3.2.18}$$

and

$$\sum_{n=0}^{\infty} a_{n2}\left(n^2 + \frac{p\ell^2}{\pi^2 \kappa_2}\right)^{\frac{1}{2}} \cos nx = 0, \qquad 0 \leq x < c. \tag{3.2.19}$$

It appears that an exact analytical solution to this set of dual series is not possible to obtain. Therefore, approximate methods are employed. A perturbation scheme for small p is used to obtain a solution valid for large t.

3.2.3 Solution by Perturbation

If we let

$$a_{n2} = \frac{1}{p}\left[a_{n2}^{(0)} + p^{\frac{1}{2}} a_{n2}^{(1)} + p a_{n2}^{(2)} + p^{3/2} a_{n2}^{(3)} + \ldots . \right], \qquad (3.2.20)$$

substitute it into (3.2.18) and (3.2.19), expand in powers of $p^{\frac{1}{2}}$, and then multiply the resulting equations by p, we obtain

$$\left[a_{02}^{(0)} + p^{\frac{1}{2}} a_{02}^{(1)} + p a_{02}^{(2)} + p^{3/2} a_{02}^{(3)} + \ldots\right]\left[1 + \frac{k_2 \kappa_1^{\frac{1}{2}}}{k_1 \kappa_2^{\frac{1}{2}}}\right]$$

$$+ \sum_{n=1}^{\infty} \left\{ a_{n2}^{(0)}\left[1 + \frac{k_2}{k_1}\right] + p^{\frac{1}{2}} a_{n2}^{(1)}\left[1 + \frac{k_2}{k_1}\right] + p\left[a_{n2}^{(2)}\left(1 + \frac{k_2}{k_1}\right)\right.\right.$$

$$\left. - \frac{\ell^2}{2n^2\pi^2} \frac{k_2}{k_1}\left(\frac{1}{\kappa_1} - \frac{1}{\kappa_2}\right) a_{n2}^{(0)}\right] + p^{3/2}\left[a_{n2}^{(3)}\left(1 + \frac{k_2}{k_1}\right)\right.$$

$$\left.\left. - \frac{\ell^2}{2n^2\pi^2} \frac{k_2}{k_1}\left(\frac{1}{\kappa_1} - \frac{1}{\kappa_2}\right) a_{n2}^{(1)}\right] + \ldots . \right\} \cos nx = 1 ,$$

$$c < x \leq \pi , \qquad (3.2.21)$$

and

$$[a_{02}^{(0)} + p^{\frac{1}{2}}a_{02}^{(1)} + pa_{02}^{(2)} + p^{3/2}a_{02}^{(3)} + \ldots.] \frac{p^{\frac{1}{2}}\ell}{\pi\kappa_2^{\frac{1}{2}}} + \sum_{n=1}^{\infty} \Big\{ a_{n2}^{(0)} + p^{\frac{1}{2}} a_{n2}^{(1)}$$

$$+ p[a_{n2}^{(2)} + \frac{1}{2} \frac{\ell^2}{n^2\pi^2} a_{n2}^{(0)}] + p^{3/2}[a_{n2}^{(3)} + \frac{1}{2}\frac{\ell^2}{n^2\pi^2} a_{n2}^{(1)}] + \ldots \Big\}$$

$$\times \cos nx = 0 , \qquad 0 \leq x < c . \tag{3.2.22}$$

By equating terms in successive powers of $p^{\frac{1}{2}}$, we obtain the following.

Order p^0

$$\left.\begin{aligned} a_{02}^{(0)} &= \frac{k_1\kappa_2^{\frac{1}{2}}}{k_1\kappa_2^{\frac{1}{2}} + k_2\kappa_1^{\frac{1}{2}}} , \qquad n = 0 , \\ \text{and} \\ a_{n2}^{(0)} &= 0 , \qquad n = 1, 2, 3, \ldots. \end{aligned}\right\} \tag{3.2.23}$$

Order $p^{\frac{1}{2}}$

$$a_{02}^{(1)}[1 + \frac{k_2\kappa_1^{\frac{1}{2}}}{k_1\kappa_2^{\frac{1}{2}}}] + \sum_{n=1}^{\infty} a_{n2}^{(1)}[1 + \frac{k_2}{k_1}]\cos nx = 0 ,$$

$$c < x \leq \pi , \tag{3.2.24}$$

and

$$a_{02}^{(0)} \frac{\ell}{\pi\kappa_2^{\frac{1}{2}}} + \sum_{n=1}^{\infty} a_{n2}^{(1)} n \cos nx = 0 , \qquad 0 \leq x < c . \tag{3.2.25}$$

For a more general case of a Fourier series of this type

$$\frac{1}{2}\lambda A_0 + \sum_{n=1}^{\infty} n A_n \cos nx = F(x), \qquad 0 \leq x < c, \tag{3.2.26}$$

and

$$\frac{1}{2}A_0 + \sum_{n=1}^{\infty} A_n \cos nx = G(x), \qquad c < x \leq \pi, \tag{3.2.27}$$

the coefficients, A_n, are given by Sneddon [6] as

$$A_0 = \frac{2}{\pi}\left\{ \frac{\pi}{2^{\frac{1}{2}}} \int_0^c h_1(t) + \int_c^{\pi} G(t)dt \right\}, \qquad n = 0, \tag{3.2.28}$$

and

$$A_n = \frac{2}{\pi}\left\{ \frac{\pi}{2^{3/2}} \int_0^c h_1(t)[P_n(\cos t) + P_{n-1}(\cos t)\,]dt + \int_c^{\pi} G(t)\cos nt\, dt \right\},$$

$$n = 1, 2, 3, \ldots. \tag{3.2.29}$$

where the auxiliary function $h_1(t)$ is

$$h_1(t) = \frac{2}{\pi}\frac{d}{dt}\int_0^t \frac{\sin\frac{1}{2}x\,dx}{(\cos x - \cos t)^{\frac{1}{2}}}\left\{ \int_0^x F(u)du - \frac{1}{2}\lambda A_0 x \right.$$

$$\left. - \sum_{n=1}^{\infty}\left[\frac{2}{\pi}\int_c^{\pi} G(u)\cos nu\, du\right]\sin nx \right\}, \quad 0 \leq t < c, \tag{3.2.30}$$

and $P_n(\cos t)$ denotes Legendre polynomials.

The equations (3.2.24) and (3.2.25) are a special case of (3.2.26) and (3.2.27) with

$$G(x) = 0 , \tag{3.2.31}$$

$$\frac{1}{2} A_0 = \frac{a_{02}^{(1)} \left[1 + \frac{k_2 \kappa_1^{\frac{1}{2}}}{k_1 \kappa_2^{\frac{1}{2}}} \right]}{\left[1 + \frac{k_2}{k_1} \right]} , \tag{3.2.32}$$

$$A_n = a_{n2}^{(1)} , \qquad n = 1, 2, 3, \ldots \tag{3.2.33}$$

$$\lambda = 0 , \tag{3.2.34}$$

and

$$F(x) = - a_{02}^{(0)} \frac{\ell}{\pi \kappa_2^{\frac{1}{2}}} , \qquad 0 \leq x < c . \tag{3.2.35}$$

By the substitution of (3.2.31) and (3.2.35) into (3.2.30) we obtain

$$h_1(t) = - \frac{2}{\pi} a_{02}^{(0)} \frac{\ell}{\pi \kappa_2^{\frac{1}{2}}} \frac{d}{dt} \int_0^t \frac{x \sin \frac{1}{2} x \, dx}{(\cos x - \cos t)^{\frac{1}{2}}} ,$$

which can be reduced [7] to

$$h_1(t) = - a_{02}^{(0)} \frac{\ell}{\pi \kappa_2^{\frac{1}{2}}} 2^{\frac{1}{2}} \tan \tfrac{1}{2} t . \tag{3.2.36}$$

Straightforward integration of (3.2.28) and (3.2.29) leads to

$$A_0 = 4\, a_{02}^{(0)} \frac{\ell}{\pi \kappa_2^{\frac{1}{2}}} \ell n(\cos \tfrac{1}{2} c) , \tag{3.2.37}$$

or

$$a_{02}^{(1)} = \frac{2k_1 \kappa_2^{\frac{1}{2}} \ell (k_1+k_2)}{(k_1 \kappa_2^{\frac{1}{2}} + k_2 \kappa_1^{\frac{1}{2}})^2} \ell n (\cos \tfrac{1}{2} c) , \tag{3.2.38}$$

and

$$A_n = a_{n2}^{(1)} = \frac{k_1 \ell}{\pi (k_1 \kappa_2^{\frac{1}{2}} + k_2 \kappa_1^{\frac{1}{2}})} \frac{1}{n} [P_n(\cos c) - P_{n-1}(\cos c)] ,$$

$$n = 1, 2, 3, \ldots . \tag{3.2.39}$$

Order p

$$a_{02}^{(2)} [1 + \frac{k_2 \kappa_1^{\frac{1}{2}}}{k_1 \kappa_2^{\frac{1}{2}}}] + \sum_{n=1}^{\infty} [a_{n2}^{(2)} (1 + \frac{k_2}{k_1}) - \frac{\ell^2}{2n^2 \pi^2} \frac{k_2}{k_1} (\frac{1}{\kappa_1} - \frac{1}{\kappa_2}) a_{n2}^{(0)}] \cos nx = 0 ,$$

$$c < x \leq \pi , \tag{3.2.40}$$

and

$$a_{02}^{(1)} \frac{\ell}{\pi \kappa_2^{\frac{1}{2}}} + \sum_{n=1}^{\infty} [a_{n2}^{(2)} + \frac{1}{2} \frac{\ell^2}{n^2 \pi^2 \kappa_2} a_{n2}^{(0)}] n \cos nx = 0 ,$$

$$0 \leq x < c . \tag{3.2.41}$$

These equations are a special case of (3.2.26) and (3.2.27) with

$$G(x) = 0 , \tag{3.2.42}$$

$$\frac{1}{2} A_0 = \frac{a_{02}^{(2)} \left[1 + \frac{k_2 \kappa_1^{\frac{1}{2}}}{k_1 \kappa_2^{\frac{1}{2}}} \right]}{1 + \frac{k_2}{k_1}} , \tag{3.2.43}$$

$$A_n = a_{n2}^{(2)} , \qquad n = 1, 2, 3, ... \tag{3.2.44}$$

$$\lambda = 0 , \tag{3.2.45}$$

and

$$F(x) = - a_{02}^{(1)} \frac{\ell}{\pi \kappa_2^{\frac{1}{2}}} , \qquad 0 \leq x < c . \tag{3.2.46}$$

For this case we have

$$h_1(t) = - \frac{2}{\pi} a_{02}^{(1)} \frac{\ell}{\pi \kappa_2^{\frac{1}{2}}} 2^{\frac{1}{2}} \tan \tfrac{1}{2} t , \tag{3.2.47}$$

which upon substitution into (3.2.29) and (3.2.30) leads to

$$A_0 = 4 a_{02}^{(1)} \frac{\ell}{\pi \kappa_2^{\frac{1}{2}}} \ell n(\cos \tfrac{1}{2} c) \left(1 + \frac{k_2}{k_1} \right) , \tag{3.2.48}$$

or

$$a_{02}^{(2)} = \frac{4k_1\kappa_2^{\frac{1}{2}}\ell^2(k_1+k_2)^2}{\pi^2(k_1\kappa_2^{\frac{1}{2}}+k_2\kappa_1^{\frac{1}{2}})^3}[\ell n(\cos\tfrac{1}{2}c)]^2 , \qquad (3.2.49)$$

and

$$A_n = a_{n2}^{(2)} = \frac{2k_1\ell^2(k_1+k_2)}{\pi^2(k_1\kappa_2^{\frac{1}{2}}+k_2\kappa_1^{\frac{1}{2}})^2}\ell n(\cos\tfrac{1}{2}c)\frac{1}{n}[P_n(\cos c)-P_{n-1}(\cos c)] ,$$

$$n = 1, 2, 3, \ldots . \qquad (3.2.50)$$

Order $p^{3/2}$

$$a_{02}^{(3)}\left(1+\frac{k_2\kappa_1^{\frac{1}{2}}}{k_1\kappa_2^{\frac{1}{2}}}\right)+\sum_{n=1}^{\infty}[a_{n2}^{(3)}(1+\frac{k_2}{k_1})-\frac{\ell^2}{2n^2\pi^2}\frac{k_2}{k_1}(\frac{1}{\kappa_1}-\frac{1}{\kappa_2})a_n^{(1)}]\cos nx = 0 ,$$

$$c < x \leq \pi , \qquad (3.2.51)$$

and

$$a_{02}^{(2)}\frac{\ell}{\pi\kappa_2^{\frac{1}{2}}}+\sum_{n=1}^{\infty}[a_{n2}^{(3)}+\frac{\ell^2}{2n^2\pi^2\kappa_2}a_{n2}^{(1)}]n\cos nx = 0 ,$$

$$0 \leq x < c . \qquad (3.2.52)$$

For this case we can let

$$G(x) = 0 , \tag{3.2.53}$$

$$\frac{1}{2} A_0 = a_{02}^{(3)} \left(1 + \frac{k_2 \kappa_1^{\frac{1}{2}}}{k_1 \kappa_2^{\frac{1}{2}}}\right), \tag{3.2.54}$$

$$A_n = [a_{n2}^{(3)} (1 + \frac{k_2}{k_1}) - \frac{\ell^2}{2n^2\pi^2} \frac{k_2}{k_1} (\frac{1}{\kappa_1} - \frac{1}{\kappa_2}) a_{n2}^{(1)}] ,$$

$$n = 1, 2, 3, \ldots . \tag{3.2.55}$$

$$\lambda = 0 , \tag{3.2.56}$$

and

$$F(x) = - a_{02}^{(2)} \frac{\ell}{\pi \kappa_2^{\frac{1}{2}}} \left(1 + \frac{k_2}{k_1}\right) + \frac{1}{2} \frac{\ell^2}{\pi^2 k_1} \left(\frac{k_1}{\kappa_2} + \frac{k_2}{\kappa_1}\right) \sum_{m=1}^{\infty} \frac{1}{m} a_{m2}^{(1)} \cos mx,$$

$$0 \leq x < c . \tag{3.2.57}$$

If we now substitute (3.2.53), (3.2.56) and (3.2.57) into (3.2.31), we obtain

$$h_1(t) = -\frac{2}{\pi} a_{02}^{(2)} \frac{\ell}{\pi \kappa_2^{\frac{1}{2}}} \left(1 + \frac{k_2}{k_1}\right) 2^{\frac{1}{2}} \tan \tfrac{1}{2}t + \frac{1}{2} \frac{\ell^2}{\pi^2 k_1} \left(\frac{k_1}{\kappa_2} + \frac{k_2}{\kappa_1}\right)$$

$$\times \sum_{m=1}^{\infty} \frac{1}{m^2} a_{m2}^{(1)} \frac{d}{dt} \int_0^t \frac{\sin mx \sin \frac{1}{2}x}{(\cos x - \cos t)^{\frac{1}{2}}} \, dx$$

$$= -\frac{2}{\pi} a_{02}^{(2)} \frac{\ell}{\pi \kappa_2^{\frac{1}{2}}} \left(1 + \frac{k_2}{k_1}\right) 2^{\frac{1}{2}} \tan \tfrac{1}{2}t + \frac{2^{\frac{1}{2}} \ell^2}{16 \pi k_1} \left(\frac{k_1}{\kappa_2} + \frac{k_2}{\kappa_1}\right)$$

$$\times \sum_{m=1}^{\infty} \frac{1}{m^2} a_{m2}^{(1)} \frac{d}{dt} [P_{m-1}(\cos t) - P_m(\cos t)] ,$$

$$0 \leq t < c . \qquad (3.2.58)$$

By using this expression for $h_1(t)$ in (3.2.29) and (3.2.30), we find that

$$A_0 = 4a_{02}^{(2)} \frac{\ell}{\pi \kappa_2^{\frac{1}{2}}} \ell n(\cos \tfrac{1}{2}c) \left(1 + \frac{k_2}{k_1}\right) + \frac{\ell^2}{16 \pi k_1} \left(\frac{k_1}{\kappa_2} + \frac{k_2}{\kappa_1}\right) \qquad (3.2.59)$$

$$\times \sum_{m=1}^{\infty} \frac{1}{m^2} a_{m2}^{(1)} [P_{m-1}(\cos c) - P_m(\cos c)]$$

or

$$a_{02}^{(3)} = \frac{8k_1\kappa_2^{\frac{1}{2}}\ell^3(k_1+k_2)^3}{\pi^3(k_1\kappa_2^{\frac{1}{2}}+k_2\kappa_1^{\frac{1}{2}})^4}[\ell n(\cos\tfrac{1}{2}c)]^3$$

$$- \frac{k_1\kappa_2^{\frac{1}{2}}\ell^3}{32\pi^2(k_1\kappa_2^{\frac{1}{2}}+k_2\kappa_1^{\frac{1}{2}})^2}(\frac{k_1}{\kappa_2}+\frac{k_2}{\kappa_1})\sum_{m=1}^{\infty}\frac{1}{m^3}[P_m(\cos c)-P_{m-1}(\cos c)] \qquad (3.2.60)$$

and

$$A_n = \frac{4\ell^3(k_1+k_2)^3}{\pi^3(k_1\kappa_2^{\frac{1}{2}}+k_2\kappa_1^{\frac{1}{2}})^3}[\ell n(\cos\tfrac{1}{2}c)]^2\frac{1}{n}[P_n(\cos c)-P_{n-1}(\cos c)]$$

$$+ \frac{\pi\ell^3}{32\pi^3(k_1\kappa_2^{\frac{1}{2}}+k_2\kappa_1^{\frac{1}{2}})}(\frac{k_1}{\kappa_2}+\frac{k_2}{\kappa_1})\sum_{m=1}^{\infty}\frac{1}{m^3}[P_m(\cos c)-P_{m-1}(\cos c)]B_{mn},$$

$$n = 1,2,3,\ldots \qquad (3.2.61)$$

where B_{mn} denotes the integral

$$B_{mn} = -\int_0^c \{\frac{d}{dt}[P_m(\cos t)-P_{m-1}(\cos t)]\}[P_n(\cos t)+P_{n-1}(\cos t)]dt$$

$$= \int_{\cos c}^{1}[P_m'(x)-P_{m-1}'(x)][P_n(x)+P_{n-1}(x)]dx \ . \qquad (3.2.62)$$

By making use of the following properties of Legendre polynomials:

$$[(1 - x^2)P_k'(x)]' + k(k + 1)P_k(x) = 0 , \qquad k = 0, 1, 2, \ldots \tag{3.2.63}$$

$$P_{k+1}'(x) - P_{k-1}'(x) = (2k + 1)P_k(x) , \qquad k = 1, 2, 3, \ldots \tag{3.2.64}$$

We obtain

$$B_{m+1,n} + B_{mn} = \int_{\cos c}^{1} [P_{m+1}'(x) - P_m'(x) + P_m'(x) - P_{m-1}'(x)]$$

$$\times [P_n(x) - P_{n-1}(x)]dx = (2m+1) \int_{\cos c}^{1} P_m(x)[P_n(x) + P_{n-1}(x)]dx , \tag{3.2.65}$$

and

$$n(n+1) \int_{\cos c}^{1} P_m(x)P_n(x)dx = - \int_{\cos c}^{1} [(1-x^2)P_n'(x)]' P_m(x)dx$$

$$= -(1-x^2)P_n'(x)P_m(x) \Big|_{\cos c}^{1} + \int_{\cos c}^{1} (1-x^2)P_n'(x)P_m'(x)dx \tag{3.2.66}$$

$$= \sin^2 c \, P_n'(\cos c)P_m(\cos c) + (1-x^2)P_n(x)P_m'(x) \Big|_{\cos c}^{1}$$

$$- \int_{\cos c}^{1} P_n(x)[(1-x^2)P_m'(x)]' dx$$

$$= \sin^2 c[P_n'(\cos c)P_m(\cos c) - P_n(\cos c)P_m'(\cos c)] + m(m+1) \int_{\cos c}^{1} P_m(x)P_n(x)dx.$$

As a result, we find that

$$\int_{\cos c}^{1} P_m(x)P_n(x) = \frac{\sin^2 c}{n(n+1)-m(m+1)}[P_n'(\cos c)P_m(\cos c)-P_n(\cos c)P_m'(\cos c)] ,$$

$$m \neq n. \qquad (3.2.67)$$

For $m = n$, we have

$$\int_{\cos c}^{1} P_m^2(x)dx = \frac{1}{(2m+1)}\left[1 - \cos c\, P_m(\cos c) + \frac{2(m-1)P_m(\cos c)P_{m-1}(\cos c)}{(2m-1)}\right.$$

$$\left. - 2\sum_{k=1}^{m} \frac{P_{k-1}(\cos c)P_{k-2}(\cos c)}{(2k-1)(2k-3)}\right] , \qquad (3.2.68)$$

which is derived from a result given by Prasad [8] for $\int_o^x P_m^2(x)dx$.

With the use of equations (3.2.67) and (3.2.68) the right side of (3.2.65) can be written in explicit form. If we denote this right side by C_{mn}, we have

$$B_{m+1,n} + B_{mn} = C_{mn} = (2m+1) \int_{\cos c}^{1} P_m(x)[P_n(x) + P_{n-1}(x)]dx , \qquad (3.2.69)$$

and

$$B_{1,n} = C_{0,n} . \qquad (3.2.70)$$

This set of difference equations can be solved to give

$$B_{mn} = \sum_{k=1}^{m} (-1)^{m-k} C_{k-1,n} . \qquad (3.2.71)$$

An expression for $a_{2n}^{(3)}$ can now be obtained from (3.2.55) and (3.2.61); it is given by

$$a_{n2}^{(3)} = \left\{ \frac{4k_1 \ell^3 (k_1 + k_2)^2}{\pi^3 (k_1 \kappa_2^{\frac{1}{2}} + k_2 \kappa_1^{\frac{1}{2}})^3} [\ell n(\cos \tfrac{1}{2} c)]^3 \right.$$

$$\left. + \frac{k_1 k_2 \ell^3}{2\pi^3 (k_1 \kappa_2^{\frac{1}{2}} + k_2 \kappa_1^{\frac{1}{2}})(k_1 + k_2)} (\frac{1}{\kappa_1} - \frac{1}{\kappa_2}) \frac{1}{n^3} \right\} [P_n(\cos c) - P_{n-1}(\cos c)]$$

$$+ \frac{\ell^3 k_1}{32\pi^2 (k_1 \kappa_2^{\frac{1}{2}} + k_2 \kappa_1^{\frac{1}{2}})(k_1 + k_2)} (\frac{k_1}{\kappa_2} + \frac{k_2}{\kappa_1}) \sum_{m=1}^{\infty} \frac{1}{m^3} [P_m(\cos c) - P_{m-1}(\cos c)] B_{mn},$$

$$n = 1, 2, 3, \ldots \qquad (3.2.72)$$

Terms of higher order are exceedingly complicated but may, nevertheless, be calculated in terms of the constants B_{mn}. The coefficients of the perturbation solution can be used to obtain the temperature distribution in region 2. For region 1, the coefficients, $a_{n1} = a_{n1}^{(0)} + p^{\frac{1}{2}} a_{n1}^{(1)} + p a_{n1}^{(2)} + \ldots$, can be obtained from the relation (3.2.17). For $n = 0$, we have

$$a_{01}^{(i)} = - \frac{k_2 \kappa_1^{\frac{1}{2}}}{k_1 \kappa_2^{\frac{1}{2}}} a_{02}^{(i)}, \qquad i = 0, 1, 2, \text{ and } 3; \qquad (3.2.73)$$

and for $n \geq 1$, simple expansion of (3.2.17) for small p gives

$$a_{n1}^{(0)} + p^{\frac{1}{2}} a_{n1}^{(1)} + p a_{n1}^{(2)} + \ldots = -\frac{k_2}{k_1}\left[1 - \frac{p}{2n^2\pi^2}\left(\frac{1}{\kappa_1} - \frac{1}{\kappa_2}\right) + \ldots\right]$$

$$\times \left[a_{n2}^{(0)} + p^{\frac{1}{2}} a_{n2}^{(1)} + p a_{n2}^{(2)} + \ldots\right] = -\frac{k_2}{k_1} a_{n2}^{(0)} - p^{\frac{1}{2}} \frac{k_2}{k_1} a_{n2}^{(1)} - p \frac{k_2}{k_1}$$

$$\times \left[a_{n2}^{(2)} - \frac{1}{2n^2\pi^2}\left(\frac{1}{\kappa_1} - \frac{1}{\kappa_2}\right) a_{n2}^{(0)}\right] - p^{3/2} \frac{k_2}{k_1}\left[a_{n2}^{(3)} - \frac{1}{2n^2\pi^2}\left(\frac{1}{\kappa_1} - \frac{1}{\kappa_2}\right) a_{n2}^{(1)}\right] + \ldots,$$

$$n = 1, 2, 3, \ldots\ldots \qquad (3.2.74)$$

By equating the terms in like powers of $p^{\frac{1}{2}}$, we obtain for $n = 1, 2, 3, \ldots$

$$a_{n1}^{(0)} = -\frac{k_2}{k_1} a_{n2}^{(0)} ,$$

$$a_{n1}^{(1)} = -\frac{k_2}{k_1} a_{n2}^{(1)} ,$$

$$a_{n1}^{(2)} = -\frac{k_2}{k_1}\left[a_{n2}^{(2)} - \frac{1}{2n^2\pi^2}\left(\frac{1}{\kappa_1} - \frac{1}{\kappa_2}\right) a_{n2}^{(0)}\right] = -\frac{k_2}{k_1} a_{n2}^{(2)} ,$$

$$a_{n1}^{(3)} = -\frac{k_2}{k_1}\left[a_{n2}^{(3)} - \frac{1}{2n^2\pi^2}\left(\frac{1}{\kappa_1} - \frac{1}{\kappa_2}\right) a_{n2}^{(1)}\right] ,$$

(3.2.75)

3.2.4 Inversion of the Solution

The Laplace transform of the solution may be written as

$$\Theta_i(x, y, p) = \left[\frac{1}{p}(a_{0i}^{(0)} + \delta_{1,i}) + \frac{1}{p^{\frac{1}{2}}} a_{0i}^{(1)} + a_{0i}^{(2)} + p^{\frac{1}{2}} a_{0i}^{(3)} + \ldots.\right] \exp\left[-\frac{p^{\frac{1}{2}} \ell |y|}{\pi \kappa_i^{\frac{1}{2}}}\right]$$

$$+ \sum_{n=1}^{\infty} \left[\frac{1}{p^{\frac{1}{2}}} a_{ni}^{(1)} + a_{ni}^{(2)} + p^{\frac{1}{2}} a_{ni}^{(3)} + \ldots.\right] \exp\left[-\left(n^2 + \frac{p\ell^2}{\pi^2 \kappa_i}\right)^{\frac{1}{2}} |y|\right] \cos nx \ ,$$

$$i = 1, 2. \qquad (3.2.76)$$

The inverses of all the terms outside the summation sign and the second term under it may be obtained directly from tables. The other terms may be inverted by using the convolution integral. If $\mathcal{L}^{-1}$ is used to denote the inverse operation, then we have

$$\mathcal{L}^{-1} \exp[-\alpha(p + \beta)^{\frac{1}{2}}] = \frac{\alpha}{2(\pi t^3)^{\frac{1}{2}}} \exp\left[-\left(\frac{\alpha^2}{4t} + \beta t\right)\right] , \qquad (3.2.77)$$

and

$$\mathcal{L}^{-1} \frac{1}{p^{\frac{1}{2}}} = \frac{1}{(\pi t)^{\frac{1}{2}}} . \qquad (3.2.78)$$

We can write, by making use of the convolution property,

$$\mathcal{L}^{-1} \frac{1}{p^{\frac{1}{2}}} \exp[-\alpha(p+\beta)^{\frac{1}{2}}] = \frac{\alpha}{2\pi} \int_0^t \frac{1}{(t-\tau)^{\frac{1}{2}} \tau^{3/2}} \exp\left[-\left(\frac{\alpha^2}{4\tau} + \beta\tau\right)\right] d\tau .$$

(3.2.79)

Upon the substitution $\tau = ut$, the integral becomes

$$\mathcal{L}^{-1}\frac{1}{p^{\frac{1}{2}}}\exp[-\alpha(p+\beta)^{\frac{1}{2}}] = \frac{\alpha}{2\pi t}\int_0^1 \frac{1}{(1-u)^{\frac{1}{2}}u^{3/2}}\exp[-(\frac{\alpha^2}{4ut}+\beta ut)]du$$

$$= -\frac{\alpha}{2\pi t}\int_0^1 \exp[-(\frac{\alpha^2}{4ut}+\beta ut)]d(\frac{1}{u}-1)^{\frac{1}{2}}\ , \tag{3.2.80}$$

and by the further substitution

$$v^2 = \frac{\alpha^2}{4ut} + \beta ut\ , \tag{3.2.81}$$

we obtain

$$\mathcal{L}^{-1}\frac{1}{p^{\frac{1}{2}}}\exp[-\alpha(p+\beta)^{\frac{1}{2}}] = \frac{\alpha}{2\pi t}\int_{v=(\alpha^2/4t+\beta t)^{\frac{1}{2}}}^{v=\infty} \exp(-v^2)d[\frac{1}{u(v)}-1]^{\frac{1}{2}}. \tag{3.2.82}$$

The upper limit is ∞ as long as $\alpha \neq 0$ and the lower limit is large when t is large. Therefore, it is appropriate to obtain an approximate expression for $[1/u(v)-1]^{\frac{1}{2}}$ for large v. From (3.2.81) we obtain

$$u = \frac{v^2}{2\beta t}[1-(1-\frac{\alpha^2\beta}{v^4})^{\frac{1}{2}}]$$

$$= \frac{v^2}{2\beta t}[\frac{1}{2}\frac{\alpha^2\beta}{v^4}+\frac{1}{8}\frac{\alpha^4\beta^2}{v^8}+\ldots]$$

$$= \frac{\alpha^2}{4v^2t}[1+\frac{1}{4}\frac{\alpha^2\beta}{v^4}+\ldots..]\ ,$$

and

$$d\left(\frac{1}{u} - 1\right)^{\frac{1}{2}} = d\left[\frac{4v^2t}{\alpha^2}\left(1 + \frac{1}{4}\,\frac{\alpha^2\beta}{v^4} + \ldots.\right)^{-1} - 1\right]^{\frac{1}{2}}$$

$$= d\left[\frac{4v^2t}{\alpha^2}\left(1 - \frac{1}{4}\,\frac{\alpha^2\beta}{v^4} + \ldots\right) - 1\right]^{\frac{1}{2}}$$

$$= d\,\frac{2vt^{\frac{1}{2}}}{\alpha}\left[1 - \frac{1}{4}\,\frac{\alpha^2\beta}{v^4} - \frac{\alpha^2}{4v^2t} + \ldots\right]^{\frac{1}{2}}$$

$$= d\,\frac{2vt^{\frac{1}{2}}}{\alpha}\left[1 - \frac{\alpha^2}{8v^2t} + \ldots\right]$$

$$= \frac{2t^{\frac{1}{2}}}{\alpha}\left[1 + \frac{\alpha^2}{8v^2t} + \ldots.\right]dv\ . \qquad (3.2.83)$$

The inverse given by (3.2.82) may now be written as

$$\mathcal{L}^{-1}\,\frac{1}{p^{\frac{1}{2}}}\,\exp[-\alpha(p+\beta)^{\frac{1}{2}}] = \frac{1}{\pi t^{\frac{1}{2}}}\int_{(\alpha^2/4t+\beta t)^{\frac{1}{2}}}^{\infty} \exp(-v^2)\left[1 + \frac{\alpha^2}{8v^2t} + \ldots\right]dv$$

$$= \frac{1}{2\pi t^{\frac{1}{2}}}\,\exp\left[-\left(\frac{\alpha^2}{4t} + \beta t\right)\right]\left[\frac{1}{(\beta t)^{\frac{1}{2}}} - \frac{1}{2(\beta t)^{3/2}} + \ldots\right], \qquad (3.2.84)$$

which is exponentially small for large t. From this result it is quite straightforward to show that $\mathcal{L}^{-1}p^{\frac{1}{2}}\exp[-\alpha(p+\beta)^{\frac{1}{2}}]$ is also exponentially small. Upon the application of these results for the inversion of (3.2.76) we see that the entire expression under the summation sign is

exponentially small for $|y| > 0$. By inverting the other terms, we obtain for $y > 0$,

$$\theta_1(x, y, t) = 1 - \frac{k_2\kappa_1^{\frac{1}{2}}}{(k_1\kappa_2^{\frac{1}{2}} + k_2\kappa_1^{\frac{1}{2}})} \operatorname{erfc}\left[\frac{\ell y}{2\pi(\kappa_1 t)^{\frac{1}{2}}}\right] - \left\{\frac{2k_2\kappa_1^{\frac{1}{2}}(k_1 + k_2)}{\pi^2(k_1\kappa_2^{\frac{1}{2}} + k_2\kappa_1^{\frac{1}{2}})^2}\right.$$

$$\times \ell n(\cos\tfrac{1}{2}c)\frac{\ell}{(\pi t)^{\frac{1}{2}}} + \left[\frac{4k_2(k_1 + k_2)^2}{(k_1\kappa_2^{\frac{1}{2}} + k_2\kappa_1^{\frac{1}{2}})^3}[\ell n(\cos\tfrac{1}{2}c)]^2 y - \frac{8k_2\kappa_1^{\frac{1}{2}}(k_1 + k_2)^3}{(k_1\kappa_2^{\frac{1}{2}} + k_2\kappa_1^{\frac{1}{2}})^4}\right.$$

$$\times [\ell n(\cos\tfrac{1}{2}c)]^3 - \frac{k_2\kappa_1^{\frac{1}{2}}\pi}{32(k_1\kappa_2^{\frac{1}{2}} + k_2\kappa_1^{\frac{1}{2}})^2}\left(\frac{k_1}{\kappa_2} + \frac{k_2}{\kappa_1}\right)\sum_{m=1}^{\infty}\frac{1}{m^3}$$

$$\left.\left.\times [P_m(\cos c) - P_{m-1}(\cos c)]^2\right]\frac{1}{\pi^3}\frac{\ell^3}{2(\pi t^3)^{\frac{1}{2}}} + \ldots\right\} \exp\left[-\frac{\ell^2 y^2}{4\kappa_1 t}\right], \tag{3.2.85}$$

and for $y < 0$,

$$\theta_2 = \frac{k_1\kappa_2^{\frac{1}{2}}}{(k_1\kappa_2^{\frac{1}{2}} + k_2\kappa_1^{\frac{1}{2}})} \operatorname{erfc}\left[- \frac{\ell y}{2\pi(\kappa_2 t)^{\frac{1}{2}}} \right] + \left\{ \frac{2k_1\kappa_2^{\frac{1}{2}}(k_1 + k_2)}{\pi^2(k_1\kappa_2^{\frac{1}{2}} + k_2\kappa_1^{\frac{1}{2}})^2} \right.$$

$$\times \ell n(\cos\tfrac{1}{2}c) \frac{\ell}{(\pi t)^{\frac{1}{2}}} + \frac{1}{\pi^3} \left[\frac{4k_1(k_1+k_2)^2}{(k_1\kappa_2^{\frac{1}{2}} + k_2\kappa_1^{\frac{1}{2}})^3} [\ell n(\cos\tfrac{1}{2}c)]^2 \ (-y) \right.$$

$$- \frac{8k_1\kappa_2^{\frac{1}{2}}(k_1+k_2)^3}{(k_1\kappa_2^{\frac{1}{2}}+k_2\kappa_1^{\frac{1}{2}})^4} [\ell n(\cos\tfrac{1}{2}c)]^3 - \frac{k_1\kappa_2^{\frac{1}{2}}\pi}{32(k_1\kappa_2^{\frac{1}{2}}+k_2\kappa_1^{\frac{1}{2}})^2} \left(\frac{k_1}{\kappa_2} + \frac{k_2}{\kappa_1}\right)$$

$$\left. \times \sum_{m=1}^{\infty} \frac{1}{m^3} [P_m(\cos c) - P_{m-1}(\cos c)]^2 \right] \left. \frac{\ell^3}{2(\pi t^3)^{\frac{1}{2}}} + \ldots. \right\} \exp\left[- \frac{\ell^2 y^2}{4\kappa_2 t} \right] .$$

(3.2.86)

At $y = 0$, the temperature distribution on each side of the interface may be obtained by inverting $\bar{\theta}_1(x, 0, p)$, which may be obtained by letting $y \to 0$ in (3.2.76). However, a difficulty arises in the inversion of $p^{\frac{1}{2}}$ because this expression by itself does not have an inverse. But we are only interested in a solution for long time and also, the expression $p^{\frac{1}{2}}$ is valid only for small p. Under these circumstances we can obtain a meaningful inverse of $p^{\frac{1}{2}}$. Let us consider the function

$$F(p) = p^{\frac{1}{2}} \exp[-\alpha p^{\frac{1}{2}}] , \qquad \alpha > 0. \tag{3.2.87}$$

The inverse, $f(t)$, of $F(p)$ is given by

$$f(t) = \mathcal{L}^{-1}F(p) = \left[- \frac{1}{2(\pi t^3)^{\frac{1}{2}}} + \frac{\alpha^2}{4(\pi t^5)^{\frac{1}{2}}} \right] \exp\left[- \frac{\alpha^2}{4t} \right] . \tag{3.2.88}$$

For $\alpha \ll 1$ and small p, $F(p) \sim p^{\frac{1}{2}}$; and $f(t) \sim \frac{1}{2} (\pi t^3)^{-\frac{1}{2}}$ for large t. Therefore, for small p and large t, it is valid to interpret $- \frac{1}{2} (\pi t^3)^{-\frac{1}{2}}$ as the inverse of $p^{\frac{1}{2}}$. The temperature distributions on each side of the interface may now be obtained by setting $y = 0$ in (3.2.76) and then inverting $\Theta_i(x, 0, p)$. Upon carrying out this operation we find that

$$\theta_i(x, 0, t) = \delta_{1,i} + a_{0i}^{(0)} + \frac{1}{(\pi t)^{\frac{1}{2}}} \sum_{n=o}^{\infty} a_{ni}^{(1)} \cos nx$$

$$- \frac{1}{2(\pi t^3)^{\frac{1}{2}}} \sum_{n=o}^{\infty} a_{ni}^{(3)} \cos nx + \ldots, \qquad i = 1, 2. \tag{3.2.89}$$

In this result, the inverses of the terms independent of p, i.e., $a_{ni}^{(2)}$, $i = 0, 1, 2, \ldots$ are taken to be zero as opposed to $a_{ni}^{(2)} \delta(t)$ because we are only interested in large values of t.

By the substitution of expressions for $a_{0i}^{(0)}$, $a_{ni}^{(1)}$ and $a_{ni}^{(2)}$, $i = 1, 2$, $n = 1, 2, 3, \ldots$ and carrying out the summation [5] of the first series, we obtain

$$\theta_1(x,0,t) = \frac{k_1\kappa_2^{\frac{1}{2}}}{(k_1\kappa_2^{\frac{1}{2}} + k_2\kappa_1^{\frac{1}{2}})} - \frac{\ell}{\pi(\pi t)^{\frac{1}{2}}}\left\{\frac{2k_1k_2(\kappa_2^{\frac{1}{2}} - \kappa_1^{\frac{1}{2}})}{(k_1\kappa_2^{\frac{1}{2}} + k_2\kappa_1^{\frac{1}{2}})^2}\ell n(\cos\tfrac{1}{2}c)\right.$$

$$\left. + \frac{k_2}{(k_1\kappa_2^{\frac{1}{2}} + k_2\kappa_1^{\frac{1}{2}})} H(c-x)\ell n\left[\frac{\cos\frac{1}{2}x}{\cos\frac{1}{2}c} + \left(\frac{\cos^2\frac{1}{2}x}{\cos^2\frac{1}{2}c} - 1\right)^{\frac{1}{2}}\right]\right\} + \ldots\ldots, \tag{3.2.90}$$

and

$$\theta_2(x,0,t) = \frac{k_1\kappa_2^{\frac{1}{2}}}{(k_1\kappa_2^{\frac{1}{2}} + k_2\kappa_1^{\frac{1}{2}})} + \frac{\ell}{\pi(\pi t)^{\frac{1}{2}}}\left\{\frac{2k_1k_2(\kappa_1^{\frac{1}{2}} - \kappa_2^{\frac{1}{2}})}{(k_1\kappa_2^{\frac{1}{2}} + k_2\kappa_1^{\frac{1}{2}})^2}\ell n\,(\cos\tfrac{1}{2}c)\right.$$

$$\left. + \frac{k_1}{(k_1\kappa_2^{\frac{1}{2}} + k_2\kappa_1^{\frac{1}{2}})} H(c-x)\ell n\left[\frac{\cos\frac{1}{2}x}{\cos\frac{1}{2}c} + \left(\frac{\cos^2\frac{1}{2}x}{\cos^2\frac{1}{2}c} - 1\right)^{\frac{1}{2}}\right]\right\} + \ldots\ldots, \tag{3.2.91}$$

where H denotes the Heaviside step function.

The average heat flux per unit area, q_{av}, across the interface is given by

$$q_{av} = -(T_{10} - T_{20})\frac{1}{\ell}\int_0^{\ell}\left[\mathcal{L}^{-1}\, k_1\, \frac{\partial \Theta_1}{\partial y^*}\bigg|_{y^*=0}\right] dx^*$$

$$= -(T_{10} - T_{20})\,\frac{k_1}{\ell}\int_0^{\pi}\left[\mathcal{L}^{-1}\,\frac{\partial \Theta_1}{\partial y}\bigg|_{y=0}\right] dx$$

$$= (T_{10} - T_{20})k_1\,\frac{\pi}{\ell}\,\mathcal{L}^{-1}\,\frac{\ell}{\pi\kappa_1^{\frac{1}{2}}}\left[\frac{1}{p^{\frac{1}{2}}}\,a_{01}^{(0)} + a_{01}^{(1)} + p^{\frac{1}{2}}\,a_{01}^{(2)} + \ldots\right.$$

$$= (T_{10} - T_{20})\,\frac{k_1 k_2}{(k_1 + k_2)}\;\frac{\pi}{\ell}\;\frac{k_1 + k_2}{\pi(k_1\kappa_2^{\frac{1}{2}} + k_2\kappa_1^{\frac{1}{2}})}\;\frac{\ell}{(\pi t)^{\frac{1}{2}}}$$

$$\left. - \frac{(k_1 + k_2)^3}{\pi^3(k_1\kappa_2^{\frac{1}{2}} + k_2\kappa_1^{\frac{1}{2}})^3}\,[\ell\, n(\cos\tfrac{1}{2}c)]^2\;\frac{\ell^3}{(\pi t)^3)^{\frac{1}{2}}} + \ldots.\right] .$$

(3.2.92)

By taking the reciprocal of this result we obtain the average resistance, R, for a unit area as

$$R = \frac{(k_1\kappa_2^{\frac{1}{2}} + k_2\kappa_1^{\frac{1}{2}})}{k_1 k_2}\;(\pi t)^{\frac{1}{2}}\left[1 - \frac{(k_1 + k_2)^2}{(k_1\kappa_2^{\frac{1}{2}} + k_2\kappa_1^{\frac{1}{2}})^2}[\ell n(\cos\tfrac{1}{2}c)]^2\,\frac{\ell^2}{\pi^2 t} + \ldots\right]^{-1}$$

$$= \frac{(k_1\kappa_2^{\frac{1}{2}} + k_2\kappa_1^{\frac{1}{2}})}{k_1 k_2}\;(\pi t)^{\frac{1}{2}}\left[1 + \frac{(k_1 + k_2)^2}{(k_1\kappa_2^{\frac{1}{2}} + k_2\kappa_1^{\frac{1}{2}})^2}\,[\ell n(\cos\tfrac{1}{2}c)]^2\,\frac{\ell^2}{\pi t} + \ldots\right] ,$$

(3.2.93)

which may also be written as

$$R = R_{fc}\left[1 + \frac{(1 + \frac{k_2}{k_1})^2}{[1 + \frac{k_2}{k_1}(\frac{\kappa_1}{\kappa_2})^{\frac{1}{2}}]^2}[\ell n(\cos\tfrac{1}{2}c)]^2\,(\pi Fo_2)^{-1} + \ldots\right], \tag{3.2.94}$$

where $R_{fc} = (k_1\kappa_2^{\frac{1}{2}} + k_2\kappa_1^{\frac{1}{2}})(\pi t)^{\frac{1}{2}}/(k_1k_2)$ is the full contact resistance, and $Fo_2 = \kappa_2 t/\ell^2$ is the Fourier number based on the lower thermal diffusivity. This result is presented in Fig. 3.2.1, where R/R_{fc} is plotted as a function of $Fo_2/[\ell n(\cos\frac{1}{2}c)]^2$ for contacts between copper and steel, steel and glass, and copper and glass.

3.2.5 Discussion

The present analysis provides useful results for situations in which we have a large fraction of the interface in contact. This corresponds to the case in which $c/\pi \ll 1$. In fact, when $c = 0$, we have full contact and the only terms in the solution that count are those of leading order. These terms then satisfy the set of equations (3.2.5-3.2.8) exactly. For cases when $c/\pi \lesssim 1$, however, the higher order corrections become unrealistically large, except for correspondingly large values of the Fourier number, $Fo_i = \kappa_i t/\ell^2$. As a suitable criterion of validity, we can require that the dominant term in the highest order be much smaller than the next lower order term. For equations (3.2.85), (3.2.86) and (3.2.90-3.2.93) such a criterion would lead to the condition that

$$\frac{(k_1 + k_2)^2}{(k_2\kappa_1^{\frac{1}{2}} + k_1\kappa_2^{\frac{1}{2}})^2} [\ell n(\cos \tfrac{1}{2} c)]^2 \frac{\ell^2}{\pi t} \ll 1. \qquad (3.2.95)$$

Although the validity of this analysis is restricted by (3.2.94), the results expose the interaction of the different parameters involved. Being analytical solutions, they have the usual advantage over numerical solutions in which the role of the various parameters is often difficult and laborious to interpret. The present set of results provides an incentive for experimental work associated with the measurement of the transient resistance for varying fraction of contact.

REFERENCES

[1] Carslaw, H. S., and Jaeger, J. C., Conduction of Heat in Solids, Cambridge University Press, Cambridge, 356-357 (1963).

[2] Schneider, G. E., Strong, A. B., and Yovanovich, M. M., "Transient Thermal Response of Two Bodies Communicating Through a Small Circular Contact Area", International Journal of Heat and Mass Transfer 20, 301-308 (1977).

[3] Heasley, J. H., "Transient Heat Flow Between Contacting Solids", International Journal of Heat and Mass Transfer 8, 147-154 (1965).

[4] Norminton, E. J., and Blackwell, J. H., "Transient Heat Flow from Constant Temperature Spheroids and the Thin Circular Disk", Quarterly Journal of Mechanics and Applied Mathematics 17 (1), 65-72 (1964).

[5] Dundurs, J., and Panek, C., "Heat Conduction Between Bodies with Wavy Surfaces", International Journal of Heat and Mass Transfer 19, 731-736 (1976).

[6] Sneddon, I. N., Mixed Boundary Value Problems in Potential Theory, North Holland Publishing Company, Amsterdam (1966).

[7] Gradshteyn, I. S. and Ryzhik, I. W., Tables of Integrals, Series and Products, 4th edition, Academic Press, London (1965).

[8] Prasad, G., A Treatise on Spherical Harmonics and the Functions of Bessel and Lame, part I, Benares Mathematical Society, Mahamandal Press, Benares (1930).

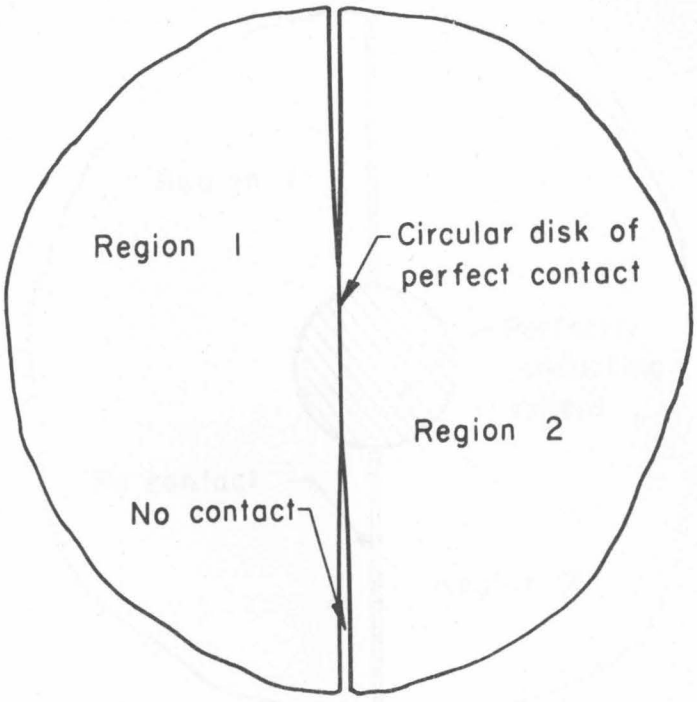

Fig. 3.0.1. Two solids in contact over a finite circular disk.

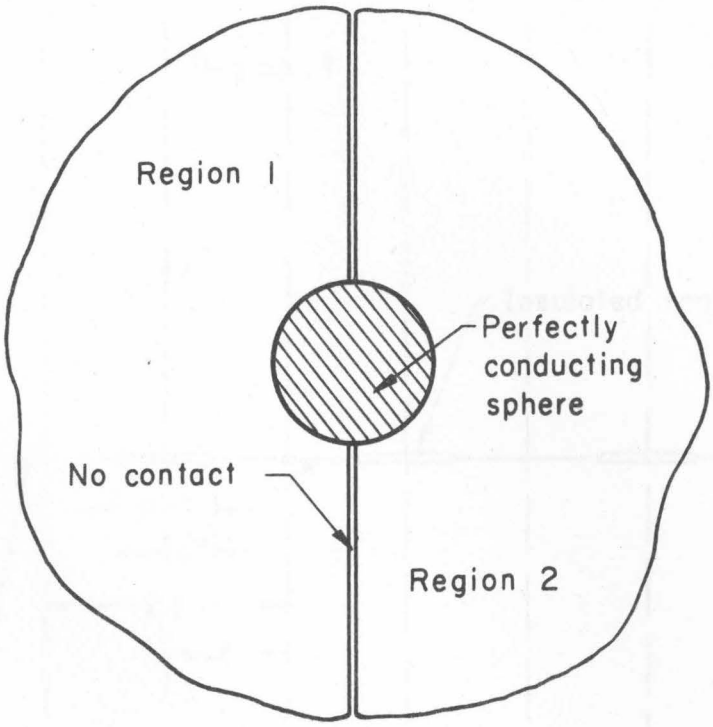

Fig. 3.0.2. Heasley's model: a perfectly conducting sphere between two solids.

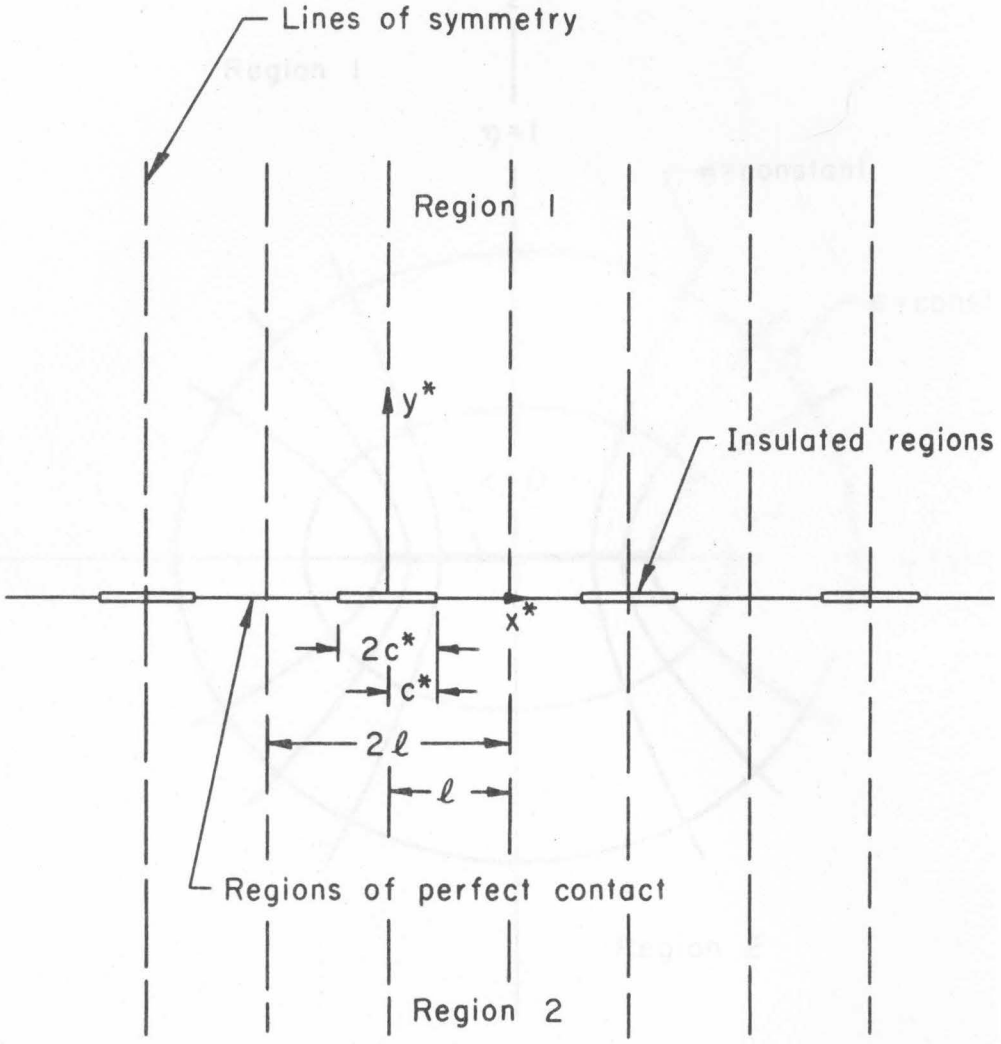

Fig. 3.0.3. Two solids in contact over a series of identical, equally spaced strips.

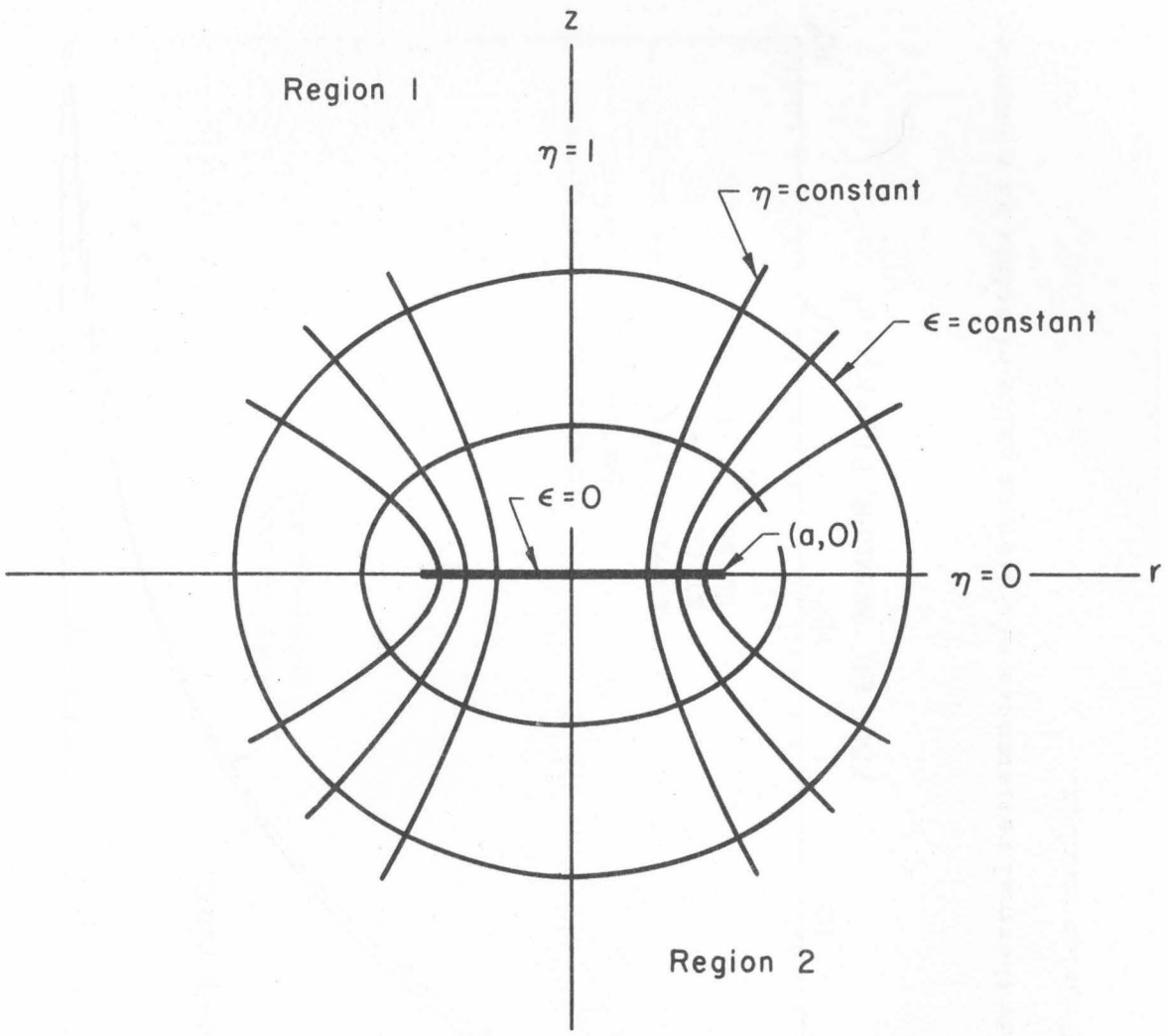

Fig. 3.1.1. Oblate spheroidal coordinate system.

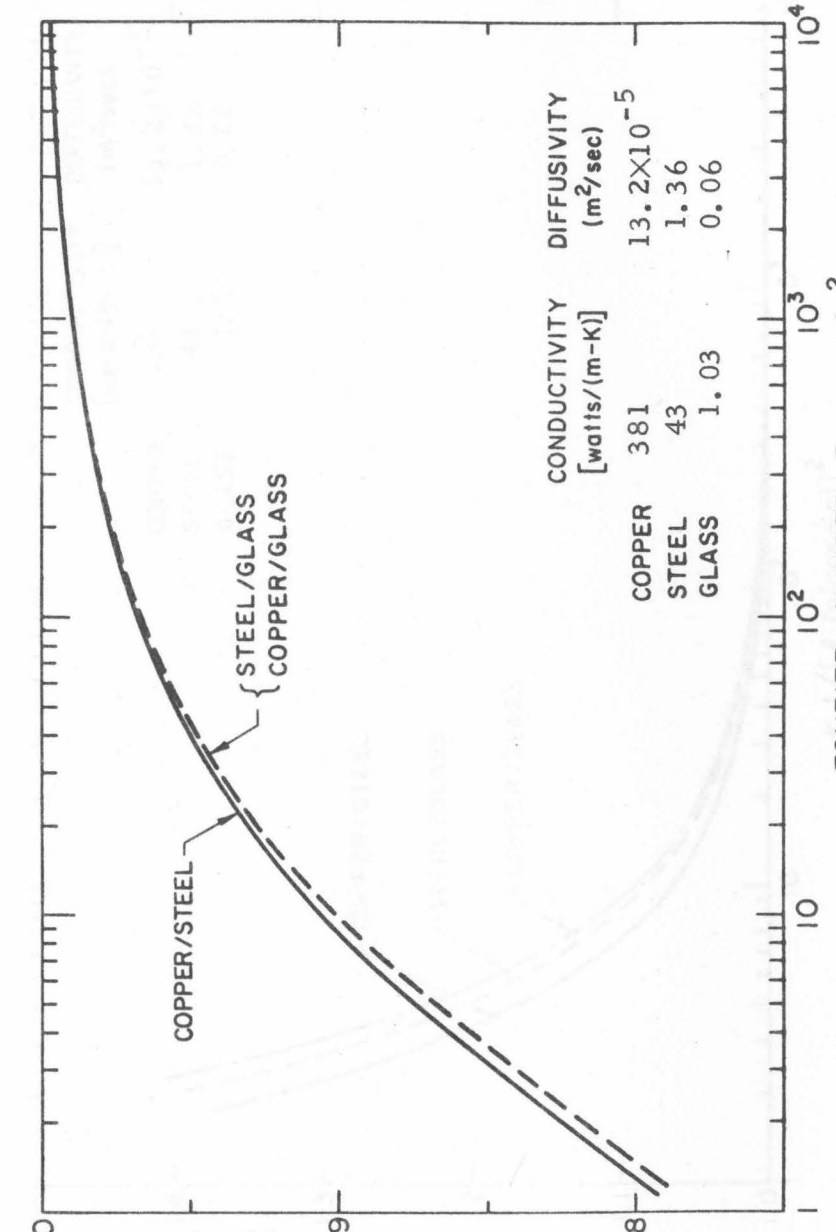

Fig. 3.1.2. Unsteady thermal resistances of different pairs of solids as a function of the Fourier number.

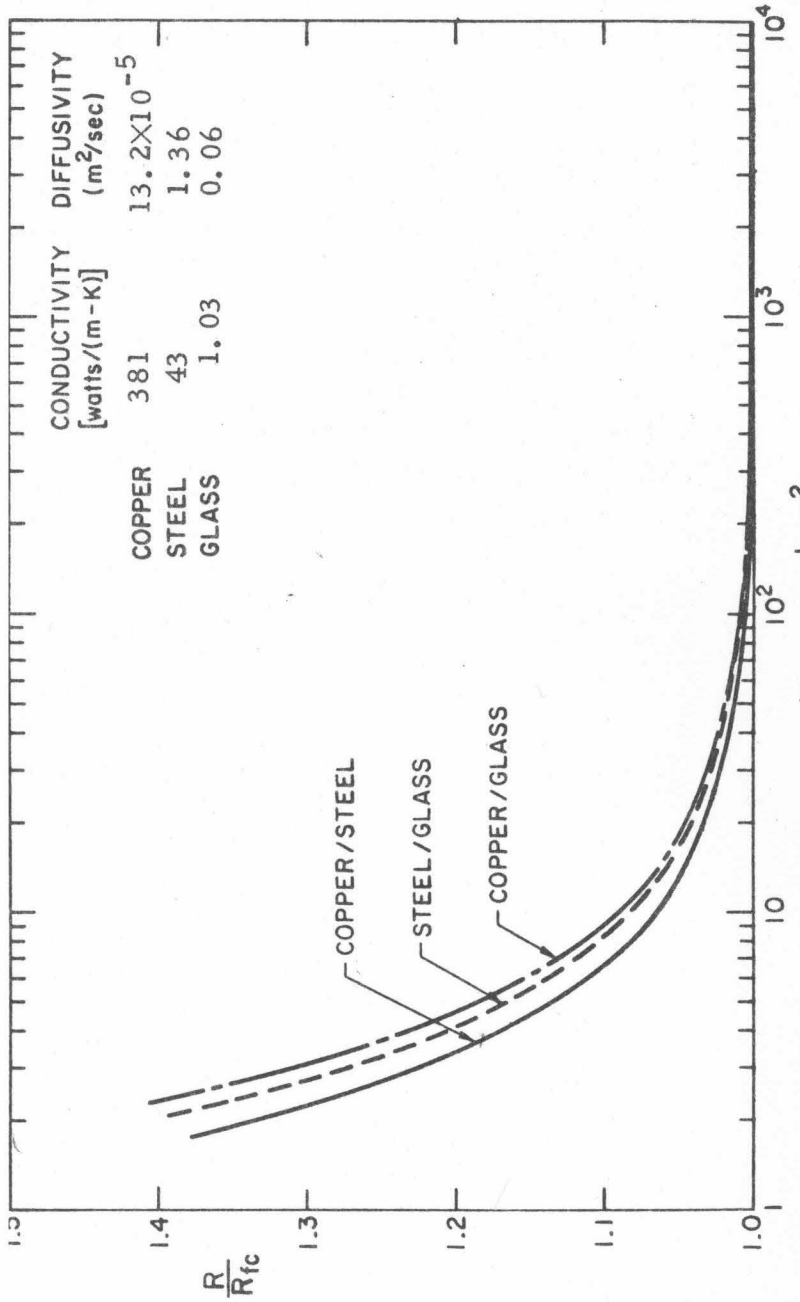

Fig. 3.2.1. Unsteady thermal resistances of different pairs of solids as a function of $\kappa_2 t/[\ell \ln(\cos \frac{1}{2}c)]^2$.